Lattice models, cylinder partition functions, and the affine coxeter element

Robert Paul Thomas Talbot

Lattice Models, Cylinder Partition Functions, and the Affine Coxeter Element.

Robert Paul Thomas Talbot

A thesis for the degree of
Doctor of Philosophy

Department of Mathematical Sciences
University of Durham
Durham DH1 3LE
England

30 September 1998

Lattice Models, Cylinder Partition Functions, and the Affine Coxeter Element.

Robert Paul Thomas Talbot

Ph.D. Thesis 1998

Abstract

The partition functions of the affine Pasquier models on the cylinder are calculated in the continuum limit. The partition functions of the models based upon the $\widehat{A}_n$ cycle graphs are first found from the appropriate Coulomb-gas equivalence. Their relationship with the $\widehat{D}_n$ and $\widehat{E}_{6,7,8}$ models is established by constructing an affine analogue to the classical intertwiners using a Temperley-Lieb algebraic equivalence. From this relationship, each of the partition functions is constructed. We write our results in terms of 'generating polynomials' establishing explicitly the precise operator content of the conformally invariant continuum field theories.

A numerical study is undertaken to establish the validity of the partition functions as calculated. We conclude that the partition functions calculated are correct.

The partition functions are further studied and the connection with the McKay correspondence established. We establish a simple form for the partition functions in terms of degenerate $c = 1$ Virasoro characters and Chebychev polynomials of the second kind. From this, we establish the role within the partition functions played by the affine Coxeter element, a particular member of the Weyl group associated with the defining graph of the model. Some of the resulting consequences of this role are explored.

Declaration

This thesis is the result of research carried out between April 1995 and June 1998. The special study described has been carried out and composed by me. This work has not been presented towards any other degree or professional qualification.

Chapters 1 and 4, excepting part of section 1.2.7, review necessary background material and apart from the author's own interpretation, no claim of originality is made. Chapters 2, 3, 5, the appendices and part of section 1.2.7 describe the original study carried out by the author. Apart from the description, in section 3.1, of the power method algorithm, this work is original and has been carried out solely by the author. This work forms the bulk of a paper currently in preparation. Chapter 6 summarises the results of the earlier chapters and attempts to place them within the context of current research.

Copyright

Acknowledgements

Most importantly I wish to express my gratitude to all my family. Most especially to my parents, Robert and Angela, my siblings, David, Richard and Victoria and to my Aunt Maureen. I am deeply indebted to them for their constant support and encouragement.

I thank Jennifer Robertson for her constant advice, for her inspiration, for being my best friend and for putting up with me while I wrote this thesis. I especially thank her for dragging me off to see the film *Good Will Hunting*. This particular film inspired me towards the approach used in section 2.5 of this thesis and which eventually developed into chapter 5. As pure entertainment, it wasn't bad either.

I would also like to thank the numerous friends I made whilst in Durham, in particular: David Barton, Ilona Bausch, Simon Brown, Stefan Calvert, *Αθανασια Χατζηφωτιου*, Paul Embleton, Michael Evason, Ashwina Gayan, Esther Jubb, Cristina Licata, Isobel Martin, Jane Maupin, Anthony Mosakowski, Simon Pierce, Kim Stabler, Momme von Sydow, Kevin Thompson, Steven Vandevenne and Dean Wood. They and many others made my time in Durham worthwhile.

I also thank Dr. M. Richardson, principal of the Graduate Society, for much helpful advice; and also together with the staff of the society, for an enjoyable residence in Durham.

I thank Michel Bauer, Vincent Pasquier and Jean-Bernard Zuber for helpful discussions and the organisers and staff of the Institut Henri Poincaré, Paris, for their hospitality during November–December 1996.

I thank the library staff of Imperial College London for supplying a number of vital references at short notice, unobtainable in Durham University library.

I wish to thank Gabor Takacs for his assistance in running some programs on my behalf on the computing systems of the INFN Bologna, Italy (see chapter 3).

I thank Edward Corrigan and Robert Weston for constructive and encouraging remarks made during the examination of this thesis.

Much thanks are due to Patrick Dorey for interesting me in and supervising this project, and also for numerous invaluable discussions.

But some there are who deem themselves most free
When they within this gross and visible sphere
Chain down the wingéd thought, scoffing ascent,
Proud in their meanness: and themselves they cheat
With noisy emptiness of learnéd phrase,
Their subtle fluids, impacts, essences,
Self-working tools, uncaused effects, and all
Those blind Omniscients, those Almighty Slaves,
Untenanting creation of its God.

— *Samuel Taylor Coleridge.*
"The Destiny of Nations".

The core of nature is in the heart of Man.

— *Friedrich Wilhelm Nietzsche.*

To Angela and Robert.

Forte et Fidele

Contents

Figures

Chapter 1

Lattice Models and Conformal Field Theory

In this chapter we establish the theoretical framework behind the first part of the study which is conducted in chapters 2 and 3. The material of this chapter follows a variety of sources and, except for the second half of section 1.2.7 (the calculation of equation (1.152)), no claim of originality is made. Further background material is given as chapter 4.

1.1 Pasquier Lattice Models

In this section, we introduce the idea of a graph lattice model. We present the concept of integrability and apply it to introduce the integrable lattice models of Pasquier [43]. These models may be thought of generalisations of the familiar Q-state Potts model and of the integrable lattice models of Andrews *et al.* [1]. Using the Q-state Potts model as a guide, the Temperley-Lieb algebra is introduced. This is a sufficient condition for the integrability of a lattice model. Representations of this algebra and hence integrable lattice models are constructed by restricting the degrees of freedom of the model to a graph.

Although the models were first constructed in the form discussed below by Pasquier [43], this review also makes use of the articles [25], [31] and [57].

1.1.1 Statistical Mechanics

Statistical mechanics is the science concerned with describing systems with large numbers of degrees of freedom. Such systems abound in nature: the air we breathe, the water we drink and the matter of which we ourselves are made being familiar examples. Each is composed of huge numbers of particles, each with its own position and momentum. One cannot hope to describe the behaviour of each and every single particle. Statistical mechanics takes its name by concentrating on the bulk statistical properties of these systems, deriving such from the typically short range interactions of the individual subsystems. It faces two major problems: Often the underlying interactions are unknown. We are forced to guess and approximate quite complex interactions. The second problem is that of mathematical tractability. The underlying interactions often do not afford an easy derivation of the bulk properties. So we are forced to approximate yet further. One such approximation is to restrict to the examination of 2-dimensional systems, simplifying the physics. The degrees of freedom may be simplified too, perhaps just considering one physical parameter and modelling the complex interactions solely upon this. Both strategies are employed in the systems discussed in this section.

We shall also assume that the systems in which we are interested are in *equilibrium*. That is, the bulk physical properties of interest to us do not change over some given timescale. For such a system at temperature T, at any given time the *relative probability* or *Boltzmann weight* that the system is in the configuration labelled by c is

$$\mathbb{W}(\mathsf{c}) = \exp\{-E(\mathsf{c})/k_{\mathrm{B}}\,T\}\;; \tag{1.1}$$

where $E(\mathsf{c})$ is the energy of the configuration c and k_{B} the *Boltzmann constant*. Thus at low temperature, a configuration of higher overall energy is less likely to occur than a less energetic configuration. As the temperature is raised, highly energetic configurations are eventually permitted. The probability, therefore, of the specific configuration c is

$$\mathbb{P}(\mathsf{c}) = \frac{1}{Z}\exp\{-E(\mathsf{c})/k_{\mathrm{B}}\,T\}\;; \tag{1.2}$$

where

$$\mathcal{Z} \equiv \sum_{\mathsf{c}' \in \mathcal{C}} \exp\{-E(\mathsf{c}')/k_{\mathrm{B}}\,T\}\ , \tag{1.3}$$

the sum of all the weights over all the possible configurations $\mathcal{C}$, is the *partition function*. It normalises the Boltzmann weights and may be thought of as a generating function for the statistical properties of the system.

1.1.2 The Q-State Potts Model

The *Q-state Potts model* is defined [4] for $Q \in \mathbb{Z}^+$ by associating to each site a on a rectangular lattice Λ a height σ_a which may take any of Q distinct values. (We adopt the notation whereby the non-negative integers are denoted by $\mathbb{Z}^+ \equiv \{0, 1, 2, \dots\}$ and the non-positive integers by $\mathbb{Z}^- \equiv -\mathbb{Z}^+ = \{0, -1, -2, \dots\}$.) Two adjacent heights or spins at sites a and b interact with energy $-J\,\delta_{\sigma_a \sigma_b}$. We will assume that J is positive so that we consider the *ferromagnetic* case where at low temperature, adjacent heights tend to align. The partition function is therefore

$$\mathcal{Z}_Q = \sum_{\substack{\text{All} \\ \text{configurations} \\ \{\sigma\}}} \exp\left\{ K \sum_{\langle a,b \rangle} \delta_{\sigma_a \sigma_b} \right\}\ ; \tag{1.4}$$

where $K \equiv J/k_{\mathrm{B}}\,T$ and $\langle , \rangle$ denotes nearest neighbour pairs. The choice $Q = 2$ defines the *Ising model.*

The partition function (1.4) defines a system of spins in thermal equilibrium. The expected value for the spin at site a is simply the thermal average over a timescale equivalent to that defining the notion of equilibrium, i.e.

$$\langle \sigma_a \rangle = \sum_{\substack{\text{All} \\ \text{configurations} \\ \{\sigma\}}} \sigma_a\, \mathbb{P}(\{\sigma\}) \tag{1.5}$$

$$= \frac{1}{\mathcal{Z}} \sum_{\substack{\text{All} \\ \text{configurations} \\ \{\sigma\}}} \sigma_a \exp\left\{ K \sum_{\langle a,b \rangle} \delta_{\sigma_a \sigma_b} \right\}\ . \tag{1.6}$$

Of particular interest is the 2-point correlation defined by

$$\langle \sigma_a \, \sigma_b \rangle = \sum_{\substack{\text{All} \\ \text{configurations} \\ \{\sigma\}}} \sigma_a \, \sigma_b \, \mathbb{P}(\{\sigma\}) \; . \tag{1.7}$$

This can be used to examine the distance, the *correlation length* ζ, over which the spins exert a significant influence on each other. A spin σ_a will influence and will be influenced by those other spins within a distance ζ. When ζ is finite, it is related to the 2-point correlation, where the distance r between the sites a and b is large, by

$$\langle \sigma_a \, \sigma_b \rangle = \frac{e^{-r/\zeta}}{r^{\tau}} \; . \tag{1.8}$$

The exponent τ is an example of a *critical exponent.*

The model (1.4) is generalised to $Q \in \mathbb{R}$ by analytic continuation, making use of the *high-temperature expansion*: Each neighbouring and alike pair of spins contributes a factor e^K while each unlike pair contributes a factor of 1. Thus, equation (1.4) can be rewritten as

$$\mathcal{Z}_Q = \sum_{\substack{\text{All} \\ \text{configurations} \\ \{\sigma\}}} \prod_{\langle a,b \rangle} \left\{ 1 + \left(e^K - 1 \right) \delta_{\sigma_a \sigma_b} \right\} . \tag{1.9}$$

Each term in the product is represented graphically in terms of bonds on the lattice. A bond is present if the $\left(e^K - 1\right)$ term is present in the expansion of the product (1.9). These bonds form clusters of constant height (refer to figure 1.1). Performing the summation over the configurations $\{\sigma\}$ yields a factor of Q for each independent cluster. Thus

$$\mathcal{Z}_Q = \sum_{\text{Graphs}} \left(e^K - 1 \right)^{N_{\mathrm{B}}} Q^{N_{\mathrm{C}}} \; ; \tag{1.10}$$

where N_{B} and N_{C} are the numbers of bonds and clusters respectively. The expression (1.10) is clearly analytic in Q. So the definition (1.9) of the Potts model can be extended to general values of $Q \in \mathbb{R}$ by using this new expression (1.10). If to each bond-graph is associated the set of closed loops (polygons) around the clusters, as demonstrated in figure 1.1, then the number of closed loops, N_{L} in a given graph in (1.10) is given by

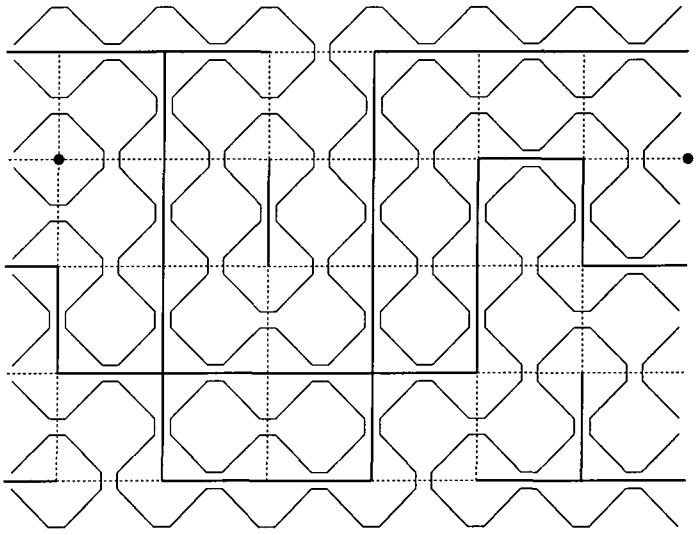

Figure 1.1: The Q-state Potts model with free boundary conditions on the rectangular lattice (dashed lines), here shown in a finite cylindrical geometry. The lattice is periodic in the 'horizontal' direction. Each configuration may be represented by a graph of bonds (thick lines) denoting clusters of like heights. Equivalently, each configuration may be represented by the set of closed loops or polygons (thin lines) about the clusters

Euler's relation

$$N_{\mathrm{L}} = N_{\mathrm{B}} + N_{\mathrm{C}} - N_{\mathrm{S}} \; ; \tag{1.11}$$

with N_{S} the total number of sites in the lattice. For planar or cylindrical geometries, the number of polygons is

$$N_{\mathrm{P}} = N_{\mathrm{L}} + N_{\mathrm{C}} \; . \tag{1.12}$$

Hence (1.10) can be rewritten as

$$\mathcal{Z}_Q = Q^{N_{\mathrm{S}}/2} \sum_{\text{Graphs}} \left\{ \left(e^K - 1\right) Q^{-1/2} \right\}^{N_{\mathrm{B}}} Q^{N_{\mathrm{P}}/2} \; . \tag{1.13}$$

The critical point of the model defined by (1.10), the point where the correlation length ζ becomes infinite, is known from duality arguments (see [46] and [33]) to be at the point

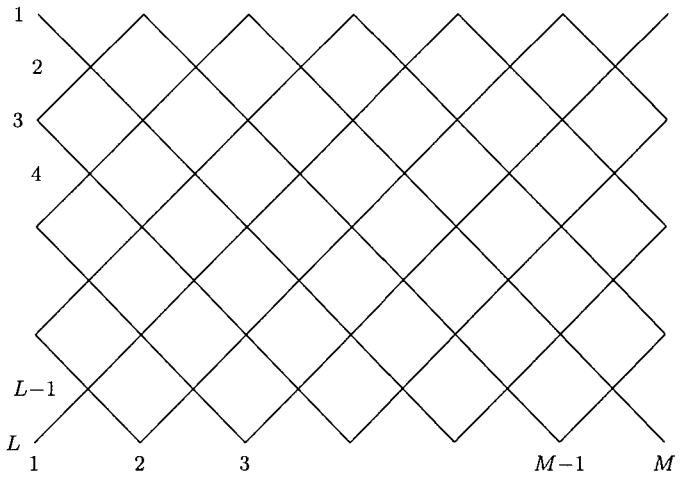

Figure 1.2: A standard regular rectangular $M \times L$ lattice Λ.

where

$$\left(e^K - 1\right) Q^{-1/2} = 1 \,. \tag{1.14}$$

Furthermore, the transition is second order for $Q \in [0, 4]$ and first order outside this interval. Duality arguments relate the free energy of a system to that of an equivalent system constructed on the dual lattice (the lattice constructed by building a lattice with sites centred on the faces of the original) but at a different temperature [56]. Such a duality argument is presented in section 1.1.5.

1.1.3 General Graph Lattice Models

Consider a standard rectangular lattice Λ as in figure 1.2. To each point a of Λ is assigned a value of a *spin* or *height* function σ_a which is allowed to be one of a discrete set of values $\mathcal{G}$. The generalisations of the Potts models are found by restricting the configurations of the model so that neighbouring heights on the lattice should be close to each other; i.e. that no strongly fluctuating configuration should be allowed. This contrasts with the Potts models themselves, where there are no restrictions on the heights associated to two adjacent lattice sites. Hence the set $\mathcal{G}$ is extended to be a *directed graph*: the height variable σ takes values which are the nodes of the graph $\mathcal{G}$. The bonds of the rectangular lattice are chosen to be oriented (downwards as in figure 1.3 for example) and the following "*$\mathcal{G}$-restriction*

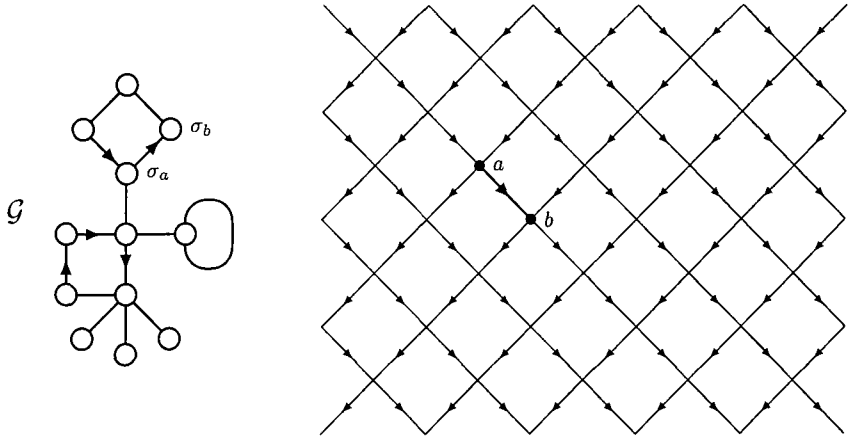

Figure 1.3: The $\mathcal{G}$-restriction condition: two sites a and b with an arrow pointing from a to b have heights σ_a and σ_b such that an arrow points from σ_a to σ_b on the graph $\mathcal{G}$; i.e. if one follows an arbitrary path on the lattice in the direction of the arrows only, then the heights must also follow a path which obeys the arrows on the graph $\mathcal{G}$. The nodes or elements of $\mathcal{G}$ are here denoted by circles and the links between the nodes are denoted by a directed-line drawn between a and b if a connects to b. Two-way links are represented by undirected lines.

condition" is imposed on σ:

> If one follows an arbitrary path on the lattice in the direction of the arrows only, then the heights σ must also follow a path which obeys the arrows on the graph $\mathcal{G}$; (1.15)

(see again figure 1.3). In other words, to each path on the lattice, there is a corresponding path of heights on the graph $\mathcal{G}$.

One sees that with this restriction, the configuration spaces of the Ising, 3-state Potts and 4-state Potts models are recovered by

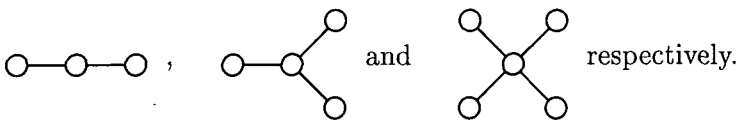

In each case half of the lattice points take the height-value of the central node of the graph; the remaining lattice points take heights corresponding to the 'leg' nodes. Hence the original lattice factorises into two interpenetrating lattices: one trivial lattice with fixed configuration and one with the configuration space of the Ising/Potts model (see

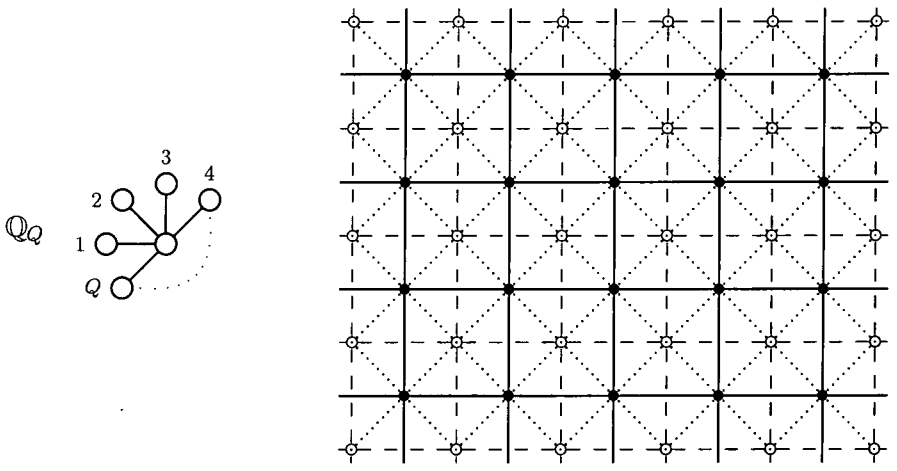

Figure 1.4: When the graph $\mathcal{G}$ is $\mathbb{Z}_2$-colourable, the lattice Λ factorises into two interpenetrating lattices, respectively denoted by dashed-lines with light sites and thick lines with dark sites. In the case of the graph $\mathbb{Q}_Q$ (left), the height function σ has the fixed value of the central node on one set of sites (the dark coloured sites for example) and on the other lattice sites there is a lattice model with degrees of freedom corresponding to the Q-state Potts model.

figure 1.4). Indeed this will always be the case if the graph $\mathcal{G}$ is $\mathbb{Z}_2$-*colourable*; i.e. if there exists a map between the nodes of the graph $\mathcal{G}$ and the set $\mathbb{Z}_2$ which is non-constant as one traverses the links of the graph. Similarly the configuration space of the Q-state Potts model with $Q \in \mathbb{Z}^+$ is recovered by considering the graph $\mathbb{Q}_Q$ consisting of one central node with Q 'legs' attached (see figure 1.4).

At the local level, one considers a single *square*, *plaquette* or *face* of the lattice. The statistics of the model are governed by local *Boltzmann weights*,

$$w(\sigma_a, \sigma_b, \sigma_c, \sigma_d) = \quad , \tag{1.16}$$

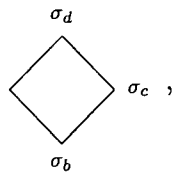

which depend solely upon the values of the height variable around the face (a, b, c, d) of Λ. Such a model is termed an *interaction round a face* or *IRF-model*. The partition function

of the model with given boundary conditions on the height function σ is

$$\mathcal{Z} = \sum_{\substack{\{\sigma\} \\ \text{Subject to} \\ \text{boundary} \\ \text{conditions}}} \prod_{\substack{\text{All} \\ \text{faces} \\ (a,b,c,d)}} \sigma_a \begin{array}{ccc} & \sigma_d & \\ \sigma_a & \square & \sigma_c \\ & \sigma_b & \end{array} \sigma_c \ , \tag{1.17}$$

If juxtaposition of the weights (1.16) is considered as multiplication and all vertices are summed over subject to the restriction (1.15), then the partition function (1.17) is represented graphically by the lattice of 1.2. We shall see the Boltzmann weights for the Potts models in section 1.1.5.

To further analyse these models, it is useful to label the horizontal and vertical directions 'time' and 'space' respectively. One considers a vertical "*zigzag*" of sites to be a fixed-time slice; i.e. the configuration space of the heights on a zigzag is taken to be the basis of a Hilbert space (see figure 1.6). This procedure allows the transfer matrix to be expressed as a trace as we shall see. We now examine the operators which propagate between zigzags, these provide the 'time'-evolution of the model:

Define [4] the *face-transfer matrices* as

$$X^j_{\sigma\sigma'} \equiv \begin{array}{ccc} & \sigma_{j-1} & \\ \sigma_j & \square & \sigma'_j \\ & \sigma_{j+1} & \end{array} \prod_{i \neq j} \delta_{\sigma_i \sigma'_i} \ . \tag{1.18}$$

These act between two neighbouring rows of L lattice sites, with height configurations $\sigma \equiv (\sigma_1, \ldots, \sigma_L)$ and $\sigma' \equiv (\sigma'_1, \ldots, \sigma'_L)$ (see figure 1.5). We may now write "*zigzag-to-zigzag transfer matrices*" as:

$$\begin{aligned} V &\equiv \prod_{j=0}^{L/2} X^{2j} \ , \\ W &\equiv \prod_{j=1}^{L/2} X^{2j-1} \ . \end{aligned} \tag{1.19}$$

It is clear that we have two types of zigzag (figure 1.6) depending on whether the first node is in the right or the left position. V propagates from '*even*' to '*odd*' zigzags, W from odd

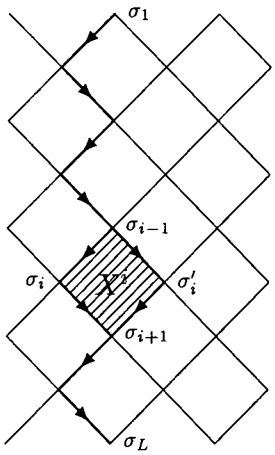

Figure 1.5: The face transfer matrix X^i; i.e. the evolution of a zigzag: $\sigma_i \mapsto \sigma'_i$.

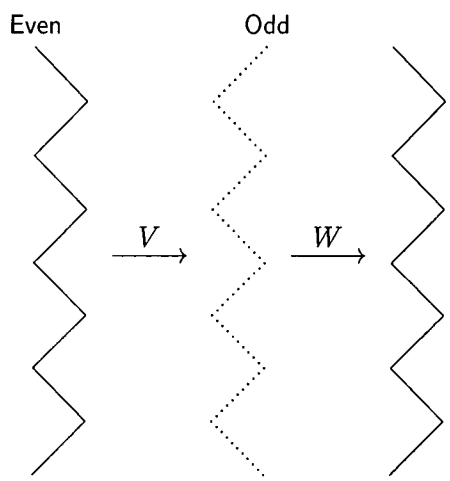

Figure 1.6: The two types of zigzags. V propagates from even to odd zigzags, W from odd to even. The configuration space on each zigzag provides the basis of a Hilbert space.

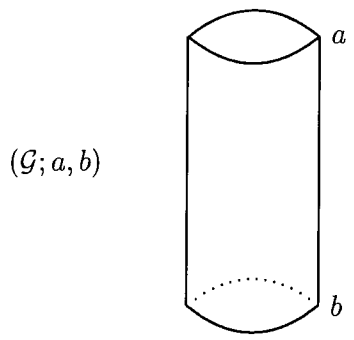

Figure 1.7: The cylindrical lattice Γ of circumference M and length L. On the cylinder boundaries, the spin function σ takes the values a and b on the 'top' and 'bottom' respectively. We denote by $(\mathcal{G}; a, b)$ the cylindrical Pasquier model whose configuration space is specified by the graph $\mathcal{G}$ with boundary conditions a and b on either end of the cylindrical lattice. The order of the specification a, b is irrelevant due to symmetry.

to even. Together they describe the time-evolution of the system with the *transfer matrix*

$$T \equiv V W \tag{1.20}$$

describing the propagation from even to even zigzags. Simarily $\overline{T} \equiv W V$ describes the propagation between odd zigzags. As T (or $\overline{T}$) acts as a time propagator, we see that it is related to the Hamiltonian H by $T = \exp(-\sqrt{2}\, d H)$ with d the interlattice spacing (i.e. the distance between neighbouring sites of the lattice).

If we impose periodic boundary conditions in the temporal direction (i.e. $\sigma_{M+1} \equiv \sigma_1$), the lattice becomes geometrically a cylinder of circumference M and length L (figure 1.7). We denote a lattice in this geometry by Γ. The partition function (1.17) on the lattice is

$$\mathcal{Z} = \underset{\substack{\text{Subject to}\\ \text{boundary}\\ \text{conditions}}}{\text{Tr}} T^M = \underset{\substack{\text{Subject to}\\ \text{boundary}\\ \text{conditions}}}{\text{Tr}} \left((V W)^M \right), \tag{1.21}$$

which is a simple trace of the transfer matrix raised to some power. Up to this point we have not mentioned the boundary conditions which might be imposed on the ends of the model. However, we point out that the trace above must take these into account.

1.1.4 Integrability

A necessary and sufficient condition for a given model to be *exactly-solvable* or *integrable* is often taken to be the existence of an infinite number of independent mutually commuting conserved charges. At least in principle, one may reformulate the equations of motion in terms of these charges, so the time evolution of the system is simplified.

Such charges may be constructed by introducing a family of Boltzmann weights [4],

$$w(\sigma_a, \sigma_b, \sigma_c, \sigma_d|\xi) = \quad ; \tag{1.22}$$

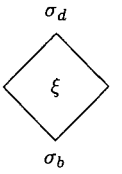

where ξ is a continuous parameter in some interval $\mathcal{J}$.

It is convenient, temporarily, to rotate the temporal and spatial directions by $\frac{\pi}{4}$, assume a periodicity of L in the (new) 'spatial' direction and define the *row-to-row transfer matrix* $R(\xi)$ [4], propagating from row to row, by

$$R(\xi)_{\sigma\sigma'} \stackrel{\text{def}}{=} \prod_{j=1}^{L} w(\sigma_i, \sigma_{i+1}, \sigma'_{i+1}, \sigma'_i|\xi) \tag{1.23}$$

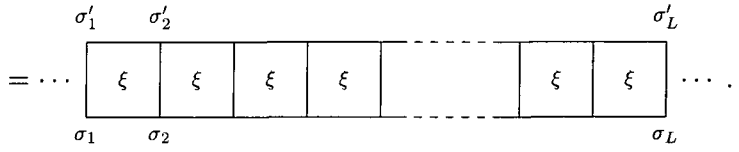

If it can be established that the resulting family, $\{\, R(\xi) \mid \xi \in \mathcal{J} \,\}$, of row-to-row transfer matrices is a mutually commuting and infinite set, then one may at least in principle proceed via the Bethe ansatz [4] to find the highest eigenvalue $\widehat{r}(\xi)$ of $R(\xi)$ and therefore the thermodynamic free energy per site of the model,

$$F(\xi) = -\lim_{L,M\to\infty} \frac{1}{LM} \ln \mathcal{Z} = -\lim_{L\to\infty} \frac{1}{L} \ln \widehat{r}(\xi) \,. \tag{1.24}$$

The ability to find this free energy is generally what is meant by terming the model *integrable* or *solvable*. The parameter ξ in equation (1.22) is called the *spectral-* or *anisotropy-parameter* as it may be thought of as modulating the strengths of the different interactions around a face.

Now, consider the conditions sufficient for

$$[R(\xi)\,,\,R(\xi')] = 0, \quad \text{with } \xi,\xi' \in \mathcal{J}\,. \tag{1.25}$$

First, write the product $R(\xi)\,R(\xi')$ as

$$\big(R(\xi)\,R(\xi')\big)_{\sigma\sigma'} = \sum_{\sigma''}\prod_{i=1}^{L} w(\sigma_i,\sigma_{i+1},\sigma''_{i+1},\sigma''_i|\xi)\,w(\sigma''_i,\sigma''_{i+1},\sigma'_{i+1},\sigma'_i|\xi')$$

$$= \cdots$$

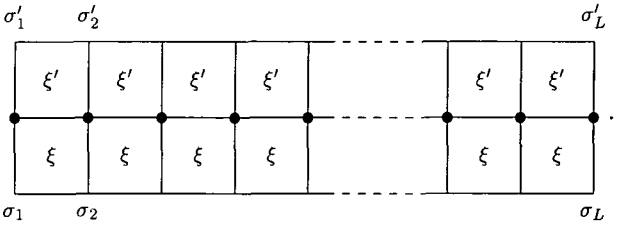

$$\cdots \tag{1.26}$$

$$= \mathrm{Tr}\prod_{i=1}^{L} D(\sigma_i,\sigma'_i;\sigma_{i+1},\sigma'_{i+1}|\xi,\xi')\;;$$

where

$$D(\sigma_i,\sigma'_i;\sigma_{i+1},\sigma'_{i+1}|\xi,\xi')_{\sigma''_i,\sigma''_{i+1}} \stackrel{\text{def}}{=} w(\sigma_i,\sigma_{i+1},\sigma''_{i+1},\sigma''_i|\xi)\,w(\sigma''_i,\sigma''_{i+1},\sigma'_{i+1},\sigma'_i|\xi')\,. \tag{1.27}$$

A sufficient condition for (1.25) to hold is the existence of a matrix $S(\sigma,\sigma')$ such that

$$D(\mu,\mu';\nu,\nu'|\xi,\xi') = S(\mu,\mu')\,D(\mu,\mu';\nu,\nu'|\xi',\xi)\,S^{-1}(\nu,\nu')\,, \tag{1.28}$$

or

$$S\,D(\xi,\xi') = D(\xi',\xi)\,S \tag{1.29}$$

for any permissable configuration (w.r.t. $\mathcal{G}$). As an ansatz for $S(\mu,\mu')$, take it to be itself a Boltzmann weight with spectral parameter ξ'', i.e.

$$S(\mu,\mu')_{p,q} = w(p,\mu,q,\mu'|\xi'')\,. \tag{1.30}$$

Substituting into (1.29), this ansatz will be consistent provided

$$\sum_q w(\mu,\nu,q,p|\xi)\, w(p,q,\nu',\mu'|\xi')\, w(q,\nu,r,\nu'|\xi'') = \sum_q w(p,\mu,q,\mu'|\xi'')\, w(\mu,\nu,r,q|\xi')\, w(q,r,\nu',\mu'|\xi)\ . \quad (1.31)$$

Which, perhaps more clearly, in the notation of (1.22) is

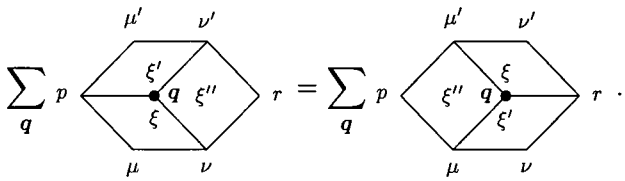

(1.32)

Baxter [4] has shown that in most cases it is possible to choose the parametrisation of the weights so that

$$\xi'' = \xi' - \xi\ . \quad (1.33)$$

This is indeed the case for the models of interest to us later.

Returning to the "diagonal lattice" picture of the last section (i.e. without the $\frac{\pi}{4}$ rotation), the integrability condition takes the form

$$X^i(\xi)\, X^{i+1}(\xi')\, X^i(\xi'') = X^{i+1}(\xi'')\, X^i(\xi')\, X^{i+1}(\xi) \quad (1.34)$$

in terms of the face transfer matrices.

Equations (1.31), (1.32) and (1.34) are equivalent and known as the *Yang-Baxter equation*. One of the most important problems in the theory of integrable lattice models is to find its solutions.

1.1.5 The Algebraic Content of the Potts Model

Reconsider the Q-state Potts model with partition function

$$\mathcal{Z} = \sum_{\substack{\text{All} \\ \text{configurations} \\ \{\sigma\}}} \exp\left(\sum_{\langle i,j \rangle_h} K_h \, \delta_{\sigma_i \sigma_j} + \sum_{\langle i,j \rangle_v} K_v \, \delta_{\sigma_i \sigma_j} \right) ; \tag{1.35}$$

where $\langle , \rangle_{h,v}$ indicate nearest neighbour sites in the horizontal and vertical directions, and K_v and K_h denote the temperature dependent couplings in the vertical and horizontal directions respectively.

The model is reformulated in the language of the preceding sections as follows:

Note that as mentioned earlier, the configuration space of the Q-state Potts model is given by the $\mathbb{Q}_Q$ graph. Degrees of freedom exist only at every second lattice site; every other site has a height fixed to take the value of the centre node of the $\mathbb{Q}_Q$ graph (refer again to figure 1.4). This means that the face-transfer matrices may be written as

$$\begin{aligned} X^{2j}_{\sigma\sigma'} &\equiv \exp\left(K_v \, \delta_{\sigma_{2j-1}\sigma_{2j+1}}\right) \delta_{\sigma_{2j}\sigma'_{2j}} \prod_{i \neq 2j} \delta_{\sigma_i \sigma'_i} , \\ X^{2j+1}_{\sigma\sigma'} &\equiv \exp\left(K_h \, \delta_{\sigma_{2j+1}\sigma'_{2j+1}}\right) \prod_{i \neq 2j+1} \delta_{\sigma_i \sigma'_i} ; \end{aligned} \tag{1.36}$$

which are manifestly of the form (1.18). The $\{X^{2j}\}$ serve to build up the contributions to the partition function coming from alike vertical neighbours on the Potts sublattice and the $\{X^{2j+1}\}$ serve to build up the contributions from alike horizontal neighbours. Defining the zigzag-to-zigzag operators U, V and T as before (equation (1.19)), it is easily seen that the partition function (1.35) is recovered from equation (1.21). Define operators $\{e_j\}$ by

$$\begin{aligned} e_{2j} &\equiv Q^{\frac{1}{2}} \, \delta_{\sigma_{2j-1}\sigma_{2j+1}} \prod_{i=0}^{L} \delta_{\sigma_i \sigma'_i} , \\ e_{2j+1} &\equiv Q^{-\frac{1}{2}} \prod_{\substack{i=0 \\ i \neq 2j}}^{L} \delta_{\sigma_i \sigma'_i} . \end{aligned} \tag{1.37}$$

It is easy to see that [4] the $\{e_i\}$ satisfy the relations:

$$\begin{aligned} e_i^2 &= \beta\, e_i \ , \\ e_i\, e_{i\pm1}\, e_i &= e_i \ , \\ e_i\, e_j &= e_j\, e_i \quad \text{for } |i-j| \geq 2 \ ; \end{aligned} \tag{1.38}$$

with $\beta \equiv Q^{\frac{1}{2}}$. Using these properties, the *Jones trace* property

$$\mathrm{Tr}(e_{i_1}\, e_{i_2} \cdots e_{i_n}) = \beta^{-n}\ \mathrm{Tr}\,\mathbb{I} \quad \text{for } i_1 < i_2 < \cdots < i_n \ , \tag{1.39}$$

may be shown by induction. These relations define the algebra generated by the $\{e_i\}$, namely a *Temperley-Lieb algebra* of parameter β [54]. The face-transfer matrices in terms of these operators are

$$\begin{aligned} X^{2j} &= \mathbb{I} + \xi_v\, e^{2j} \ , \\ X^{2j+1} &= Q^{\frac{1}{2}} \left\{ \xi_h\, \mathbb{I} + e^{2j+1} \right\} \ ; \end{aligned} \tag{1.40}$$

with $\xi_{v,h} \equiv Q^{-\frac{1}{2}} \{\exp(K_{v,h}) - 1\}$.

We now find the critical temperature T_c at which the thermodynamic free energy per site (1.24) is singular in T. For a large lattice, the transformation $e^i \to e^{i+1}$ will produce only boundary effects and therefore does not affect the volume dependence of the partition function in the infinite limit ($L, M \to \infty$) such as we might consider in the thermodynamic- or continuum-limits. Note that the shift $e^i \to e^{i+1}$ is entirely analogous to moving onto the dual lattice in the Potts case. The interpenetrating lattices of figure 1.4 are dual to each other. Inspecting equations (1.19), (1.21), (1.24) and (1.40) and using the cyclic property of the trace, we see that F satisfies the relation

$$F(\xi_v, \xi_h) = F(\xi_h^{-1}, \xi_v^{-1}) - \ln(\xi_v \xi_h) \ . \tag{1.41}$$

This is a *duality relation*: it relates a high-temperature Potts model to a low-temperature Potts model.

Assume that K_v and K_h are both positive so that the Potts system describes a ferromag-

net: heights which are nearest-neighbours either vertically or horizontally 'prefer' to align. On physical grounds, the ferromagnetic Potts model is expected to possess a disordered high-temperature phase ($K_{v,h}$ and $\xi_{v,h}$ small) in which all Q height values are equiprobable, separated by a transition from an ordered low-temperature phase ($K_{v,h}$ and $\xi_{v,h}$ large) in which each site of the lattice assumes the same height value. Therefore, in the two-dimensional coupling space ($\xi_{v,h}$), one expects a curve separating the ordered and disordered regions. If F is non-analytic at the point (ξ_v, ξ_h), then by (1.41) it must also be non-analytic at the point (ξ_h^{-1}, ξ_v^{-1}). The simplest possibility is that it is non-analytic only on the self-dual curve $\xi_v\, \xi_h = 1$ where the phase transition must therefore occur. This is indeed the case [33].

On this self-dual and critical curve, the parameter $\xi \equiv \xi_v = \xi_h^{-1}$ describes the vertical/horizontal anisotropy; it is the anisotropy- or spectral-parameter introduced in equation (1.22). Setting $\xi = 1$ results in an isotropic Potts model. Rescaling by an irrelevant overall factor, the partition function at criticality may be written as equation (1.21) with zigzag-to-zigzag transfer matrices (1.19) built from the face transfer matrices

$$X^j(\xi) = \mathbb{I} + \xi\, e_j\,, \quad 0 \leq j \leq L\,. \tag{1.42}$$

(Ignoring the factor $\xi_h\, Q^{\frac{1}{2}}$ in the face transfer matrix X^{2j+1} corresponds to scaling the partition function which in turn corresponds to a constant shift in the free energy density and this may be ignored.)

Thus, the model is self-dual if and only if the face transfer matrices X^{2j+1} and X^{2j} are 'proportional'. This in turn is the condition that we can apply the Yang-Baxter discussion of the last section (after a rotation of the lattice by $\frac{\pi}{4}$).

Note that we are not constrained use the representation (1.37) of the Temperley-Lieb algebra, the partition function is ultimately defined solely in terms of the operators $\{\, e_j \mid 1 \leq j \leq L \,\}$ which are in turn defined completely by properties (1.38) for the specified value of β. Thus we are free to choose any convenient representation with the same value $\beta \equiv Q^{\frac{1}{2}}$ [54]. Moreover, as is easily seen by checking, the conditions (1.38) for any value of β are in fact sufficient for (1.42) to satisfy the Yang-Baxter equation ((1.31), (1.32)

or (1.34)). Indeed, the expression (1.42) provides a solution to (1.34) provided

$$\xi'' = \frac{\xi - \xi'}{1 + \xi\,\xi' + \beta\,\xi'} \,. \tag{1.43}$$

Thus ξ'' has a solution in terms of ξ, ξ' and β. The parameter ξ may be reparametrised so that (1.33) is satisfied. For $\beta < 2$, $\beta = 2$ and $\beta > 2$, this leads respectively to trigonometric, rational and hyperbolic parametrisations (see [25] for example). Hence we see that the Q-state Potts model is integrable everywhere on the critical and self-dual curve $\xi_v\,\xi_h = 1$.

We remark that the requirements for integrability might still in principle be met using face transfer matrices of the form (1.40); we may yet be able to construct an infinite set of commuting transfer matrices. However, with both parameters $\xi_{v,h}$ independent, the integrability requirements are more involved than in the discussion of the last section. We are interested only in the critical case given by $\xi_v\,\xi_h = 1$, as for $Q \in [0, 4]$ this leads to a conformally invariant field theory in the continuum limit. This critical case, as we have just seen, is indeed integrable.

We remark also that, the single parameter ξ of (1.42) which describes the anisotropy in the interactions in the vertical and horizontal directions, becomes irrelevant in the continuum limit. This is because the way in which the limit is taken can be used to bring the value of ξ to whatever we wish, just by taking the limit in different ways in the vertical and horizontal directions. Thus, once this limit is taken (see later), the parameter ξ will no longer play an explicit role.

1.1.6 The Lattice Models of Pasquier

Define for each graph $\mathcal{G}$ an associated *incidence-* or *adjacency-matrix*, also denoted $\mathcal{G}$, by

$$\mathcal{G}_{ab} = \begin{cases} 1 & ; \text{ if node } a \text{ is connected to node } b. \\ 0 & ; \text{ otherwise.} \end{cases} \quad ; \tag{1.44}$$

where $a, b \in \mathcal{G}$ (i.e. a and b are nodes of the graph $\mathcal{G}$). For example, the graph

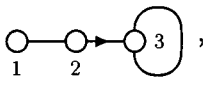

has adjacency matrix

$$\begin{pmatrix} 0 & 1 & 0 \\ 1 & 0 & 1 \\ 0 & 0 & 1 \end{pmatrix} . \tag{1.45}$$

We may in fact allow entries greater than 1 in the matrix $\mathcal{G}$. This corresponds to having more than one link between two nodes. We do not consider such cases here. Graphs with the property that there is no more than one link between any two nodes are termed *simply-laced.*

The adjacency matrix associated with any graph $\mathcal{G}$ is symmetric iff the graph $\mathcal{G}$ is undirected. An adjacency matrix decomposes into block-diagonal form iff its graph can be separated into two or more disconnected subgraphs. If $\underset{\sim}{\psi}$ is an eigenvector of $\mathcal{G}$ with eigenvalue β, then

$$\begin{aligned} \left(\mathcal{G}\,\underset{\sim}{\psi}\right)_a &= \sum_{b \in \mathcal{G}} \mathcal{G}_{ab}\,\psi_b \\ &= \sum_{b:a} \psi_b \\ &= \beta\,\psi_a \ ; \end{aligned} \tag{1.46}$$

where the notation "b:a" indicates that the summation is over all nodes b adjacent to (i.e. connected to by) a w.r.t. the graph $\mathcal{G}$.

Consider for simplicity only undirected and simply-laced graphs $\mathcal{G}$ and consider representations of the Temperley-Lieb algebra (1.38) of the form (ansatz)

$$(e_j)_{\sigma\sigma'} = \sqrt{\frac{\psi_{\sigma_j}\psi_{\sigma'_j}}{\psi_{\sigma_{j-1}}\psi_{\sigma_{j+1}}}}\,\delta_{\sigma_{j-1}\sigma_{j+1}} \prod_{i\neq j} \delta_{\sigma_i\sigma'_i}\,, \tag{1.47}$$

where σ, σ' are two permissable adjacent configurations w.r.t. the graph $\mathcal{G}$ and the vector $\underset{\sim}{\psi}$ is yet to be determined. The last two of the relations (1.38) are satisfied by this form. The first relation is also satisfied provided $\underset{\sim}{\psi}$ is an eigenvector of $\mathcal{G}$ with eigenvalue β. In particular, close examination of the Boltzmann weight generated by (1.47) indicates that the path

$$\sigma_{j-1} \to \sigma_j \to \sigma_{j+1} \to \sigma'_j \to \sigma_{j-1} \tag{1.48}$$

and hence the entire lattice, satisfies the $\mathcal{G}$-restriction condition (1.15).

In the thermodynamic limit, any model defined by the relations (1.38) has the same partition function up to boundary effects as the Q-state Potts model with $Q^2 = \beta$. Such a model, therefore, exhibits a second-order phase transition and hence conformal symmetry along the self-dual line, only for $Q \in [0,4]$, i.e. $\beta \in [0,2]$. Furthermore, the Boltzmann weights defined by (1.47) ought to be strictly positive so that the conformal theory at criticality in the thermodynamic and continuum limits is unitary. Also, the graphs under consideration satisfy the conditions of the Perron-Frobenius theorem which states:

Theorem 1.1 (Perron-Frobenius) A finite real matrix with strictly non-negative entries has maximal eigenvalue strictly greater than zero, the corresponding eigenvector to which is the unique eigenvector with strictly positive components. □

Hence the two conditions identify $\underset{\sim}{\psi}$ as the maximal *Perron-Frobenius eigenvector* of those undirected, simply-laced graphs with maximal eigenvalue $\beta \in [0,2]$.

The classification of all such graphs arises elsewhere, e.g. in the problem of classifying the simply-laced Lie algebras. Those graphs with $\beta = 2$ are, with some additions, the Coxeter-Dynkin diagrams of the affine Lie algebras; see table 1.1. Excepting the graphs $\widehat{A}_{2n-1}/\mathbb{Z}_2$

and $\widehat{D}_{2n-1}/\mathbb{Z}_2$, we will refer to these diagrams as the *affine* and/or $\widehat{A}\widehat{D}\widehat{E}$ *graphs*. To find those graphs with $\beta \in (0,2)$, use is made of the Kronecker lemma:

Lemma 1.2 (Kronecker) The maximal eigenvalue of the adjacency graph $\mathcal{G}$ is a strictly increasing function of its matrix elements. Thus adding (removing) an oriented link to (from) $\mathcal{G}$ will increase (decrease) the highest eigenvalue. Therefore a graph always has a strictly higher largest eigenvalue than any of its proper subgraphs. □

This lemma implies that these graphs have:

(1) No internal loop, or otherwise $\widehat{A}_n$ would be a subgraph;

(2) Any node has at most three legs, otherwise $\widehat{D}_4$ would be a subgraph;

(3) There is at most one three-legged node, or else $\widehat{D}_n$ would be a subgraph;

(4) No graph with a fork may also have a node linked to itself, or $\widehat{D}_{2n-1}/\mathbb{Z}_2$ would be a subgraph; and

(5) No graph may have more than one node linked to itself, or $\widehat{A}_{2n-1}/\mathbb{Z}_2$ would be a subgraph.

Exploring all possible subgraphs, only those of table 1.2 satisfy these conditions. With the exception of the graph $A_{2n}/\mathbb{Z}_2$, these graphs are the graphs of the simply-laced simple Lie algebras. We will refer to all but the graph $A_{2n}/\mathbb{Z}_2$ as the *classical* and/or *ADE graphs*.

We exclude from consideration the models based upon the graphs $A_{2n}/\mathbb{Z}_2$, $\widehat{A}_{2n-1}/\mathbb{Z}_2$ and $\widehat{D}_{2n-1}/\mathbb{Z}_2$. These models possess nodes linked to themselves. Such graphs are not $\mathbb{Z}_2$-colourable so that the factorisation of the lattices depicted in figure 1.4 does not occur.

The Ising, 3-state Potts and 4-state Potts models are recovered as the models labelled by A_3, D_4 and $\widehat{D}_4$ respectively. The models labelled A_n in table 1.2 are identified as the *restricted solid-on-solid (RSOS)* models found earlier by Andrews *et al.* [1]. These models were shown to be part of the greater classification of tables 1.1 and 1.2 by Pasquier [43].

The graphs of tables 1.1 and 1.2 (excluding those graphs with self-linked nodes) all possess the useful property that their eigenvalues may be written in the form $\beta^{(\mu)} = 2\cos\frac{\mu\pi}{h}$; where the $\{\mu\} \equiv \mathrm{v}^*(\mathcal{G})$, called the *exponents*, are positive integers and h, also an integer,

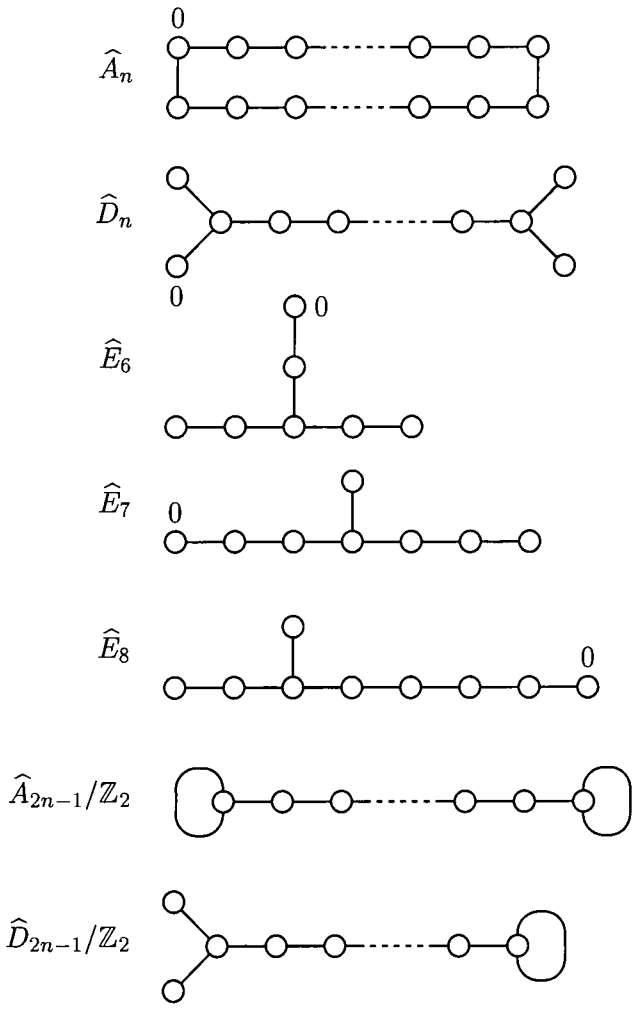

Table 1.1: The graphs having highest eigenvalue $\beta = 2$. Excepting the last two, these are recognised as the simply-laced affine Coxeter-Dynkin diagrams $\widehat{A}$, $\widehat{D}$ and $\widehat{E}$. The so-called 'affine node' of each such diagram is labelled 0. Removal of this node from the diagram "$\widehat{X}_n$" results in the corresponding classical Coxeter-Dynkin diagram "X_n" appearing in table 1.2. The diagrams $\widehat{A}_{2n-1}/\mathbb{Z}_2$ and $\widehat{D}_{2n-1}/\mathbb{Z}_2$ are not $\mathbb{Z}_2$-colourable.

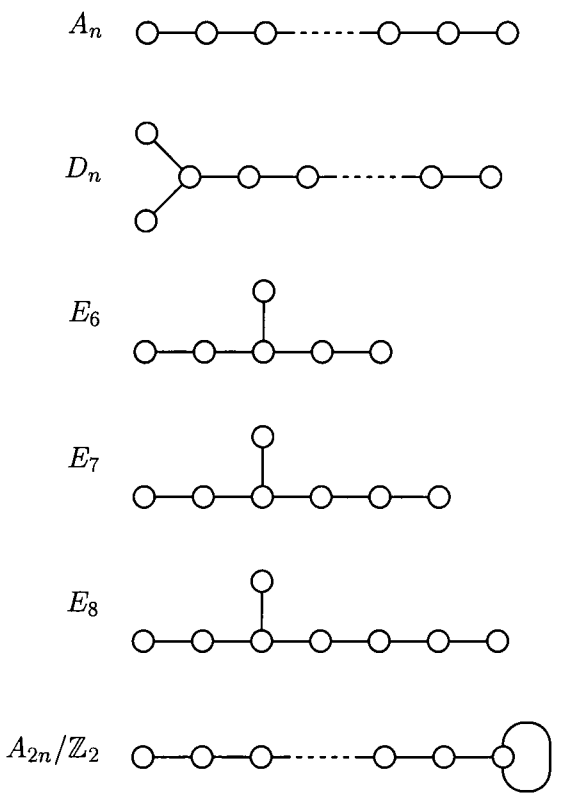

Table 1.2: The graphs with eigenvalue $\beta < 2$. Note that, excluding the final set of graphs $A_{2n}/\mathbb{Z}_2$, these are the (non-affine) classical simply-laced Coxeter-Dynkin ADE diagrams.

is the *Coxeter number* of the graph. We introduce the notation, whereby a general graph and/or its associated Lie algebra is denoted by $\mathcal{G}$. The eigenvectors and eigenvalues of such a graph are labelled by the exponents of the graph and denoted by $\underset{\sim}{\psi}^{(\mu)}$ and $\beta^{(\mu)}$ respectively. When referring specifically to the eigenvectors of an A_n or $\widehat{A}_n$ model we will often use the symbol $\underset{\sim}{\phi}^{(\mu)}$ instead. In all cases, we denote by $\underset{\sim}{\psi}$ (or $\underset{\sim}{\phi}$) and β, i.e. without superscripts, the Perron-Frobenius eigenvector and eigenvalue of a model. For the classical models, $\underset{\sim}{\psi} \equiv \underset{\sim}{\psi}^{(1)}$ and $\beta \equiv \beta^{(1)}$; and for the affine models, $\underset{\sim}{\psi} \equiv \underset{\sim}{\psi}^{(0)}$ and $\beta \equiv \beta^{(0)}$. Often it is useful to label a graph by its Coxeter number h (or affine Coxeter number if appropriate) rather than by the usual index n. In this case, we subscript the Coxeter number in square-parentheses on the graph, e.g. "$\mathcal{G}_{[h]}$" or "$\widehat{D}_{[6]} \equiv \widehat{D}_5$". The notation we adopt for labelling the nodes, the exponents for each of the affine models and the components of the corresponding eigenvectors in the $\widehat{A}_n$ and $\widehat{D}_n$ cases are given in appendix A.

Each of the graphs A_n, D_n, $E_{6,7,8}$, $\widehat{A}_n$, $\widehat{D}_n$ and $\widehat{E}_{6,7,8}$ defines a representation of the Temperley-Lieb algebra through equation (1.47) and therefore, at least for $\xi_v\,\xi_h = 1$, an integrable lattice model. We denote by $(\mathcal{G}; a, b)$ the integrable lattice model of figure 1.7, defined on the cylindrical lattice Γ (periodic in the time direction), based on the graph $\mathcal{G}$ with boundary conditions a and b on either end of the cylinder. We denote by $\mathcal{Z}_\Gamma^{(\mathcal{G};a,b)}$ the partition function of such a model. The face transfer matrices are defined [44] as in (1.42). Since the models undergo a second-order phase transition at the self-dual point $\xi_v\,\xi_h = 1$, their continuum limits are conformally invariant [15]. As the Boltzmann weights of the lattice models are required to be real and positive, the corresponding conformal theories are unitary. In the case of the classical graphs A_n, D_n and $E_{6,7,8}$, the conformal theories obtained in the thermodynamic limit provide representatives of the unitary minimal series [45] (and see [26]) with central charge

$$c = 1 - \frac{6}{h(h-1)}\,; \tag{1.49}$$

where h is the Coxeter number of the appropriate graph. Indeed the complete classification of two-dimensional conformal field theories, the *ADE-classification*, has been found by Cappelli *et al.* [9]. The complete set of minimal modular invariant partition functions on the torus fall into two series: one labelled by $(A_{[h]}, \mathcal{G}_{[h']})$ and the other by $(\mathcal{G}_{[h]}, A_{[h']})$; where $\mathcal{G}$ is a classical ADE graph, h and h' are the Coxeter numbers labelling the graphs

and $h' > h$. Unitary models correspond to the requirement $h' = h + 1$. The modular invariant partition functions defined by (1.47) precisely realise the $(A_{[h-1]}, \mathcal{G}_{[h]})$ series [45].

The affine graphs $\widehat{A}_n$, $\widehat{D}_n$ and $\widehat{E}_{6,7,8}$ provide unitary $c = 1$ models (see references [45] and [29]. This will also be demonstrated explicitly in the following chapter).

1.1.7 Intertwiners

The partition function of the model $(\mathcal{G}; a, b)$ may be written as

$$\mathcal{Z}_\Gamma^{(\mathcal{G};a,b)} = \sum_{k=0}^{M} \sum_{\substack{i_1,\dots,i_k=1 \\ i_1<\cdots<i_k}}^{L} g_{i_1,\dots,i_k}(\beta) \operatorname*{Tr}_{(a,b)} (e_{i_1} \cdots e_{i_k}) \ . \tag{1.50}$$

This expression is obtained by writing $\mathcal{Z}_\Gamma^{(\mathcal{G};a,b)}$ as a trace over the face transfer matrices which in turn may be expressed in a representation- and graph-independent fashion as sums over the identity $\mathbb{I}$ and Temperley-Lieb operators $\{ e_j \mid 1 \leq j \leq M \}$. The properties (1.38) together with the cyclicity of the trace allow the partition function to be reduced to this form [51]. Moreover, the numbers $\{g_{i_1,\dots,i_k}\}$ are functions only of the parameter β appearing in (1.38); in particular, these numbers are positive and depend upon the graph defining the model only through the Perron-Frobenius eigenvalue β. Thus to calculate the partition function $\mathcal{Z}_\Gamma^{(\mathcal{G};a,b)}$ it will be necessary to calculate the trace over products of Temperley-Lieb operators $\{e_j\}$.

Denote by $\mathrm{Tr}_{(a,b)}$ the trace subject to the boundary conditions (a, b). It is useful to introduce the *Markov trace* defined for any operator Y on the Hilbert space of a model based on the graph $\mathcal{G}$ by

$$\begin{aligned} \mathrm{Tr}_{\sigma_1}^{(\nu)} \mathsf{Y} &\stackrel{\text{def}}{=} \sum_{\sigma_L} \frac{\psi_{\sigma_L}^{(\nu)}}{\psi_{\sigma_1}^{(\nu)}} \operatorname*{Tr}_{(\sigma_1,\sigma_L)} \mathsf{Y} \\ &\equiv \sum_{\sigma_2,\dots,\sigma_L} \frac{\psi_{\sigma_L}^{(\nu)}}{\psi_{\sigma_1}^{(\nu)}} \langle \sigma_1, \dots, \sigma_L | \, \mathsf{Y} \, | \sigma_1, \dots, \sigma_L \rangle \ ; \end{aligned} \tag{1.51}$$

where the $\left\{ \underset{\sim}{\psi}^{(\mu)} \mid \mu \in \mathrm{v}^*(\mathcal{G}) \right\}$ are the eigenvectors of the graph $\mathcal{G}$ labelled by the exponents

of $\mathcal{G}$. The *modified partition function* is defined [51] in terms of this trace by

$$\begin{aligned} \mathcal{Z}_{\Gamma}^{[\mathcal{G};\nu]} &\stackrel{\text{def}}{=} \mathrm{Tr}_a^{(\nu)}\, T^M \\ &\equiv \sum_{b\in\mathcal{G}} \frac{\psi_b^{(\nu)}}{\psi_a^{(\nu)}}\, \mathcal{Z}_{\Gamma}^{(\mathcal{G};a,b)} \ . \end{aligned} \tag{1.52}$$

We remark that this partition function is independent of a as will be seen in lemma 1.3.

Write

$(\mathbb{I})_{\sigma\sigma'} =$ 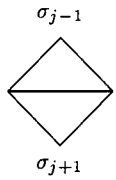

, $(e_j)_{\sigma\sigma'} =$ 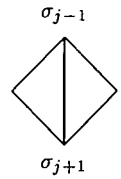

; (1.53)

then it follows from (1.47) that

$\sum_{d\in\mathcal{G}}$ 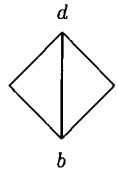

$\psi_d^{(\mu)} = \dfrac{\psi_a\, \psi_b^{(\mu)}}{\psi_b}$ (1.54)

and

$\sum_{c,d\in\mathcal{G}}$ 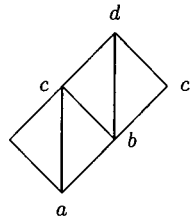

$\psi_d^{(\mu)} = \psi_b^{(\mu)}$. (1.55)

The eigenvector property of $\underset{\sim}{\psi}^{(\mu)}$ yields

$\sum_{d\in\mathcal{G}}$ 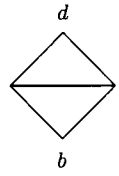

$\psi_d^{(\mu)} = \beta^{(\mu)}\, \psi_a^{(\mu)}$, (1.56)

as the summation, due to the $\mathcal{G}$-restriction condition, is over all d adjacent to a.

The following is a result of Sochen [51], slightly adapted for our purposes later on:

Lemma 1.3 (Sochen [51]) The modified partition function defined by (1.52) is graph independent in that

$$\mathcal{Z}_\Gamma^{[\mathcal{G};\nu]} = f(\beta, \beta^{(\nu)}) \; ; \tag{1.57}$$

i.e. the modified trace depends on the graph $\mathcal{G}$ only through the eigenvalues β and $\beta^{(\mu)}$. In particular, the function f is completely independent of the chosen representation of the Temperley-Lieb algebra. It depends only upon the details of the lattice Λ. Thus, for two graphs sharing the exponent ν and having the same Perron-Frobenius eigenvalue β, the modified partition functions $\{\mathcal{Z}_\Gamma^{[\mathcal{G};\nu]}\}_\mathcal{G}$ will be identical. □

Proof Combining (1.50) and (1.52),

$$\mathcal{Z}_\Gamma^{[\mathcal{G};\nu]} = \sum_{k=0}^{M} \sum_{\substack{i_1,\dots,i_k=1 \\ i_1<\cdots<i_k}}^{L} g_{i_1,\dots,i_k}(\beta)\, \mathrm{Tr}_a^{(\nu)}\left(e_{i_1}\cdots e_{i_k}\right) \; . \tag{1.58}$$

Therefore examining the traces on the RHS (it is useful to bear in mind the notation of (1.53) in the calculations that follow): For $k = 0$,

$$\mathrm{Tr}_a^{(\nu)}\left(\mathbb{1}\right) = \left(\beta^{(\nu)}\right)^{L-1} \; . \tag{1.59}$$

This is obtained by repeated application of (1.56). The RHS is a function of β and $\beta^{(\mu)}$ only and has the same functional form for all $\mathcal{G}$. It is independent of the boundary condition a. For $k = 1$, using (1.54) and (1.56),

$$\mathrm{Tr}_a^{(\nu)}\left(e_{i_1}\right) = \beta \left(\beta^{(\nu)}\right)^{L-2} \; . \tag{1.60}$$

The proof proceeds by induction on the number of operators in the trace. We use the symbol f to denote some unknown/general representation-independent and graph-independent function (not necessarily the same each time the symbol is used however). Suppose

$$\mathrm{Tr}_a^{(\nu)}\left(e_{i_1}\cdots e_{i_k}\right) = f(\beta, \beta^{(\nu)}) \; , \tag{1.61}$$

then for $p > 1$,

$$\begin{aligned} \mathrm{Tr}_a^{(\nu)}\left(e_{i_1}\cdots e_{i_k}\, e_{i_k+p}\right) &= \frac{\beta}{\beta^{(\nu)}}\,\mathrm{Tr}_a^{(\nu)}\left(e_{i_1}\cdots e_{i_k}\right) \\ &= f(\beta,\beta^{(\nu)})\;; \end{aligned} \tag{1.62}$$

and for $p = 1$,

$$\begin{aligned} \mathrm{Tr}_a^{(\nu)}\left(e_{i_1}\cdots e_{i_k}\, e_{i_k+p}\right) &= \beta^{(\nu)}\,\mathrm{Tr}_a^{(\nu)}\left(e_{i_1}\cdots e_{i_k}\right) \\ &= f(\beta,\beta^{(\nu)})\;, \end{aligned} \tag{1.63}$$

using (1.55) and (1.56).

The conjecture (1.57) follows by induction. ■

An immediate consequence of lemma 1.3 is that for any classical ADE graph $\mathcal{G}_{[h]}$ with the same Coxeter number h as the graph $A_{[h]}$, that

$$\mathcal{Z}_\Gamma^{[\mathcal{G}_{[h]};\nu]} = \mathcal{Z}_\Gamma^{[A_{[h]};\nu]}\;. \tag{1.64}$$

Thus, provided the $\left\{\, \underset{\sim}{\psi}^{(\mu)} \;\middle|\; \mu \in \mathrm{v}^*(\mathcal{G}) \,\right\}$ are chosen to be orthonormal,

$$\mathcal{Z}_\Gamma^{(\mathcal{G}_{[h]};a,b)} = \sum_{\lambda\in A_{[h]}} \left\{ \sum_{\mu\in \mathrm{v}^*(\mathcal{G})} \frac{\phi_\lambda^{(\mu)}}{\phi_\alpha^{(\mu)}}\,\psi_a^{(\mu)*}\,\psi_b^{(\mu)} \right\} \mathcal{Z}_\Gamma^{(A_{[h]};\alpha,\lambda)}\;; \tag{1.65}$$

where α may be chosen arbitrarily on the graph $A_{[h]}$. The object relating the two partition functions is known as an *intertwiner*; i.e.

$$\mathcal{Z}_\Gamma^{(\mathcal{G}_{[h]};a,b)} = \sum_{\lambda\in A_{[h]}} \left(V_{(\alpha)}^\lambda\right)_{ab} \mathcal{Z}_\Gamma^{(A_{[h]};\alpha,\lambda)}\;, \tag{1.66}$$

with the intertwiner,

$$\left(V_{(\alpha)}^\lambda\right)_{ab} \equiv \sum_{\mu\in \mathrm{v}^*(\mathcal{G})} \frac{\phi_\lambda^{(\mu)}}{\phi_\alpha^{(\mu)}}\,\psi_a^{(\mu)*}\,\psi_b^{(\mu)}\;. \tag{1.67}$$

Intertwiners provide mappings between the Hilbert spaces of different models. In par-

ticular, fixing α and a in (1.67), they provide the rectangular (i.e. non-square) matrices $(V)_b^\lambda \equiv \left(V_{(\alpha)a}\right)_b^\lambda$ that relate the adjacency matrices,

$$A_{[h]}\, V = V\, G_{[h]}\ . \tag{1.68}$$

1.1.8 Further Graph Lattice Models

The set of models of tables 1.1 and 1.2 is obtained by restricting the set of graphs considered to be simply-laced and undirected. Also, substituting the form (1.42) into the Yang-Baxter equation (1.34) results in the conditions:

$$\begin{aligned} &e_i^2 = \beta\, e_i\ , \\ &e_i\, e_{i+1}\, e_i - e_i = e_{i+1}\, e_i\, e_{i+1} - e_{i+1}\ , \\ &e_i\, e_j = e_j\, e_i \quad \text{for } |i-j| \geq 2\ , \end{aligned} \tag{1.69}$$

as the sufficient conditions for integrability. (The trace property (1.39) is also satisfied.) The algebra of the $\{e_i\}$ is therefore more generally a *Hecke algebra* of which the Temperley-Lieb algebras form a subclass. Furthermore, the form (1.47) is nothing more than an ansatz for providing a representation of the Temperley-Lieb algebra. Thus we might expect to find more integrable models once these restrictions have been lifted.

Di Francesco and Zuber [23] have defined a series of representations of subalgebras of the Hecke algebra. They define a SU(N)*-vertex model* as one whose transfer matrix commutes with the quantum group SU$(N)_q$ for some q. This quantum group restriction of the transfer matrix requires that the Boltzmann weights are to be found in the commutant of the quantum group SU$(N)_q$. This commutant is a quotient of the Hecke algebra. In this classification, the models of Pasquier are synonymous with "SU(2)-height models". The quotient of the Hecke algebra from which their Boltzmann weights are built is none other than the Temperley-Lieb algebra (1.38).

Roche [47] and independently also Warnaar *et al.* [55] construct integrable lattice models based on an alternative form to (1.47) for the Boltzmann weights, also based upon the Perron-Frobenius eigenvector, $\underset{\sim}{\psi}$, of ADE graphs. These *dilute ADE-lattice models* can

be shown [8] to provide realisations of both the $(A_{[h-1]}, \mathcal{G}_{[h]})$ and $(\mathcal{G}_{[h-1]}, A_{[h]})$ series of unitary minimal models.

1.2 Conformal Field Theory

Conformally invariant quantum field theories describe the critical behaviour of systems at second order phase transitions [5], [15]. In this section we review the 2-dimensional theory, particularly its application to the case when the central charge $c = 1$ and the geometry of the system under consideration is cylindrical. This review follows [5], [7], [10], [11], [13], and [16] and also uses some elements of the review article [30].

1.2.1 The Conformal Group

Consider the space $\mathbb{R}^d$ with flat metric $g_{\mu\nu} = \eta_{\mu\nu}$ of signature (p, q) and line element $\mathrm{d}s^2 = g_{\mu\nu}\,\mathrm{d}x^\mu\,\mathrm{d}x^\nu$. Under the general change of coordinates $x \to x'$:

$$g_{\mu\nu}(x) \mapsto g'_{\mu\nu}(x') = \frac{\partial x^\alpha}{\partial x'^\mu}\,\frac{\partial x^\beta}{\partial x'^\nu}\,g_{\alpha\beta}(x)\ . \tag{1.70}$$

The *conformal group* is the subgroup of coordinate transformations that leaves the metric invariant up to a local scale change,

$$g_{\mu\nu}(x) \mapsto g'_{\mu\nu}(x') = \Lambda(x)\,g_{\mu\nu}(x)\ . \tag{1.71}$$

The infinitesimal generators of the conformal group are determined by considering the infinitesimal coordinate transformations of the form $x^\mu \to x'^\mu = x^\mu + \varepsilon^\mu$ so that

$$\mathrm{d}s^2 \to \mathrm{d}s^2 + (\partial_\mu\varepsilon_\nu + \partial_\nu\varepsilon_\mu)\,\mathrm{d}x^\mu\,\mathrm{d}x^\nu\ . \tag{1.72}$$

For (1.71) to be satisfied, $\partial_\mu\varepsilon_\nu + \partial_\nu\varepsilon_\mu$ must be proportional to $\eta_{\mu\nu}$. Tracing both sides of this proportionality relation yields the *conformal Killing equation*:

$$\partial_\mu\varepsilon_\nu + \partial_\nu\varepsilon_\mu = \frac{2}{d}\,(\partial\cdot\varepsilon)\,\eta_{\mu\nu}\ . \tag{1.73}$$

For $d > 2$ the general solution is

$$\varepsilon^\mu = a^\mu + \omega^\mu_\nu\,x^\nu + b^{-1}\,x^\mu + (\lambda^\mu\,x^2 - 2\,x^\mu\lambda\cdot x)\ ; \tag{1.74}$$

the parts on the RHS corresponding in turn to translations, rotations, dilatations and the so-called special conformal transformations. The conformal group for $d > 2$ therefore is finite dimensional.

In contrast, for $d = 2$ and $g_{\mu\nu} = \delta_{\mu\nu}$, (1.73) reduces to the Cauchy-Riemann equations:

$$\partial_1 \varepsilon_1 = \partial_2 \varepsilon_2 \,, \qquad \partial_1 \varepsilon_2 = -\partial_2 \varepsilon_1 \,. \tag{1.75}$$

It is now natural to write $\varepsilon(z) = \varepsilon^1 + i\varepsilon^2$ and $\overline{\varepsilon}(\overline{z}) = \varepsilon_1 - i\varepsilon^2$ in the complex coordinates $z = x^1 + ix^2$ and $\overline{z} = x^1 - ix^2$; with $x^1, x^2, \varepsilon^1, \varepsilon^2 \in \mathbb{C}$. z and $\overline{z}$ are taken to be independent quantities (not complex conjugates) in calculations, with the reality condition $\overline{z} \equiv z^*$ imposed afterwards. (We adopt the notation z^* to denote the complex conjugate of z.) The group of conformal transformations in $d = 2$ is thus isomorphic to the infinite-dimensional group of arbitrary analytic coordinate transformations:

$$z \to f(z) \,, \qquad \overline{z} \to \overline{f}(\overline{z}) \,. \tag{1.76}$$

We will use the convention whereby functions of the coordinate z (i.e. purely holomorphic functions) are denoted by unbarred quantities and functions of $\overline{z}$ (i.e. antiholomorphic functions) by barred quantities and also write $\partial \equiv \partial_z \equiv \frac{\partial}{\partial z}$ and $\overline{\partial} \equiv \partial_{\overline{z}} \equiv \frac{\partial}{\partial \overline{z}}$.

Infinitesimally, the transformations (1.76) are $z \to z + \varepsilon(z)$ and $\overline{z} \to \overline{z} + \overline{\varepsilon}(\overline{z})$. Written as Laurent series, these become:

$$\varepsilon(z) = -\sum_{n=-\infty}^{\infty} \varepsilon_n \, z^{n+1} \,, \qquad \overline{\varepsilon}(\overline{z}) = -\sum_{n=-\infty}^{\infty} \overline{\varepsilon}_n \, \overline{z}^{n+1} \,. \tag{1.77}$$

So that the Lie algebra of the conformal group is generated by:

$$l_n = -z^{n+1}\,\partial \,, \qquad \overline{l}_n = -\overline{z}^{n+1}\,\overline{\partial} \,; \qquad n \in \mathbb{Z} \,. \tag{1.78}$$

These are the generators of the *Witt algebra*. This loop algebra has commutation relations:

$$\begin{aligned} [l_n\,,\,l_m] &= (n-m)\,l_{m+n}\,, \\ [\bar{l}_n\,,\,\bar{l}_m] &= (n-m)\,\bar{l}_{m+n}\,, \\ [l_n\,,\,\bar{l}_m] &= 0\,. \end{aligned} \tag{1.79}$$

This is the *local conformal algebra*. The last of these commutators indicates that this algebra is the direct sum of two subalgebras, one generated by the $\{l_n\}$ and the other by the $\{\bar{l}_n\}$. Indeed, it is clear from (1.76), that the conformal group in $d = 2$ is the direct product of two identical subgroups. The separate algebras (groups) are referred to as the holomorphic and antiholomorphic algebras (groups) respectively. As they are isomorphic, we will generally choose to neglect to mention the antiholomorphic algebra (group); similar results for the holomorphic algebra (group) apply equally to the antiholomorphic case.

Clearly l_n is regular at $z = 0$ for all $n \geq -1$ and is singular for $n \leq -2$. Performing the coordinate transformation $z = 1/w$ one finds $l_n \mapsto -w^{-n+1}\partial_w$ which is regular at $w = 0$ (i.e. $z = \infty$) for $n \leq 1$ and singular for $n \geq 2$. Therefore only the subalgebra of transformations generated by $\{l_{-1}, l_0, l_1\} \cup \{\bar{l}_{-1}, \bar{l}_0, \bar{l}_1\}$ is well defined everywhere on the Riemann sphere ($\mathbb{C}^\infty \equiv \mathbb{C} \cup \{\infty\}$). The finite form of these transformations are maps $\mathbb{C}^\infty \to \mathbb{C}^\infty$ which are analytic everywhere and possess global inverses. They are called the *global-* or *projective-conformal transformations* and are isomorphic to the group $\mathsf{SL}(2,\mathbb{C})/\mathbb{Z}_2$ of Möbius transformations on the Riemann sphere. In general the *local conformal transformations* generated by the entire local algebra (i.e. the conformal group) are typically meromorphic and do not possess global inverses.

The generators l_{-1} and $\bar{l}_{-1}$ may be identified as the generators of translations, $l_0 + \bar{l}_0$ as the generator of dilatations, $i(l_0 - \bar{l}_0)$ as the generator of rotations, and l_1 and $\bar{l}_1$ as the generators of the special conformal transformations. The Cartan subalgebra is generated by $\{l_0, \bar{l}_0\}$. The physical operators, or fields, will be eigenstates of these operators with eigenvalues h and $\bar{h}$ respectively, called the *conformal weights*. As $l_0 + \bar{l}_0$ and $i(l_0 - \bar{l}_0)$ generate dilatations and rotations respectively, the *scaling dimension* x and *spin* s of an

operator are given by:

$$x = h + \overline{h}\,, \qquad s = h - \overline{h}\,. \tag{1.80}$$

The transformation of the line element under the conformal group in complex coordinates is

$$\mathrm{d}s^2 \equiv \mathrm{d}z\,\mathrm{d}\overline{z} \mapsto \partial f\,\overline{\partial f}\,\mathrm{d}z\,\mathrm{d}\overline{z} = \partial f\,\overline{\partial f}\,\mathrm{d}s^2\,. \tag{1.81}$$

This transformation may be generalised to

$$\Phi(z,\overline{z}) \mapsto (\partial f)^h\,(\overline{\partial f})^{\overline{h}}\,\Phi(f(z),\overline{f}(\overline{z}))\;; \tag{1.82}$$

where h and $\overline{h}$ are the conformal weights of the operator $\Phi(z,\overline{z})$. If an operator $\Phi(z,\overline{z})$ transforms in this way under the entire conformal group then Φ is said to be a *primary operator.* If it behaves in this fashion only under the global group, then it is a *quasiprimary operator.* A conformal field theory typically consists of an infinite set of local operators $\{\phi(z,\overline{z})\}$, which includes the identity operator, with the property that if a field is one such operator then so will be all its derivatives. The sets of primary and quasiprimary operators are special subsets of these operators; the remaining operators, known as *secondary operators*, being linear combinations of the quasiprimary operators and their derivatives. In general, the conformal group of transformations can alter the geometry of the system and may therefore change the physical ground state of the theory. However global transformations do not change the geometry so that the vacuum is invariant under the global group.

From (1.82), under the local (global) transformation $z \to z+\varepsilon(z)$, $\overline{z} \to \overline{z}+\overline{\varepsilon}(\overline{z})$, a primary (quasiprimary) operator $\Phi(z,\overline{z})$ will transform as

$$\delta_{\varepsilon,\overline{\varepsilon}}\Phi(z,\overline{z}) = \big(\,(h\,\partial\varepsilon + \varepsilon\,\partial) + (\overline{h}\,\overline{\partial}\overline{\varepsilon} + \overline{\varepsilon}\,\overline{\partial})\,\big)\,\Phi(z,\overline{z})\,. \tag{1.83}$$

This places severe constraints on the 2- and 3-point correlation functions of any such operators.

1.2.2 Quantisation

Consider flat Euclidean space with space and time coordinates y^1 and y^0 together with the complex coordinates $\zeta = y^0 + iy^1$ and $\overline{\zeta} = y^0 - iy^1$. To eliminate possible infrared divergences, the spatial coordinate is compactified so that $y^1 \equiv y^1 + 2\pi$. This defines an infinite cylinder in the y^0, y^1-coordinates. Now consider the conformal map $\zeta \to z = \exp\zeta = \exp(y^0 + iy^1)$ that maps the cylinder to the complex plane coordinatised by z. Infinite past and future on the cylinder, $y^0 = \mp\infty$, are mapped to the points $z = 0, \infty$ on the plane. Equal-time surfaces, $y^0 =$ constant, become circles of constant radius on the z-plane and time-reversal corresponds to $z \to 1/z^*$. Dilatations in the z-plane, $z \to e^a z$, are the time-translations $y^0 \to y^0 + a$ on the cylinder. So the dilatation generator on the conformal plane may be regarded as the Hamiltonian of the system and the Hilbert space is built up on surfaces of constant radius. This procedure for defining a quantum theory on the plane is known as *radial quantisation*.

Under the general coordinate transformation $x^\mu \to x^\mu + \varepsilon^\mu(x)$ the Hamiltonian of a theory will transform as

$$\delta_\varepsilon H = -\frac{1}{2\pi}\int \mathrm{d}^2x\, \partial^\mu \varepsilon^\nu\, \Theta_{\mu\nu}\ ; \tag{1.84}$$

which defines the *energy-momentum* or *stress-energy tensor* $\Theta_{\mu\nu}$. For a conformally invariant theory, invariance under infinitesimal rotations ($\varepsilon^\mu = \omega^\mu_\nu\, x^\nu$) implies that $\Theta_{\mu\nu}$ is symmetric and global scale invariance ($\varepsilon^\mu = \lambda\, x^\mu$) implies $\mathrm{Tr}\,\Theta = 0$.

In terms of correlation functions, (1.84) is equivalent to [5]:

$$\sum_{k=1}^{n}\langle \Phi_1(x_1)\cdots\delta_\varepsilon\Phi_k(x_k)\cdots\Phi_n(x_n)\rangle = -\frac{1}{2\pi}\int \mathrm{d}^2x\, \partial^\mu\varepsilon^\nu\, \langle \Theta_{\mu\nu}(x)\, \Phi_1(x_1)\cdots\Phi_n(x_n)\rangle\ . \tag{1.85}$$

Suppose the variation $\varepsilon^\mu(x)$ is conformal within some domain D containing the points $x_1, \ldots, x_n$ and non-conformal but differentiable on the complement D', the boundary between these domains being the contour C. Assume also that $\varepsilon^\mu(x)$ vanishes as $x^\nu \to \infty$.

Then integrating by parts the RHS of (1.85) yields

$$\frac{1}{2\pi}\int_{D'} \mathrm{d}^2x\, \varepsilon^\nu(x)\,\langle \partial^\mu \Theta_{\mu\nu}(x)\,\Phi_1\cdots\Phi_n\rangle - \frac{1}{2\pi}\oint_C \mathrm{d}\mathcal{S}\, n^\mu\, \varepsilon^\nu(x)\,\langle \Theta_{\mu\nu}(x)\,\Phi_1\cdots\Phi_n\rangle\ ; \quad (1.86)$$

where n^μ is orthonormal to the contour C. The arbitrariness of ε^μ in D' implies that the first term must vanish for any ε^μ. This yields the conservation law

$$\partial^\mu \Theta_{\mu\nu} = 0\ . \quad (1.87)$$

As Θ is traceless and satisfies (1.87), there are only two non-vanishing components which may be written as:

$$\begin{aligned} \Theta \equiv \Theta(z) \equiv \Theta_{zz} &= \Theta_{00} - \Theta_{11} + 2\,i\,\Theta_{01}\ , \\ \overline{\Theta} \equiv \overline{\Theta}(\overline{z}) \equiv \Theta_{\overline{z}\overline{z}} &= \Theta_{00} - \Theta_{11} - 2\,i\,\Theta_{01}\ ; \end{aligned} \quad (1.88)$$

i.e. with solely holomorphic and antiholomorphic dependence respectively, and which satisfy $\partial\overline{\Theta} = \overline{\partial}\Theta = 0$. Also from (1.86), we may write the generator of the variations in (1.85) as

$$\begin{aligned} Q &= -\frac{1}{2\pi}\oint_C \mathrm{d}\mathcal{S}\, n^\mu\, \varepsilon^\nu(x)\,\Theta_{\mu\nu}(x) \\ &= \frac{1}{2\pi i}\oint_C \left(\mathrm{d}z\,\varepsilon(z)\,\Theta(z) - \mathrm{d}\overline{z}\,\overline{\varepsilon}(\overline{z})\,\overline{\Theta}(\overline{z})\right)\ . \end{aligned} \quad (1.89)$$

Thus the variation of any field $\phi(w,\overline{w})$ is given by the equal-time commutator

$$\delta_{\varepsilon,\overline{\varepsilon}}\,\phi(w,\overline{w}) = \frac{1}{2\pi i}\oint \Big([\mathrm{d}z\,\Theta(z)\,\varepsilon(z)\,,\ \phi(w,\overline{w})] - [\mathrm{d}\overline{z}\,\overline{\Theta}(\overline{z})\,\overline{\varepsilon}(\overline{z})\,,\ \phi(w,\overline{w})] \Big)\ . \quad (1.90)$$

Products of operators $A(z)\,B(w)$ in Euclidean space radial quantisation are only defined for $|z| > |w|$; so the radial ordering operation R is defined as

$$R(\ A(z)\,B(w)\ ) = \begin{cases} A(z)\,B(w) & ;\ \text{if } |z| > |w|. \\ B(w)\,A(z) & ;\ \text{if } |z| < |w|. \end{cases}\ . \quad (1.91)$$

The holomorphic part of (1.90) may therefore be written

$$\begin{aligned}\delta_\varepsilon \phi(w) &= \frac{1}{2\pi i}\left(\oint_{|z|>|w|} - \oint_{|z|<|w|}\right) \mathrm{d}z\, \varepsilon(z)\, R(\,\Theta(z)\,\phi(w)\,) \\ &= \frac{1}{2\pi i}\oint_{C_w} \mathrm{d}z\, \varepsilon(z)\, R(\,\Theta(z)\,\phi(w)\,)\;;\end{aligned} \tag{1.92}$$

with a similar result (with a minus sign from (1.89)) for the antiholomorphic variation $\overline{\varepsilon}(\overline{z})$. C_w here, denotes an infinitesimal contour about the point w. Comparison with (1.83) for a primary (or quasiprimary) field $\Phi(w,\overline{w})$ implies that

$$R(\,\Theta(z)\,\Phi(w,\overline{w})\,) = \left(\frac{h}{(z-w)^2} + \frac{1}{z-w}\partial_w\right)\Phi(w,\overline{w}) + \text{analytic terms}\,, \tag{1.93}$$

This is another way of stating that $\Phi(w,\overline{w})$ is a conformal field with conformal weight h.

We shall adopt the convention whereby the radial-ordering operator is dropped and all operator-products are understood to be radially-ordered.

1.2.3 The Virasoro Algebra

The generators of the (quantised) algebra of conformal transformations may be found by considering the generator of a variation $\varepsilon_3(z)$ defined by

$$Q_{\varepsilon_3} = [\,Q_{\varepsilon_2}\,,\, Q_{\varepsilon_1}]\,. \tag{1.94}$$

From (1.89), this becomes

$$\begin{aligned}Q_{\varepsilon_3} = \frac{1}{(2\pi i)^2}\Bigg\{&\oint_{C_2} \mathrm{d}z_2\, \varepsilon_2(z_2)\,\Theta(z_2) \oint_{C_1} \mathrm{d}z_1\, \varepsilon_1(z_1)\,\Theta(z_1) \\ &- \oint_{C_1} \mathrm{d}z_1\, \varepsilon_1(z_1)\,\Theta(z_1) \oint_{C_2} \mathrm{d}z_2\, \varepsilon_2(z_2)\,\Theta(z_2)\Bigg\}\,.\end{aligned} \tag{1.95}$$

Note that the operator products above are radially-ordered so that in the first term on the RHS, C_2 encloses C_1 and in the second C_1 encloses C_2. Fixing z_1 and deforming the

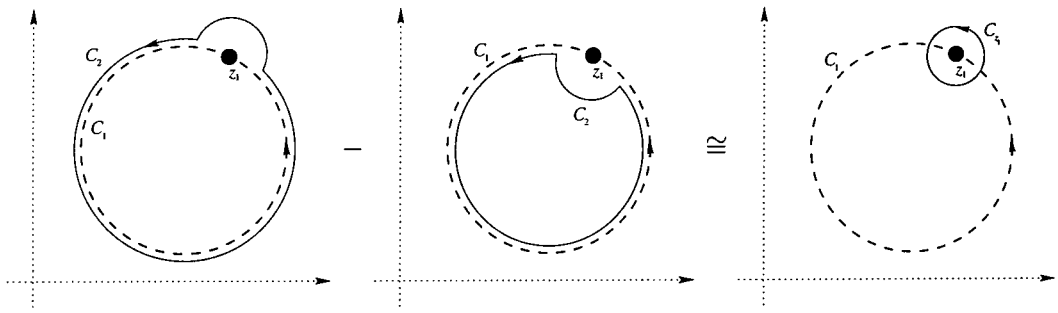

Figure 1.8: Contour choices in the evaluation of the contour integrals of equation (1.95)

inner and outer contours as in figure 1.8, Q_{ε_3} becomes

$$Q_{\varepsilon_3} = \frac{1}{(2\pi i)^2} \oint_{C_1} \mathrm{d}z_1 \, \varepsilon_1(z_1)\, \Theta(z_1) \oint_{C_{z_1}} \mathrm{d}z_2 \, \varepsilon_2(z_2)\, \Theta(z_2) \; ; \tag{1.96}$$

where C_{z_1} is an infinitesimal contour enclosing z_1. From (1.83) and (1.90)

$$\delta_{\varepsilon_3} = h\, \partial\varepsilon_3 + \varepsilon_3\, \partial = \delta_{\varepsilon_2}\, \delta_{\varepsilon_1} - \delta_{\varepsilon_1}\, \delta_{\varepsilon_2} \; , \tag{1.97}$$

so that

$$\varepsilon_3 = \varepsilon_1\, \partial\varepsilon_2 - \varepsilon_2\, \partial\varepsilon_1 \; . \tag{1.98}$$

Thus

$$\begin{aligned} Q_{\varepsilon_3} &= \frac{1}{2\pi i} \oint_{C_3} \mathrm{d}z_1 \, \varepsilon_3(z_1)\, \Theta(z_1) \\ &= \frac{1}{2\pi i} \oint_{C_3} \mathrm{d}z_1 \left\{ \varepsilon_1(z_1)\, \partial\varepsilon_2(z_1) - \varepsilon_2(z_1)\, \partial\varepsilon_2(z_1) \right\} \Theta(z_1) \; . \end{aligned} \tag{1.99}$$

Integrating by parts and applying Cauchy's theorem,

$$Q_{\varepsilon_3} = \frac{1}{(2\pi i)^2} \oint_{C_3} \mathrm{d}z_1 \, \varepsilon_1(z_1) \oint_{C_{z_1}} \mathrm{d}z_2 \, \varepsilon_2(z_2) \left\{ \frac{2\,\Theta(z_1)}{(z_2 - z_1)^2} + \frac{\partial\Theta(z_1)}{z_2 - z_1} \right\} \; . \tag{1.100}$$

Choosing $C_3 = C_1$, the product $\Theta(z_2)\,\Theta(z_1)$ is determined by comparison with (1.96). By dimensional analysis, the most general form this product could have is

$$\Theta(z_2)\,\Theta(z_1) = \frac{A(z_1)}{(z_2-z_1)^4} + \frac{B(z_1)}{(z_2-z_1)^3} + \frac{C(z_1)}{(z_2-z_1)^2} + \frac{D(z_1)}{z_2-z_1} + \text{analytic terms}\,. \quad (1.101)$$

A must be constant, as from (1.93), Θ has dimension -2 (in powers of length units). Choose this constant to be $c/2$. For B to appear, it must have dimension -1, so that $B(z_1) \sim (z_1+k)^{-1}$ which may be absorbed into the A-term. Therefore: $A(z_1) = c/2$, $B(z_1) = 0$, $C(z_1) = 2\,\Theta(z_1)$ and $D(z_1) = \partial_{z_1}\Theta(z_1)$, so that

$$\Theta(z)\,\Theta(w) = \frac{c/2}{(z-w)^4} + \frac{2\,\Theta(z)}{(z-w)^2} + \frac{\partial\Theta(z)}{z-w} + \text{analytic terms}\,. \quad (1.102)$$

The parameter c is known as the *central charge*; it describes a set of particular realisations of conformal symmetry. A similar expression to (1.102) holds for the antiholomorphic terms, defining the analogous parameter $\bar{c}$. Similarly also, $\Theta(z)\,\overline{\Theta}(\overline{w}) = 0$.

In terms of Laurent series:

$$\Theta(z) = \sum_{n=-\infty}^{\infty} L_n\, z^{-n-2}\,, \qquad \overline{\Theta}(\overline{z}) = -\sum_{n=-\infty} \overline{L}_n\, \overline{z}^{-n-2}\,; \quad (1.103)$$

with the modes $\{L_n\}$ and $\{\overline{L}_n\}$ satisfying:

$$L_n = \frac{1}{2\pi i}\oint_C \mathrm{d}z\, z^{n+1}\,\Theta(z)\,, \qquad \overline{L}_n = -\frac{1}{2\pi i}\oint_C \mathrm{d}\overline{z}\, \overline{z}^{n+1}\,\overline{\Theta}(\overline{z})\,. \quad (1.104)$$

In each case, the contour C encloses the argument of the field upon which the modes act. The algebra of the modes is the direct sum of two *Virasoro algebras*:

$$\begin{aligned}
[L_m\,,\,L_n] &= (m-n)\,L_{m+n} + \frac{c}{12}\,(m^3-m)\,\delta_{m+n,0}\,,\\
[\overline{L}_m\,,\,\overline{L}_n] &= (m-n)\,\overline{L}_{m+n} + \frac{\bar{c}}{12}\,(m^3-m)\,\delta_{m+n,0}\,, \qquad (1.105)\\
[L_m\,,\,\overline{L}_n] &= 0\,.
\end{aligned}$$

This is clearly the central extension of the loop algebra (1.79).

Comparing (1.102) with (1.93), and noting that Θ must be invariant under a global confor-

mal transformation, it is clear that Θ is a quasiprimary field; i.e. it may transform under the action of a general conformal transformation. From (1.102) the variation in Θ is

$$\delta_\varepsilon \Theta(z) = \varepsilon(z)\,\partial\Theta(z) + 2\,\partial\varepsilon(z)\,\Theta(z) + \frac{c}{12}\,\partial^3\varepsilon(z)\ . \tag{1.106}$$

For the finite transformation $z \to f(z)$, this may be integrated to give

$$\Theta(z) \mapsto (\partial f)^2\,\Theta(f(z)) + \frac{c}{12}\,\{f,z\}\ ; \tag{1.107}$$

where the *Schwartzian derivative* $\{f,z\}$ is

$$\{f,z\} = \frac{\partial f\,\partial^3 f - \frac{3}{2}\,(\partial^2 f)^2}{(\partial f)^2}\ . \tag{1.108}$$

1.2.4 Representations of the Virasoro Algebra

A *highest weight*, or *primary*, *state* $\big|h,\overline{h}\big\rangle$ is defined by the action of a primary field on the vacuum:

$$\big|h,\overline{h}\big\rangle \stackrel{\text{def}}{=} \Phi_{h,\overline{h}}(0)\,|0\rangle \equiv \lim_{z,\overline{z}\to 0} \Phi_{h,\overline{h}}(z,\overline{z})\,|0\rangle\ ; \tag{1.109}$$

where the subscripts on the operator $\Phi_{h,\overline{h}}$ denote its conformal weights. The regularity of $\Theta(z)\,|0\rangle$ at $z=0$ and $z=\infty$ leads to the annihilation formulae:

$$\begin{aligned} L_n\,|0\rangle &= 0 \quad \text{for } n \geq -1\ , \\ \langle 0|\,L_n &= 0 \quad \text{for } n \leq 1\ . \end{aligned} \tag{1.110}$$

Choosing $\varepsilon(z) = z^{n+1}$ in (1.90) yields

$$[L_n\,,\,\Phi_{h,\overline{h}}(z,\overline{z})] = \big(h\,(n+1)\,z^n + z^{n+1}\,\partial\big)\,\Phi_{h,\overline{h}}(z,\overline{z})\ ; \tag{1.111}$$

which implies that the state $\big|h,\overline{h}\big\rangle$ satisfies the *highest weight conditions*:

$$\begin{aligned} L_0\,\big|h,\overline{h}\big\rangle &= h\,\big|h,\overline{h}\big\rangle\ , \\ L_n\,\big|h,\overline{h}\big\rangle &= 0 \quad \text{for all } n > 0\ ; \end{aligned} \tag{1.112}$$

and similarly for the action of the $\{\overline{L}_n\}$.

The central extension term, proportional to the central charge c, in (1.105) vanishes for the commutators of L_{-1}, L_0 and L_1. Therefore these generators, which generate a subalgebra, have the same interpretation as the global conformal generators l_{-1}, l_0 and l_1. Note that $|0\rangle$ is annihilated by L_{-1}, L_0 and L_1 so that the vacuum is conformally invariant.

Each primary field together with its descendants

$$\left\{ \Phi_{h,\overline{h}}^{(k_1,\ldots,k_m;\overline{k}_1,\ldots,\overline{k}_n)}(z,\overline{z}) \equiv L_{-k_1}\cdots L_{-k_m}\overline{L}_{-\overline{k}_1}\cdots\overline{L}_{-\overline{k}_n}\Phi_{h,\overline{h}}(z,\overline{z}) \;\middle|\; \text{all } k_i,\overline{k}_j \in \mathbb{Z}^+ \right\} , \tag{1.113}$$

form the *conformal family* $[\Phi_{h,\overline{h}}]$ of operators. States of the form

$$\Phi_{h,\overline{h}}^{(k_1,\ldots,k_m;\overline{k}_1,\ldots,\overline{k}_n)}(0)\,|0\rangle \quad \text{with all } k_i > 0 \tag{1.114}$$

are *descendant states*. The weights (shifted by h) k and $\overline{k}$ of this state are termed the *levels* of the state. The level k is given by

$$L_0\,\Phi_{h,\overline{h}}^{(k_1,\ldots,k_m;\overline{k}_1,\ldots,\overline{k}_n)}(0)\,|0\rangle = (k+h)\,\Phi_{h,\overline{h}}^{(k_1,\ldots,k_m;\overline{k}_1,\ldots,\overline{k}_n)}(0)\,|0\rangle \ , \tag{1.115}$$

with $k \equiv \sum_{i=1}^{m} k_i$. A similar equation holds for $\overline{k}$. The state $|h,\overline{h}\rangle$ together with its descendants under the action of the holomorphic (antiholomorphic) algebra forms the *Verma module* V_h ($V_{\overline{h}}$). V_h and $V_{\overline{h}}$ carry representations of the holomorphic and antiholomorphic Virasoro algebras (defined in (1.105)) respectively. As is clear by the definition (1.113), in a given representation V_h, the levels of the states are integers.

The representation V_h of the Virasoro algebra is irreducible except for particular, special, values of h [37]. For these values, the vector space V_h contains a *null state* (or *null vector*) $|\chi\rangle \in V_h$ which satisfies the highest weight conditions (1.112); i.e.

$$\begin{aligned} L_0\,|\chi\rangle &= (h+k)\,|\chi\rangle \ , \\ L_n\,|\chi\rangle &= 0 \quad \text{for } n > 0 \ ; \end{aligned} \tag{1.116}$$

where k is the level of $|\chi\rangle$. In general, the state $|\chi\rangle$ can be considered to be a primary state of its own Verma module V_{h+k}. Thus, the representation V_h is reducible. This representation may be consistently made irreducible by setting the null vector $|\chi\rangle = 0$. No contradictions arise as $|\chi\rangle$ has the property of being orthogonal to every other state in V_h and, in particular, has zero norm; i.e.

$$\begin{aligned} &\langle\psi|\chi\rangle = 0 \quad \text{for all } |\psi\rangle \in V_h \,, \\ &\langle\chi|\chi\rangle = 0 \,. \end{aligned} \tag{1.117}$$

In terms of fields, the conformal family $[\Phi_h(z)]$ will contain a special secondary field, $X_{h+k}(z)$, which possesses the property (1.83) and consequently all the other properties of a primary field. This field corresponds to the null state $|\chi\rangle$ and is called a *null field*. It originates from the conformal family $[X_{h+k}(z)]$ embedded within $[\Phi_h(z)]$. Its correlation functions with other (non-null) fields within $[\Phi_h(z)]$ are zero, so the null field $X_{h+k}(z)$ may be consistently regarded as the zero field. Doing this, $[X_{h+k}(z)] = \{0\}$, and the true irreducible conformal family $[\Phi_h(z)]$ of the field $\Phi_h(z)$ is obtained. In such a case, the conformal family $[\Phi_h(z)]$ contains 'less' fields than expected and it is termed a *degenerate conformal family*. The primary field $\Phi_h(z)$ is termed a *degenerate primary field*.

The special values of h at which the representations V_h are reducible (for a given central charge c) are found by computing the matrix of inner products of states at a given level within the Verma module. This "*Kac-determinant*" is (see [37] and [5])

$$\det M_m(c,h) = \prod_{\substack{p,q \\ pq \leq m}} \left(h - h_{p,q}(c)\right)^{P(m-pq)} \,; \tag{1.118}$$

where $P(n)$ is the number of (integer) partitions of the integer n, and

$$\begin{aligned} h_{p,q} &\equiv h_0 + \frac{(\alpha_+ p + \alpha_- q)^2}{4} \,, \\ h_0 &\equiv \frac{c-1}{24} \,, \\ \alpha_\pm &\equiv \frac{\sqrt{1-c} \pm \sqrt{25-c}}{\sqrt{24}} \,. \end{aligned} \tag{1.119}$$

A zero value of the determinant (1.118) indicates the existence of a null state at level m.

As the generator L_0 provides the Hamiltonian for a conformal theory, it will be useful to count the number of L_0-eigenstates with a given eigenvalue (i.e. weight or level) in a given representation, V_h, of the theory. This is simply the dimension of the level-k L_0-eigenspace of the Verma module V_h.

In the case of a non-degenerate representation V_h, the dimension of this level-k eigenspace is easily determined. From (1.113) and (1.115), any state at level k is of the form

$$L_{-k_1} L_{-k_2} \cdots L_{-k_m} |h\rangle \ ; \tag{1.120}$$

with $\sum_{n=1}^{m} k_n = k$. Therefore there are $P(k)$ basis vectors at any level, where $P(k)$ denotes the number of integer partitions of the integer n.

For a degenerate representation, the dimension of the level-k subspace will be $Q(k)$ with $Q(k) \leq P(k)$ for any given level k. This information is collected into a generating function as follows: Consider the trace over the representation V_h of the operator q^{L_0}; i.e.

$$\begin{aligned} \operatorname*{Tr}_h q^{L_0} &= \sum_{|\alpha\rangle \in V_h} \langle\alpha| \, q^{L_0} \, |\alpha\rangle \\ &= \sum_{\substack{\text{level} \\ k}} \sum_{\substack{|\alpha\rangle \in V_h \\ L_0|\alpha\rangle = (h+k)|\alpha\rangle}} \langle\alpha| \, q^{L_0} \, |\alpha\rangle \\ &= q^h \sum_k Q(k) \, q^k \ . \end{aligned} \tag{1.121}$$

This last is, up to the factor q^h, the generating function for $Q(k)$. The *Virasoro character*, $\chi_h(q)$, of the representation labelled by (c, h), is canonically defined in terms of this generating function as

$$\chi_h(q) = q^{-c/24} \operatorname*{Tr}_h q^{L_0} \ . \tag{1.122}$$

The *Dedekind eta function*, $\eta(q)$, is defined by

$$\eta^{-1}(q) = q^{-c/24} \sum_{k=0}^{\infty} P(k) \, q^k = q^{-c/24} \prod_{k=1}^{\infty} \frac{1}{1-q^k} \ ; \tag{1.123}$$

so that for V_h non-degenerate,

$$\chi_h(q) = \eta^{-1}(q)\, q^h \,. \tag{1.124}$$

As a demonstration of the degenerate case, consider the example of $c = 1$, which will prove useful later on. The Kac determinant (1.118) for $c = 1$ may be written as

$$\det M_m(1,h) = \prod_{\substack{p,q \\ pq \leq m \\ p \leq q}} \left(h - \tfrac{1}{4}(q-p)^2\right)^{2\,P(m-pq)} \,. \tag{1.125}$$

It is clear from this expression that the determinant has a zero iff $h = \frac{1}{4}n^2$ with $n \in \mathbb{Z}^+$. For other values of h therefore, the character is given by (1.124). Considering specifically the degenerate cases and writing $h = \frac{1}{4}n^2$, the determinant is

$$\det M_m(1, \tfrac{1}{4}n^2) \propto \prod_{\substack{p,q \\ pq \leq m \\ p \leq q}} \left(n^2 - (q-p)^2\right)^{2\,P(m-pq)} \,. \tag{1.126}$$

Thus the lowest level m at which a null vector occurs in the representation $V_{\frac{n^2}{4}}$ is given by $q = p + n$, so that $m = n + 1$. With $n = 1$ the first null vector occurs at level 2, with $n = 2$ the null vector first occurs at level 3, etc. The weight of the degenerate vector is $\frac{n^2}{4} + n + 1 = \frac{(n+2)^2}{4}$. Thus the representation $V_{\frac{(n+2)^2}{4}}$ is contained within the representation $V_{\frac{n^2}{4}}$. Further degenerate levels within $V_{\frac{n^2}{4}}$ occur for $m = p(n+p)$ with $p \in \mathbb{Z}^+$. These correspond to the subrepresentations $\left\{ V_{\frac{(n+2p)^2}{4}} \,\middle|\, p \in \mathbb{Z}^+, p \geq 1 \right\}$.

To build the appropriate Virasoro character, we begin with $\eta^{-1}(q)\, q^{n^2/4}$ which would count the states correctly were it not for the presence of the degenerate subrepresentations. To account for these, the null states of each $V_{\frac{(n+2p)^2}{4}}$ must be subtracted at each level of $V_{\frac{n^2}{4}}$. Therefore, we subtract $\sum_{p=1}^{\infty} \eta^{-1}(q)\, q^{(n+2p)^2/4}$. However, each of these representations is itself degenerate and the subtraction therefore eliminates from the count more states than is necessary. To counteract this, we look to the first ($p = 1$) degenerate subrepresentation $V_{\frac{(n+2)^2}{4}}$. It contains all the degenerate subrepresentations $V_{\frac{(n+2p)^2}{4}}$ for $p \geq 2$. Adding, therefore, $\sum_{p=2}^{\infty} \eta^{-1}(q)\, q^{(n+2p)^2/4}$ cancels out all the overcounting up to (and including) weight $\frac{(n+2)^2}{4}$. The overcounting at the higher weights still needs to be addressed; how-

ever, at this stage in the summation, there are equally balanced positive and negative terms at the higher weights. As they all require the same correction due to overcounting, these corrections are also opposite in sign and so they cancel. The degenerate character, is therefore, $\chi^{c=1}_{\frac{n^2}{4}}(q) = \eta^{-1}(q)\left(q^{n^2/4} - q^{(n+2)^2/4}\right)$. Thus the Virasoro characters at $c = 1$ may be summarised as

$$\chi^{c=1}_{\frac{n^2}{4}}(q) = \begin{cases} \eta^{-1}(q)\, q^{n^2/4} & ;\ \text{for } n \notin \mathbb{Z}^+. \\ \eta^{-1}(q)\, q^{n^2/4}\left(1 - q^{n+1}\right) & ;\ \text{for } n \in \mathbb{Z}^+. \end{cases} \quad ; \tag{1.127}$$

in agreement with Kac [37] and reference [22].

1.2.5 Conformal Field Theory on the Cylinder

In a semi-infinite or finite system, such as a Pasquier model on a (finite) cylinder, the presence of the boundary modifies the algebra (1.105). Consider the prototype geometry of a semi-infinite half-plane defined by $\mathrm{Im}\, z > 0$ with a boundary condition, denoted (α), on the real axis. The operators $\{\phi(z, \overline{z})\}$ of the theory are defined only within the upper half-plane $\mathrm{Im}\, z > 0$. The action of the conformal field theory is locally invariant under infinitesimal conformal transformations $\varepsilon(z)$, $\overline{\varepsilon}(\overline{z})$. In order to preserve the geometry it is necessary that $\varepsilon(z)$ is restricted to be real when $z \in \mathbb{R}$. If $\varepsilon(z) = -\sum_{n=-\infty}^{\infty} \varepsilon_n\, z^{n+1}$, then the parameters $\{\varepsilon_n\}$ must be real.

The definition of $\Theta(z)$ may be extended into the lower half-plane [10] by setting

$$\Theta(z) = \overline{\Theta}(z) \quad \text{for } \mathrm{Im}\, z < 0\,. \tag{1.128}$$

In other words, $\overline{\Theta}(\overline{z})$ is regarded as the analytic continuation of $\Theta(z)$ into $\mathrm{Im}\, z < 0$. One also chooses $\Theta = \overline{\Theta}$ on the real axis; this corresponds in Cartesian coordinates to the physical condition $\Theta_{01} = 0$, i.e. there is no energy-momentum flux across the boundary.

The generator (1.89) of conformal variations is written as

$$Q = \frac{1}{2\pi i} \oint_{C+} \left(\mathrm{d}z\, \varepsilon(z)\, \Theta(z) - \mathrm{d}\overline{z}\, \overline{\varepsilon}(\overline{z})\, \Theta(\overline{z})\right)\ ; \tag{1.129}$$

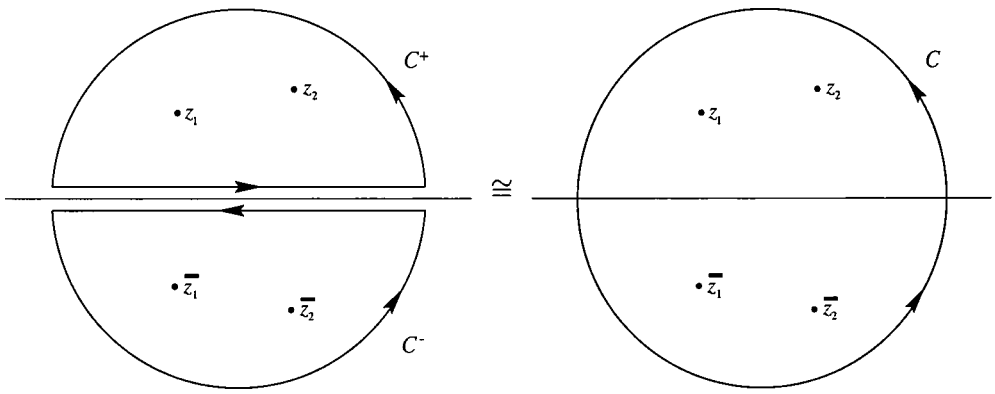

Figure 1.9: The contours C^+, C^- and $C \cong C^+ \cup C^-$.

where the contour, written C^+, is taken to lie wholly within the $\mathrm{Im}\, z > 0$ half-plane. It is convenient to choose C^+ (which must enclose the points $z_1, \ldots, z_n$ of the arguments of the fields upon which Q acts) to be a large semicircle together with a portion of the real axis. Choose the contour C^- to be the image of C^+ under reflection in the real axis (see figure 1.9). Then the restrictions on $\varepsilon(z)$, $\overline{\varepsilon}(\overline{z})$, $\Theta(z)$ and $\overline{\Theta}(\overline{z})$ imply that the generator (1.129) may be written as

$$Q = \frac{1}{2\pi i} \oint_C \mathrm{d}z\, \varepsilon(z)\, \Theta(z)\ ; \tag{1.130}$$

where the contour C is the 'net contour' $C^+ \cup C^-$. So that the presence of the boundary has 'eliminated' one of the Virasoro algebras. The generators of the remaining algebra are the $\{L_n\}$, with

$$L_n = \frac{1}{2\pi i} \oint_C \mathrm{d}z\, z^{n+1}\, \Theta(z)\ ; \tag{1.131}$$

the contour C again extends into the lower half-plane and encloses the points

$$z_1, \overline{z}_1, \ldots, z_n, \overline{z}_n$$

of the operators upon which L_n acts. The $\{L_n\}$, of course, satisfy

$$[L_m\, ,\, L_n] = (m-n)\, L_{m+n} + \frac{c}{12}\, (m^3 - m)\, \delta_{m+n,0}\ . \tag{1.132}$$

The geometry of the half-plane is brought to that of the infinitely long strip of width L by the conformal transformation

$$w = \frac{L}{\pi} \ln z \, . \tag{1.133}$$

Writing $w = a^0 + ia^1$, the generator of a^0-translations or Hamiltonian, is given in terms of the generator of dilatations in the upper-half plane, L_0, by

$$H = \int_0^L \mathrm{d}a^1 \, \Theta_{00} = \frac{\pi}{L} \left\{ L_0 - \frac{c}{24} \right\} \, . \tag{1.134}$$

The term $\frac{c}{24}$ is introduced as a result of the Schwartzian derivative (1.108).

This strip will have the same boundary condition (α) on either side. However, the existence of a Virasoro algebra is dependent only upon the fact that the boundary conditions are conformally invariant; i.e. $\Theta_{01} = 0$ on $a^1 = 0, L$, so that the more general case when the boundary conditions are not identical on either side may also be considered. Denote this new boundary condition (α, β), and by $H^{(\alpha,\beta)}$ the corresponding Hamiltonian. The eigenstates of $H^{(\alpha,\beta)}$ will fall into irreducible representations of the Virasoro algebra. Denote by $\Lambda^h_{\alpha\beta}$ the multiplicity with which the irreducible representation with highest weight h occurs in the spectrum of $H^{(\alpha,\beta)}$. Transforming the strip with this new boundary condition (α, β) back into the upper half-plane, there is a discontinuity in the boundary condition at $z = 0$. In radial quantisation, this corresponds to a "vacuum" state which is no longer annihilated by L_{-1} [16]. The vacuum is no longer translationally invariant. Such a state may be considered equivalent to the action of a boundary operator $\Phi^{(\alpha,\beta)}(0)$ acting upon the true vacuum $|0\rangle$. It is a highest weight state with weight $h_{(\alpha,\beta)}$ equal to the lowest value of h for which $\Lambda^h_{\alpha\beta} \neq 0$. Note that $\Lambda^0_{\alpha\alpha} = 1$.

To arrive at the situation reminiscent of the cylindrical Pasquier models of section 1.1, the strip with boundary condition (α, β) is made periodic in the a^0-direction (time) with period M by identifying $a^0 \equiv a^0 + M$. Topologically, this manifold is an annulus. The

modular parameter is $q \equiv \exp\{-M\pi/L\}$ and the partition function

$$\begin{aligned} \mathcal{Z}^{(\alpha,\beta)}(q) &= \mathrm{Tr}\, e^{-MH^{(\alpha,\beta)}} \\ &= \mathrm{Tr} \exp\left\{-\frac{M\pi}{L}\left(L_0 - \frac{c}{24}\right)\right\} \\ &= \sum_k \Lambda^k_{\alpha\beta}\, \chi_k(q)\ ; \end{aligned} \tag{1.135}$$

where $\chi_k(q)$ is the Virasoro character of the (Virasoro-) representation k as defined in equation (1.122).

Equation (1.134) also illustrates the 1-1 correspondence between the eigenstates of the Hamiltonian $H^{(\alpha,\beta)}$ and the scaling operators of the theory. As there is only one Virasoro algebra arising in the theory, the scaling operators are eigenvectors of L_0. Hence the scaling dimensions are given by the eigenvalues of L_0 (compare with equation (1.80)). Denote by $|x_n\rangle$ a state of scaling dimension x_n and by N_n the degeneracy of the n^{th} energy level (i.e. $|x_n\rangle$); then (1.135) may also be written

$$\begin{aligned} \mathcal{Z}^{(\alpha,\beta)}(q) &= \sum_n N_n \langle x_n | \exp\left\{-\frac{M\pi}{L}\left(L_0 - \frac{c}{24}\right)\right\} |x_n\rangle \\ &= q^{-c/24} \sum_n N_n\, q^{x_n}\ . \end{aligned} \tag{1.136}$$

Thus, the partition function of a cylindrical model may be written as a series in q with strictly non-negative integer coefficients. Furthermore, the scaling dimensions may be read off from the exponents of q once the modification by $-c/24$ has been made. The conformal invariance of the vacuum implies $x_0 = 0$. However this "true vacuum" only appears in the theory provided $\Lambda^0_{\alpha\beta} \geq 1$. In general, the ground state of the theory will be associated with the boundary operator $\Phi^{(\alpha\beta)}(z,\overline{z})$ of highest weight, or scaling dimension, $h_{(\alpha\beta)}$. Labelling by E_0 the energy of this ground state, and by Δx_n the difference in scaling dimensions $x_n - h_{(\alpha\beta)}$; then from (1.134), this difference of scaling dimensions corresponds to the energy gaps,

$$\Delta E_n \equiv E_n - E_0 = \frac{\pi}{L}\Delta x_n\ . \tag{1.137}$$

Note that although (1.127) indicates that a model in which only one irreducible Virasoro

representation appears will have the $\{x_n\}$ all integers, this is not *a priori* necessarily the case for a general model as more than one representation will be present. Now, of course, (1.136) may be written

$$Z^{(\alpha,\beta)}(q) = q^{\gamma/24} \sum_n N_n \, q^{\Delta x_n} \; ; \tag{1.138}$$

with $\gamma \equiv 24\, h_{(\alpha,\beta)} - c$.

For a model based on a given graph, $(\mathcal{G}; a, b)$ say, the height operator of the theory takes on the specified node-values a and b on either end of the cylinder. Hence we denote the boundary conditions when specifically referring to such a model by (a, b), with $a, b \in \mathcal{G}$.

1.2.6 Finite-Size Scaling

We briefly mention now, the theory of finite size scaling. This review is adapted for our purposes from Barber [3].

Phase transitions in statistical mechanical systems arise only in the thermodynamic limit, in which the volume V (i.e. the area when $d = 2$) of the system and the number of particles N (i.e. the statistical degrees of freedom) are both taken to be infinite with fixed finite density $\rho \equiv V/N$. Only in this limit is the free energy or any other thermodynamic quantity a singular function of the temperature or of external fields. However, experimental systems, such as those available within the laboratory or provided by numerical simulations have both finite volume and a finite number of degrees of freedom. Nonetheless, 'approximate singularities' may still be observed in such systems; and these often agree with the singularities predicted for the system in the thermodynamic limit. The question to be answered is to what degree can the finite system provide information concerning the infinite system of the thermodynamic limit?

Consider a 2-dimensional system infinite in extent in one dimension and finite, with width L, in the other. The example we choose of such is the infinite strip of width L. This, as mentioned before, is related to the cylindrical geometry of the Pasquier models. Let $F(T, L, N)$ be the free energy per unit length (in the infinite direction) of a lattice approximation to such a system with width L, number of particles per unit length N, at

temperature T.

We first remark that the partition function for a length M of the strip may be written as

$$\begin{aligned} \mathcal{Z}^{(\alpha,\beta)}(T,L,M,N) &\equiv e^{-MF(T,L,N)} \\ &= \operatorname{Tr} e^{-MH(T,L,N)} \\ &= \sum_{E_n} \langle E_n | \, e^{-MH(T,L,N)} \, | E_n \rangle \ . \end{aligned} \tag{1.139}$$

As $M \to \infty$, the partition function on the strip is dominated by the ground state. Thus the free energy per unit length of the infinite strip is given by $F(T,L,N) = E_0(T,L,N)$; i.e. the ground state energy and free energy per unit length are synonymous.

In the thermodynamic limit, with the density $\rho \equiv N/L$ and temperature T both held fixed, it is expected that the *(bulk) free energy density*

$$f_\infty(T,\rho) = \lim_{\substack{N,L\to\infty \\ \rho \text{ fixed}}} \frac{F(T,L,N)}{L} \tag{1.140}$$

exists and is independent of the geometry of the system and of the boundary conditions (α) and (β) imposed on either side of the 'strip'. Thus

$$F(T,L,N) = L\, f_\infty(T,\rho) + \mathcal{O}(1) \tag{1.141}$$

as the system approaches the thermodynamic limit. Thermodynamics also suggests the existence of a *boundary* or *surface free energy density* $f^{(\alpha,\beta)}(T,\rho)$, so

$$F(T,L,N) = L\, f_\infty(T,\rho) + f^{(\alpha,\beta)}(T,\rho) + \mathcal{O}(L^{-1}) \ , \tag{1.142}$$

again, as the thermodynamic limit is approached. The density $f^{(\alpha,\beta)}(T,\rho)$ will of course depend upon the boundary conditions (α,β).

At $T = T_c$, the system is described by a conformal field theory. The lattice strip may be mapped back into the semi-infinite half-plane by inverting the map (1.133). However, the canonical normalisation of $\Theta(z)$ is so that $\langle \Theta(z) \rangle = 0$ on the half-plane. Such an assumption means that the bulk and surface contributions in (1.142) have been subtracted.

Including the terms (1.142) therefore, comparison with equation (1.135) yields the expected ground state energy for a lattice-strip of width (i.e. number of sites) L:

$$E_0(L) = f_\infty L + f^{(\alpha,\beta)} + \frac{\pi}{L}\left\{h_{(\alpha\beta)} - \frac{c}{24}\right\} . \tag{1.143}$$

This is in agreement with the result of [7], once the action of the boundary operator $\Phi^{(\alpha,\beta)}(0)$ on the true vacuum is taken into account in that result. Equation (1.143) may be written as

$$E_0(L) = f_\infty L + f^{(\alpha,\beta)} + \frac{\pi}{L}\frac{\gamma}{24} ; \tag{1.144}$$

with $\gamma \equiv \gamma(\mathcal{G};\alpha,\beta) = 24\,h_{(\alpha,\beta)} - c$ the 'prefactor exponent' appearing in equation (1.138).

Note that the result (1.143) does not take into account corrections due to the departure of the Hamiltonian from the renormalisation group fixed-point Hamiltonian at the critical point. For finite values of L, the critical-point Hamiltonian is modified by terms involving 'irrelevant operators'. We ignore such corrections here. The reader is referred to references [3], [12] and [14] for further details.

1.2.7 The Model $(\widehat{A}_{2h-1}; a, b)$

The height function, σ_j, of the model $(A_\infty; a, b)$ defined in section 1.1.6 is the discrete version of a continuous free field variable $\varphi \in \mathbb{R}$. Up to rescaling of φ, this theory has partition function

$$\mathcal{Z}^{(A_\infty;a,b)}(M,L) = \int\limits_{\substack{\varphi(a^0,0)=a \\ \varphi(a^0,L)=b \\ \varphi(a^0+M,a^1)=\varphi(a^0,a^1)}} \mathrm{D}\varphi\, \exp\left\{-\frac{\pi g}{4}\int \mathrm{d}^2a\, \left|\nabla\varphi(a^0,a^1)\right|^2\right\} , \tag{1.145}$$

where $g = 1$ [49]. This model is well known in the literature to provide a $c = 1$ conformal field theory (see [30] for example). The equivalence,

$$\lim_{\substack{d\to 0 \\ M,L\to\infty \\ M/L \text{ fixed}}} \mathcal{Z}_\Gamma^{(A_\infty;a,b)} = \mathcal{Z}^{(A_\infty;a,b)}(M,L) , \tag{1.146}$$

of the lattice model in the continuum limit to the *Gaussian* or *Coulomb-gas model* (1.145) is established by examining the renormalisation-group flows of the so-called (unrestricted) solid-on-solid model mapped onto the A_∞ model via a set of transformations [42].

The partition function (1.145) is calculated by splitting $\varphi(a^0,a^1) = \varphi_0(a^0,a^1) + \varphi_{\rm Cl}(a^1)$. The field $\varphi_{\rm Cl}(a^1)$ is the classical solution to the equations of motion. The field φ_0 is periodic in the time direction and satisfies the boundary conditions $\varphi_0(a^0,0) = \varphi_0(a^0,L) = 0$. By zeta-regularisation [48],

$$\int\limits_{\substack{\varphi_0(a^0,0)=\varphi_0(a^0,L)=0\\ \varphi_0(a^0+M,a^1)=\varphi_0(a^0,a^1)}} \mathrm{D}\varphi_0 \, \exp\left\{-\frac{\pi g}{4}\int \mathrm{d}^2a\,\left|\nabla\varphi_0\right|^2\right\} = \eta^{-1}(q)\,, \tag{1.147}$$

with $q \equiv \exp\left(-M\pi/L\right)$, the modular parameter.

The classical field $\varphi_{\rm Cl}(a^1) = (b-a)\,a^1/L$ [49], so (1.145) is

$$\mathcal{Z}^{(A_\infty;a,b)}(q) = \eta^{-1}(q)\,\exp\left\{-\frac{\pi g}{4}\left(\frac{b-a}{L}\right)^2 ML\right\} = \eta^{-1}(q)\,q^{g\,(b-a)^2/4}\,. \tag{1.148}$$

The model is (manifestly) invariant under shifts in the boundary conditions $(a,b) \to (a+c,b+c)$, so we set $\varepsilon \equiv b-a$; thus, setting also $g=1$,

$$\boxed{\mathcal{Z}^{(A_\infty;0,\varepsilon)}(q) = \eta^{-1}(q)\,q^{\varepsilon^2/4}} \,. \tag{1.149}$$

By graph-symmetry, the partition function of the model $(\widehat{A}_{2h-1};a,b)$ is also invariant under 'translation' of the boundary conditions. We again rewrite the boundary condition as $\varepsilon \equiv b-a$. The continuum limit of the partition function is found by noting that the height function σ_j is here the discrete version of the continuous field $\varphi \in \mathbb{R}/2h\mathbb{Z}$; i.e. the field φ of (1.145) is now compactified on a circle of circumference $2h$ [25]. With a suitable rescaling of the field φ, the continuum partition function will be given by (1.145), again with $g=1$. The partition function (1.145) is evaluated by again splitting $\varphi(a^0,a^1) =$

$\varphi_0(a^0, a^1) + \varphi_{\text{Cl}}(a^1)$. The field $\varphi_0(a^0, a^1)$ is as before and provides the contribution (1.147). The classical field $\varphi_{\text{Cl}}(a^1)$ is modified to identify the boundary condition ε with $\varepsilon + 2nh$ for $n \in \mathbb{Z}$. Thus

$$\varphi_{\text{Cl}}(a^1) \equiv \sum_{n=-\infty}^{\infty} \varphi_{\text{Cl}}^{(n)}(a^1) \; ; \tag{1.150}$$

where $\varphi_{\text{Cl}}^{(n)}(a^1)$ is the classical field in the n^{th} instanton sector and is

$$\varphi_{\text{Cl}}^{(n)}(a^1) = (\varepsilon + 2nh)\,\frac{a^1}{L} \; . \tag{1.151}$$

Thus the continuum partition function of the model $(\widehat{A}_{2h-1}; 0, \varepsilon)$ is given by the result (1.149) with the identification $\varepsilon \equiv \varepsilon + 2\,h$, i.e.

$$\boxed{\mathcal{Z}^{(\widehat{A}_{2h-1};0,\varepsilon)}(q) = \eta^{-1}(q) \sum_{n\in\mathbb{Z}} q^{\frac{(\varepsilon+2nh)^2}{4}}} \; . \tag{1.152}$$

We continue this discussion of the partition functions in section 2.3.

We now have in place all the tools required to construct the continuum partition functions of the affine Pasquier models on the cylinder. We do this in the next chapter.

Chapter 2

Partition Functions of the Affine Models

In this chapter we discuss the calculation of the partition functions of the affine $\widehat{A}\widehat{D}\widehat{E}$ models on the cylinder with fixed, specified boundary conditions. This has been done for the classical ADE cases by Saleur and Bauer [50], also for fixed boundary conditions on the cylinder. Our motivation is to extend their results to the affine $\widehat{A}\widehat{D}\widehat{E}$ cases.

We proceed initially by analogy to Pasquier's calculation [45] of the partition functions of both classical ADE and affine $\widehat{A}\widehat{D}\widehat{E}$ models on the torus.

2.1 $\widehat{A}$ Model Decomposition

The method we set out here is to use a Temperley-Lieb equivalence to re-express the partition function $\mathcal{Z}_{\Gamma}^{(\mathcal{G};a,b)}$ of a given model, based on a graph $\mathcal{G}$ with specified boundary conditions a and b on either end of the cylinder Γ, in terms of the partition functions of the $(\widehat{A}_{2h-1};0,\varepsilon)$ models of section 1.2.7. We then use the result (1.152) to deduce the partition function in the continuum limit, i.e. the corresponding conformally invariant field theory.

Consider the evaluation of the partition function (equation (1.21)) for the model based on a (affine) graph $\mathcal{G}$ with boundary conditions a and b. We expand this trace using equations (1.19) and (1.42) and represent each term graphically using the notation (1.53): In the lattice square in the i^{th} row and j^{th} column ($i-j$ odd) we place a vertical bar if

the operator e_j is picked up in the i^{th} matrix V or W in $(V\,W)^M = V\,W\,V\,W\cdots V\,W$,

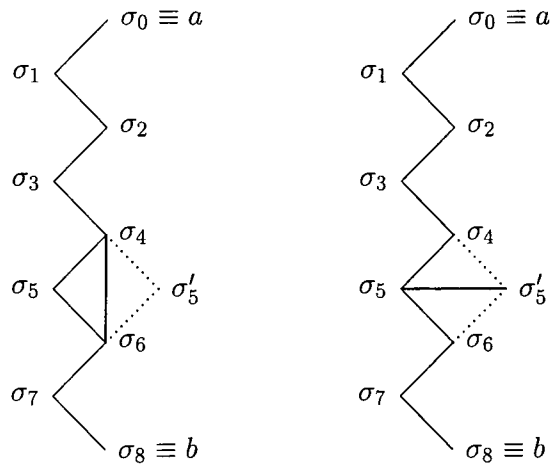

Figure 2.1: The operator e^5 is represented by a vertical bar between σ_4 and σ_6; the identity operator is represented by a horizontal bar between σ_5 and σ'_5.

see figure 2.1, and we put a horizontal bar if the identity is picked up instead. Thus for a fixed term in the expansion, in each square of the lattice Γ there is either a vertical or a horizontal bar. We may group the sites of the lattice into clusters, each site of which has the same height on $\mathcal{G}$. We separate clusters by boundaries, "*polygons*", drawn on the dual lattice; see figure 2.2. We then represent each cluster by a point; points representing clusters with a common boundary are joined by a line which represents the boundary polygon. *Irreducible clusters*, those wrapping around the cylinder, we represent with thick points; the others (*reducible*, i.e. homotopic to a point) with small points. Similarly, we represent irreducible boundary polygons with thick lines, reducible polygons with thin lines. The cluster graph corresponding to the decomposition of figure 2.2 is shown in figure 2.3. The requirement that either a horizontal or vertical bar appears in each lattice square, together with the topology of the cylinder, ensures that no cycles of clusters exist; for if we attempt to construct such a cycle, as a simple exercise demonstrates, we are forced to identify clusters until the corresponding cluster graph is a tree graph. Each cluster is therefore of the form figure 2.4; i.e. a chain, length N $(1 \leq N \leq L)$, of irreducible clusters with the reducible clusters adjoined to it in tree structures. The heights at either end of the "*N-chain*" are a and b respectively, in accord with the boundary conditions.

The contribution from each such cluster graph is a sum over all the possible height config-

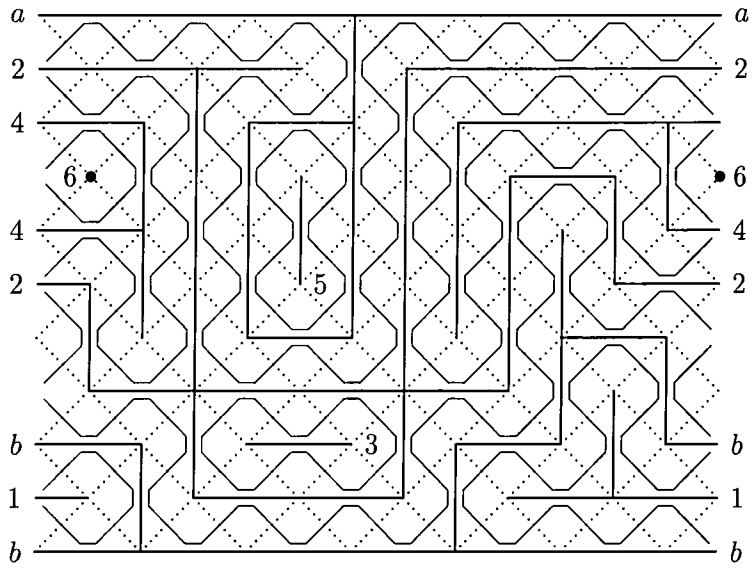

Figure 2.2: A cluster decomposition on the cylindrical lattice Γ.

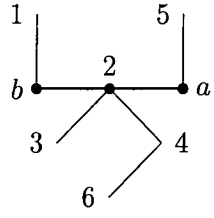

Figure 2.3: The cluster graph corresponding to the cluster decomposition of figure 2.2.

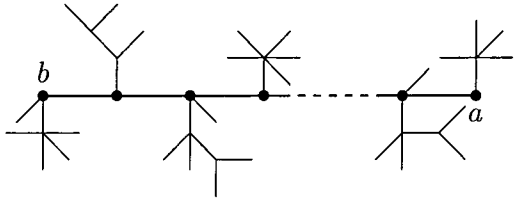

Figure 2.4: A typical cluster graph. The thick points represent irreducible clusters; the thin ones, reducible clusters. Links between points represent boundary polygons: thick lines, irreducible polygons; thin lines, reducible polygons.

urations on the graph. These inherit the graph restriction condition (1.15). The individual contributions are calculated as follows: observe, examining equation (1.47), that the contribution from the operators $\{e_j\}$ that correspond to the polygon segment

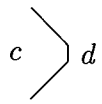

is $\dfrac{\psi_c^{1/2}}{\psi_d^{1/2}}$;

where $\underset{\sim}{\psi} \equiv \underset{\sim}{\psi}^{(0)}$ is the Perron-Frobenius eigenvector of $\mathcal{G}$. We split this contribution further so that the polygon corners give individual contributions

$= \psi_c^{1/2}$ Inside corner,

$= \psi_c^{-1/2}$ Outside corner.

The identity operators (1.53) contribute factors of 1 for the corners

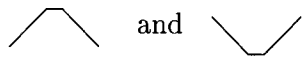

If we now follow the boundary polygons of a given cluster, we find that boundaries surrounding a cluster of height c contribute ψ_c. Boundaries surrounded by a cluster contribute a factor ψ_c^{-1}. Boundaries that wind about the cylinder contribute a factor 1. Thus the contribution from each polygon is $\psi_c^{b_+ - b_-}$; where b_+ (b_-) is the number of boundaries surrounding (surrounded by) the cluster (of height c). Thus starting at the outermost 'branches' of the tree graphs we may 'prune' each branch in turn by summing over all admissible heights at the unconnected end of the branch, whilst keeping the heights elsewhere on the graph fixed. The contribution obtained by removing each link in this way (taking the height of the unsummed end of the branch to be d) is $\psi_d^{-1} \sum_{c:d} \psi_c = \beta$; as each such link represents a boundary polygon surrounding exactly one cluster of height c (which is being summed over) and is surrounded by exactly one cluster of height d. (β is of course, the Perron-Frobenius eigenvalue of the graph $\mathcal{G}$ and is identically equal to 2 for the affine models considered here.) We prune successively, obtaining factors of β until we are left with the bare N-chain graph consisting purely of the irreducible clusters. The

partition function is therefore:

$$\mathcal{Z}_\Gamma^{(\mathcal{G};a,b)} = \sum (\text{Cluster Graphs})_{ab} \tag{2.1}$$

$$= \sum_N \left(\begin{matrix} \text{Cluster Graphs consisting} \\ \text{of an } N\text{-chain plus trees} \end{matrix} \right)_{ab} \tag{2.2}$$

$$= \sum_N \mathcal{P}_N(\beta) \; \underset{a}{1} \; 2 \; 3 \; \cdots \; N-1 \; \underset{b}{N} \; ; \tag{2.3}$$

where we sum over all graphs built around the same N-chain and collected the factors of β into the polynomial $\mathcal{P}_N(\beta)$ (thus the summations in (2.2) and (2.3) are *not* the same).

To evaluate the N-chain we must perform the summation over all configurations on the chain consistent with the boundary conditions (i.e. a and b are held fixed and cannot be summed over). This is no more than the calculation of the number of paths of length N which exist on the graph $\mathcal{G}$ between the nodes a and b. Thus the contribution of a given N-chain is $(\mathcal{G}^N)_{ab}$.

$$\underset{a}{1} \; 2 \; 3 \; \cdots \; N-1 \; \underset{b}{N} = (\mathcal{G}^N)_{ab}$$

$$= \sum_{j \in \mathrm{v}^*(\mathcal{G})} \psi_a^{(j)*} \psi_b^{(j)} \left(\beta^{(j)}\right)^N \tag{2.4}$$

$$= \sum_{j \in \mathrm{v}^*(\mathcal{G})} \psi_a^{(j)*} \psi_b^{(j)} \left(2\cos\frac{\pi j}{h}\right)^N .$$

Thus

$$\mathcal{Z}_\Gamma^{(\mathcal{G};a,b)} = \sum_N \mathcal{P}_N(\beta) \sum_{j \in \mathrm{v}^*(\mathcal{G})} \psi_a^{(j)*} \psi_b^{(j)} \left(2\cos\frac{\pi j}{h}\right)^N . \tag{2.5}$$

By analogy with Pasquier [45], we now attempt to use (2.5) to rewrite the partition function of an arbitrary affine graph model, based on the graph $\mathcal{G}$, as a linear sum over partition functions of $(\widehat{A}_{[2h']}; 0, \lambda)$ models with boundary conditions on the cylinder,

$$\mathcal{Z}_\Gamma^{(\mathcal{G}_{[h]};a,b)} = \sum_{h'} \sum_{\lambda \in \widehat{A}_{[h']}} N_{0\lambda;h'}^{ab} \, \mathcal{Z}_\Gamma^{(\widehat{A}_{[h']};0,\lambda)} . \tag{2.6}$$

If we denote by $\phi^{(k)}_{[h']\lambda}$ the components of the eigenvectors of the graph $\widehat{A}_{[h']}$; then this is true iff

$$\sum_N \mathcal{P}_N(\beta) \sum_{j\in v^*(\mathcal{G}_{[h]})} \psi^{(j)*}_a \psi^{(j)}_b \left(2\cos\frac{\pi j}{h}\right)^N = \sum_{h'} \sum_{\lambda\in\widehat{A}_{[h']}} N^{ab}_{0\lambda;h'} \sum_N \mathcal{P}'_N(\beta') \sum_{k\in v^*(\widehat{A}_{[h']})} \phi^{(k)*}_{[h']0}\, \phi^{(k)}_{[h']\lambda} \left(2\cos\frac{\pi k}{h'}\right)^N , \quad (2.7)$$

as there is a one-to-one correspondence between the cluster decompositions on the cylinder for all the graphs, $\mathcal{P}_N(\beta) = \mathcal{P}'_N(\beta')$ provided $\beta = \beta'$. Of course, $\beta = \beta' = 2$ for all affine models so we have, for each N,

$$\sum_{j\in v^*(\mathcal{G}_{[h]})} \psi^{(j)*}_a \psi^{(j)}_b \left(2\cos\frac{\pi j}{h}\right)^N = \sum_{h'}\sum_{\lambda} N^{ab}_{0\lambda;h'} \sum_{k\in v^*(\widehat{A}_{[h']})} \phi^{(k)*}_{[h']0}\, \phi^{(k)}_{[h']\lambda} \left(2\cos\frac{\pi k}{h'}\right)^N . \quad (2.8)$$

To attempt a solution to this, we must first force the eigenvalues to match on either side of equation (2.8). On doing this we note that the power N on both sides of the equation corresponds to a path length between two nodes: for it is the length of two N-chains, one with boundary heights a, b on either end and the other with boundary heights $0, \lambda$. Thus, as the graphs are $\mathbb{Z}_2$-colourable, the ($\mathbb{Z}_2$-) parity of a, b must equal the parity of N which in turn must equal the parity of $0, \lambda$. Thus the *path parity is preserved* in the decomposition onto the $\widehat{A}$ models: if the original model has even (odd) boundary conditions (i.e. the path length between a and b is even (odd)) then the $\widehat{A}$ models onto which it decomposes will also have strictly even (odd) boundary conditions.

We denote the parity of a, b by $P(a, b)$, in particular

$$P(a,b) \stackrel{\text{def}}{=} \begin{cases} 0 & ; \text{if the path length between } a \text{ and } b \text{ is even.} \\ 1 & ; \text{if the path length between } a \text{ and } b \text{ is odd.} \end{cases} . \quad (2.9)$$

We remark that for a given exponent of an affine graph may be degenerate, for example

the exponent 4 is an exponent of the graph $\widehat{E}_6$ with multiplicity 2. To accommodate this in our notation we distinguish between two different but equal-valued exponents by a subscript; so that $\underset{\sim}{\psi}^{(\mu)_i}$ denotes the eigenvector of $\mathcal{G}$ labelled by the i^{th} exponent μ.

Matching the eigenvalues and comparing their coefficients, we find for each j, $1 \leq j \leq h$:

$$(-1)^{P(a,b)}\,\delta_{jh} \sum_{i\in \mathrm{d}(0)} \psi_a^{(0)_i *}\,\psi_b^{(0)_i} + \sum_{i\in \mathrm{d}(j)} \psi_a^{(j)_i *}\,\psi_b^{(j)_i} = \sum_{\substack{h' \\ \text{such that} \\ \frac{2h}{h'}|j,\ h'|2h}} \sum_{\lambda=0}^{h'} N^{ab}_{0\lambda;h'} \left\{(-1)^{P(a,b)}\,\delta_{jh}\,\phi^{(0)*}_{[h']0}\,\phi^{(0)}_{[h']\lambda} + \phi^{(h'j/h)*}_{[h']0}\,\phi^{(h'j/h)}_{[h']\lambda}\right\} . \quad (2.10)$$

where $\mathrm{d}(j)$ is an index set labelling the degeneracy of j as an exponent of the graph $\mathcal{G}$. This gives, in general, an underdetermined set of linear equations to solve for the $N^{ab}_{0\lambda;h'}$.

Because of the large number of unknowns $N^{ab}_{0\lambda;h'}$, solving (2.10) in the general case as it stands is quite difficult. We attempted a number of ansätze without success. In particular, the form (1.67) does not provide a solution. Solutions for a small number of cases were found algebraically using a computer. As the unknowns are underdetermined, there remains some freedom in the solutions. As is seen in section 2.3, we are able to use solutions to (2.10) to find the partition functions of models based on $\mathcal{G}$. Once this is done, the freedom in the solutions is found to drop out. This is to be expected as the remaining freedom should not lead to a physical effect.

To find a solution for all the $\widehat{A}\widehat{D}\widehat{E}$ models, we might attempt to proceed using lemma 1.3 as is done for the classical cases. Unfortunately, the discussion which follows lemma 1.3 does not apply directly to the affine cases. This is due to the fact that the exponent set of an affine model $\widehat{A}$ does not necessarily contain the exponent set of the affine graph $\mathcal{G}$ with the same Coxeter number. For example, $\widehat{D}_5$ has the odd exponent 3 occurring with multiplicity 2. However, not only is there no $\widehat{A}$ model with odd exponents, but no exponent of any $\widehat{A}$ graph has a multiplicity exceeding 1.

Fortunately, we may still make use of lemma 1.3, proceeding as follows:

Consider the modified partition function (1.52) for an affine graph $\mathcal{G}_{[h]}$ with affine Coxeter number h. In analogy with (2.6), we attempt to rewrite this partition function as a linear sum over modified partition functions of $\widehat{A}$ models,

$$\mathcal{Z}_\Gamma^{[\mathcal{G}_{[h]};\nu]} = \sum_{\substack{h'\in\mathbb{Z}^+ \\ \nu'\in\widehat{A}_{[h']}}} X^{h\nu}_{h'\nu'}\, \mathcal{Z}_\Gamma^{[\widehat{A}_{[h']};\nu']} \,. \tag{2.11}$$

We allow freedom both in the choice of the $\widehat{A}$ graph (labelled by its Coxeter number h') and in the exponent ν'. Substituting in the result of lemma 1.3, labelling the eigenvalues of a graph with Coxeter number k by $\beta_k^{(\mu)}$, we therefore seek a solution for the $X^{h\nu}_{h'\nu'}$ such that,

$$f(\beta_h,\beta_h^{(\nu)}) = \sum_{\substack{h'\in\mathbb{Z}^+ \\ \nu'\in\widehat{A}_{[h']}}} X^{h\nu}_{h'\nu'}\, f(\beta_{h'},\beta_{h'}^{(\nu')}) \,. \tag{2.12}$$

The unknown function f is identical (for a given lattice Γ) on each side. As we did earlier, we must choose the eigenvalues $\{\beta_k^{(\mu)}\}$ appropriately on each side of the equation. For the reason discussed, unlike the classical ADE cases, this cannot be done simply by choosing $h'=h$ and $\nu'=\nu$. Examining $\beta_k^{(\mu)} = 2\cos\frac{\mu\pi}{k}$, equality of the eigenvalues may be obtained by choosing instead $h'=2h$ and $\nu'=2\nu$, i.e.

$$X^{h\nu}_{h'\nu'} = \delta^{2h}_{h'}\,\delta^{2\nu}_{\nu'} \,. \tag{2.13}$$

This provides a solution to (2.11). We observe that in contrast to the toroidal case [45], we can construct a solution whereby a model of (affine) Coxeter number h is expressed in terms of other models, all of which have the *same* (affine) Coxeter number, namely $2h$. In the toroidal case, the extra degree of freedom provided by the summation over h' in (2.6) is necessary. Substituting this (2.13) and equation (1.52), equation (2.11) becomes,

$$\sum_{b\in\mathcal{G}_{[h]}} \frac{\psi_b^{(\nu)}}{\psi_a^{(\nu)}}\, \mathcal{Z}_\Gamma^{(\mathcal{G}_{[h]};a,b)} = \sum_{d\in\widehat{A}_{[2h]}} \frac{\phi_d^{(2\nu)}}{\phi_c^{(2\nu)}}\, \mathcal{Z}_\Gamma^{(\widehat{A}_{[2h]};c,d)} \,; \tag{2.14}$$

where the $\{\underset{\sim}{\psi}^{(\mu)}\}$ are eigenvectors of $\mathcal{G}_{[h]}$ and the $\{\underset{\sim}{\phi}^{(\mu)}\}$ eigenvectors of $\widehat{A}_{[2h]}$. Both a and c may be chosen arbitrarily on the respective graphs. Assuming the $\{\underset{\sim}{\psi}^{(\mu)}\}$ have been

chosen to be an orthonormal set, this is inverted to yield,

$$\mathcal{Z}_{\Gamma}^{(\mathcal{G}_{[h]};a,b)} = \sum_{\lambda\in\widehat{A}_{[2h]}} \left\{ \sum_{\mu\in \mathrm{v}^*(\mathcal{G})} \frac{\phi_{\lambda}^{(2\mu)}}{\phi_0^{(2\mu)}} \psi_a^{(\mu)*} \psi_b^{(\mu)} \right\} \mathcal{Z}_{\Gamma}^{(\widehat{A}_{[2h]};0,\lambda)} \; ; \tag{2.15}$$

where c has been set to 0 (the affine node) without loss of generality. This is of the form (2.6) with

$$N_{0\lambda;h'}^{ab} = \delta_{h',2h}\, N_{\lambda}^{ab} \tag{2.16}$$

and

$$\boxed{N_{\lambda}^{ab} \equiv \sum_{\mu\in \mathrm{v}^*(\mathcal{G})} \frac{\phi_{\lambda}^{(2\mu)}}{\phi_0^{(2\mu)}} \psi_a^{(\mu)*} \psi_b^{(\mu)}} \; . \tag{2.17}$$

Note again that importantly $\left\{ \underset{\sim}{\psi}^{(\mu)} \,\middle|\, \mu \in \mathrm{v}^*(\mathcal{G}) \right\}$ in (2.17) form an orthonormal eigenbasis of $\mathcal{G}$. Equation (2.16), together with equation (2.17), may be readily checked to satisfy equations (2.10). They provide a solution but not the most general one. This is of no consequence, as the remaining degrees of freedom in (2.10) must drop out once the physical partition functions are placed into (2.6).

We proceed now to examine explicitly the coefficients (2.17) and postpone comment until section 2.6.2.

2.2 The Decompositions for the Affine Models

We now calculate the coefficients (2.17) for the affine $\widehat{D}$ and $\widehat{E}$ cases. The $\widehat{D}$ models form an infinite series so we proceed in a general manner for these cases. For the exceptional $\widehat{E}$ cases, there are only a finite number ($9 + 21 + 45 = 75$ in fact) of independent models to be studied. For these cases we choose to proceed on a case by case basis.

2.2.1 $\widehat{D}_{[h]}$ Based Models

We evaluate the coefficients (2.17) for the $\widehat{D}$ based models using the eigenvectors listed in tables A.1 and A.2 together with the following result: define the *modified summation symbol* $\sum'$ by

$$\sum_{\mu}{}' f(\mu) \equiv \sum_{\mu \in v^*(\widehat{D}_{[h]})} f(\mu) - \frac{1}{2}\{f(0) + f(h)\} \ , \tag{2.18}$$

then

$$\frac{4}{h}\sum_{\mu}{}' \cos\frac{\mu\pi\varepsilon}{h} \cos\frac{\mu\pi a}{h} \cos\frac{\mu\pi b}{h} = \frac{1}{2} \sum_{\substack{n\in\mathbb{Z} \\ q,r\in\{\pm 1\}}} \delta_{\varepsilon+qa+rb,nh} \ . \tag{2.19}$$

This is demonstrated by rewriting the cosines in exponential form and evaluating the resulting geometric series. The utility of (2.19) may be seen by examining the eigenvectors of the $\widehat{D}$ models given in table A.2.

Careful use of the identity (2.19) gives the following partition function identities:

$$\begin{aligned} 2\,\mathcal{Z}_{\Gamma}^{(\widehat{D}_{[h]};a,b)} = {} & \mathcal{Z}_{\Gamma}^{(\widehat{A}_{[2h]};0,|a+b|)} + \mathcal{Z}_{\Gamma}^{(\widehat{A}_{[2h]};0,|a-b|)} + \\ & \mathcal{Z}_{\Gamma}^{(\widehat{A}_{[2h]};0,h-|a+b|)} + \mathcal{Z}_{\Gamma}^{(\widehat{A}_{[2h]};0,h-|a-b|)} + \\ & \mathcal{Z}_{\Gamma}^{(\widehat{A}_{[2h]};0,h+|a+b|)} + \mathcal{Z}_{\Gamma}^{(\widehat{A}_{[2h]};0,h+|a-b|)} + \\ & \mathcal{Z}_{\Gamma}^{(\widehat{A}_{[2h]};0,2h-|a+b|)} + \mathcal{Z}_{\Gamma}^{(\widehat{A}_{[2h]};0,2h-|a-b|)} \ ; \end{aligned} \tag{2.20}$$

where both a and b are on the chain- or A_n-like part of the $\widehat{D}$ graph. Also,

$$2\,\mathcal{Z}_{\Gamma}^{(\widehat{D}_{[h]};X,a)} = \mathcal{Z}_{\Gamma}^{(\widehat{A}_{[2h]};0,a)} + \mathcal{Z}_{\Gamma}^{(\widehat{A}_{[2h]};0,h+a)} + \mathcal{Z}_{\Gamma}^{(\widehat{A}_{[2h]};0,h-a)} + \mathcal{Z}_{\Gamma}^{(\widehat{A}_{[2h]};0,2h-a)} \ , \tag{2.21}$$

with a on the chain. The results when the boundary conditions both lie on the forks of the $\widehat{D}$ graph are:

$$2\,\mathcal{Z}_\Gamma^{(\widehat{D}_{[2h]};X,\overline{X})} = \mathcal{Z}_\Gamma^{(\widehat{A}_{[2h]};0,0)} + \mathcal{Z}_\Gamma^{(\widehat{A}_{[2h]};0,h)} \pm \sum_{\substack{\varepsilon=0 \\ 2|\varepsilon}}^{2h-2} (-1)^{\varepsilon/2}\,\mathcal{Z}_\Gamma^{(\widehat{A}_{[2h]};0,\varepsilon)}\,, \tag{2.22}$$

where the positive sign is taken in the case X and the negative sign in the case $\overline{X}$. We also have

$$2\,\mathcal{Z}_\Gamma^{(\widehat{D}_{[2h]};X,Y)} = \mathcal{Z}_\Gamma^{(\widehat{A}_{[2h]};0,\frac{h}{2})} + \mathcal{Z}_\Gamma^{(\widehat{A}_{[2h]};0,\frac{3h}{2})} \tag{2.23}$$

for boundary conditions on opposite ends of the $\widehat{D}$ graph.

These decompositions (2.20–2.23) will of course continue to hold in the continuum limit

$$\mathcal{Z}_\Gamma^{(\mathcal{G};a,b)} \xrightarrow[\substack{L,M\to\infty \\ M/L \text{ constant}}]{d\to 0} \mathcal{Z}^{(\mathcal{G};a,b)}(q)\,. \tag{2.24}$$

2.2.2 $\widehat{E}_{6,7,8}$ Based Models

The $\widehat{A}$ model decompositions for the affine exceptional cases $\widehat{E}_6$, $\widehat{E}_7$ and $\widehat{E}_8$ may of course be calculated from (2.17). This is tedious and is best carried out by computer as there is only a finite number of cases to be examined. *Mathematica*™ was used for this purpose. Once the adjacency matrix for the appropriate model has been given, the Mathematica script evaluates an orthonormal eigenbasis for the graph. From this, the coefficients (2.17) are evaluated for each of the possible boundary conditions. For the cases $\widehat{E}_6$ and $\widehat{E}_7$, the calculations are precise as Mathematica is capable of carrying out calculations symbolically provided they are not too complex. The $\widehat{E}_8$ case was calculated numerically: the numerical errors induced being extremely small with deviations from integer or half-integer quantities, as appropriate, being of the order of 10^{-6}. These errors where then rounded away. The results of the calculation were verified to show that the symmetries of the graphs are reflected in the partition functions as expected.

As our ultimate aim is to find the partition functions, the results for these decompositions do not appear here. However, evaluating the coefficients (2.17) by computer does not present any particular difficulty.

2.2.3 $\widehat{A}_{[h]}$ Based Models

In principle, we may calculate the decomposition coefficients relating the model $(\widehat{A}_{[h]}; a, b)$ to models based on the graph $\widehat{A}_{[2h]}$. Our interest however, is in finding partition functions and we already have these for both sets of models. Such coefficients are still useful though as a consistency check at this stage: the partition function (1.152) of $(\widehat{A}_{[h]}; a, b)$ may be identified with a sum of partition functions corresponding to $\widehat{A}_{[2h]}$ models. The eigenvectors of appendix A.1 are not an orthonormal set so this was verified for a number of individual cases using an extension of the same Mathematica script as used in the last section.

2.3 The Partition Functions

Having established the relationship between the $\widehat{A}$, $\widehat{D}$ and $\widehat{E}$ based models, we wish to write the partition functions of these $c = 1$ models in the form (from (1.135))

$$\mathcal{Z}^{(\mathcal{G};a,b)}(q) = \sum_{n\in\mathcal{J}} \Lambda_n^{(\mathcal{G};a,b)}\, \chi_{\frac{n^2}{4}}(q) \; ; \tag{2.25}$$

where the $\chi_{\frac{n^2}{4}}(q)$ are $c = 1$ Virasoro characters; and $\mathcal{J}$ is some index set. In fact, it turns out that in all cases of interest $\mathcal{J} = \mathbb{Z}^+$.

2.3.1 A_∞ Based Models

We begin with the classical model A_∞ as it provides a useful tool in the subsequent analysis. This model also provides a $c = 1$ conformal field theory in the continuum limit. Its partition function is given by (1.149). The degenerate $c = 1$ characters are of the form (see equation (1.127))

$$\chi_{\frac{n^2}{4}}(q) = \eta^{-1}(q)\left\{q^{\frac{n^2}{4}} - q^{\frac{(n+2)^2}{4}}\right\} \; ; \tag{2.26}$$

for $n \in \mathbb{Z}^+$. We invert this expression to find

$$\eta^{-1}(q)\, q^{\frac{n^2}{4}} = \sum_{p=0}^{\infty} \chi_{\frac{(n+2p)^2}{4}}(q) \tag{2.27}$$

for n a positive integer. Thus

$$\mathcal{Z}^{(A_\infty;0,\varepsilon)}(q) = \sum_{p=0}^{\infty} \chi_{\frac{(\varepsilon+2p)^2}{4}}(q) \; . \tag{2.28}$$

If we define the *generalised semi-infinite Kronecker comb* as

$$\Omega_{n,\varepsilon}^{(a_1,\ldots,a_k)} \equiv \sum_{m_1,\ldots,m_k=0}^{\infty} \delta_{n,\varepsilon+\sum_{i=1}^{k} m_i\, a_i} \; , \tag{2.29}$$

where δ is the usual Kronecker-δ; then (2.28) is of the form (2.25) with

$$\Lambda_n^{(A_\infty;0,\varepsilon)} = \Omega_{n,\varepsilon}^{(2)} \; . \tag{2.30}$$

2.3.2 $\widehat{A}_{[2h]}$ Based Models

The partition function of the $\widehat{A}_{[2h]}$ based models are given by equation (1.152). Hence

$$\mathcal{Z}^{(\widehat{A}_{[2h]};0,\varepsilon)}(q) = \eta^{-1}(q) \sum_{m\in\mathbb{Z}} q^{\frac{(\varepsilon+2mh)^2}{4}} \tag{2.31}$$

$$= \eta^{-1}(q) \left\{ \sum_{m=-\infty}^{-1} q^{\frac{(\varepsilon+2mh)^2}{4}} + \sum_{m=0}^{\infty} q^{\frac{(\varepsilon+2mh)^2}{4}} \right\} \tag{2.32}$$

$$= \eta^{-1}(q) \sum_{m=0}^{\infty} \left\{ q^{\frac{(2mh+2h-\varepsilon)^2}{4}} + q^{\frac{(2mh+\varepsilon)^2}{4}} \right\} \tag{2.33}$$

$$= \sum_{m=0}^{\infty} \sum_{p=0}^{\infty} \left\{ \chi_{\frac{(2p+2mh+2h-\varepsilon)^2}{4}}(q) + \chi_{\frac{(2p+2mh+\varepsilon)^2}{4}}(q) \right\} . \tag{2.34}$$

Thus

$$\Lambda_n^{(\widehat{A}_{[2h]};0,\varepsilon)} = \Omega_{n,2h-\varepsilon}^{(2,2h)} + \Omega_{n,\varepsilon}^{(2,2h)} . \tag{2.35}$$

Note that as ε has been identified with $\{\, \varepsilon + 2nh \mid n \in \mathbb{Z} \,\}$, we have chosen ε above to be defined to take values $0 \le \varepsilon \le 2h-1$ only. Outside this range it is necessary to substitute the value $\varepsilon \pmod{2h}$ for ε. Thus the $\{\Lambda_n^{(\widehat{A}_{[2h]};0,\varepsilon)}\}$ are considered to be periodic in ε with period $2h$.

2.3.3 $\widehat{D}_{[h]}$ Based Models

Using the decompositions of section 2.2.1 and the result (2.35), we evaluate the partition functions of the $\widehat{D}_{[h]}$ based models in the continuum limit. The method is to use the decomposition equations of section 2.2.1 together with the properties

$$\Omega_{n,\varepsilon}^{(\ldots,a,\ldots)} - \Omega_{n,\varepsilon+a}^{(\ldots,a,\ldots)} = \Omega_{n,\varepsilon}^{(\ldots\ldots)} \tag{2.36}$$

$$\text{and} \quad \Omega_{n,\varepsilon}^{(\ldots,2a,\ldots)} + \Omega_{n,\varepsilon+a}^{(\ldots,2a,\ldots)} = \Omega_{n,\varepsilon}^{(\ldots,a,\ldots)} \tag{2.37}$$

to add the coefficients $\Lambda_n^{(\widehat{A}_{[2h]},a,b)}$ to form the $\Lambda_n^{(\widehat{D}_{[h]};a,b)}$. It can also be shown that

$$\sum_{\substack{\varepsilon=0 \\ 2|\varepsilon}}^{2h-2} (-1)^{\varepsilon/2}\, \Lambda_n^{(\widehat{A}_{[2h]};0,\varepsilon)} = \Omega_{n,0}^{(2,4)} + \Omega_{n,4}^{(2,4)} - 2\,\Omega_{n,2}^{(2,4)} = \Omega_{n,0}^{(4)} - \Omega_{n,2}^{(4)} . \tag{2.38}$$

This allows us to evaluate the partition functions corresponding to $(\widehat{D}_{[h]}; X, {}^{(}\overline{X}{}^{)})$. (The properties of the Kronecker comb are summarised in appendix B.) The results are as follows:

$$\begin{aligned}
\Lambda_n^{(\widehat{D}_{[h]};a,b)} &= \Omega^{(2,h)}_{n,|a-b|} + \Omega^{(2,h)}_{n,h-|a-b|} + \Omega^{(2,h)}_{n,|a+b|} + \Omega^{(2,h)}_{n,h-|a+b|} \,, \\
\Lambda_n^{(\widehat{D}_{[h]};X,a)} &= \Omega^{(2,h)}_{n,a} + \Omega^{(2,h)}_{n,h-a} \,, \\
\Lambda_n^{(\widehat{D}_{[h]};X,X)} &= \Omega^{(2,h)}_{n,h} + \Omega^{(4)}_{n,0} \,, \\
\Lambda_n^{(\widehat{D}_{[h]};X,\overline{X})} &= \Omega^{(2,h)}_{n,h} + \Omega^{(4)}_{n,2} \,, \\
\Lambda_n^{(\widehat{D}_{[h]};X,Y)} &= \Omega^{(2,h)}_{n,\frac{h}{2}} \,.
\end{aligned} \tag{2.39}$$

The results (2.30), (2.35) together with the $(\widehat{D}_{[h]}; a, b)$ results (2.39), are summarised graphically in table 2.2 (page 76).

2.3.4 $\widehat{E}_{6,7,8}$ Based Models

Similarly, we find the partition functions for the $\widehat{E}_6$, $\widehat{E}_7$ and $\widehat{E}_8$ models from (2.35) and the decompositions discussed in section 2.2.2. We leave a statement of the results until after section 2.5.

2.4 Correspondence with Other Results

There appears to be very little in the literature concerning the partition functions of the models we have examined. We know of two results, that of Baake *et al.* [2] and that of Saleur and Bauer [50], both for the 4-state Potts model with free boundary conditions on the cylinder. Unfortunately, we found the former reference quite cryptic and an admittedly naïve reading of this paper suggests that the two results do not agree.

The 4-state Potts model with free boundary conditions on the cylinder may be represented graphically, in the notation of table 2.2, as

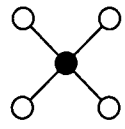

Looking at figure 1.4, the dark lattice sites (say) assume the value of the centre (dark coloured) node while the light lattice sites assume values of the leg-nodes (light coloured). Thus ignoring the 'dark lattice' upon which the configuration is constrained to be fixed, the remaining 'light lattice' provides a 4-state Potts model with free boundary conditions. Result (2.39) or table 2.2 therefore gives in this case

$$\begin{aligned} \mathcal{Z}^{(\widehat{D}_4;1,1)}(q) &= \sum_{n=0}^{\infty} \left\{ \Omega_{n,0}^{(2,4)} + \Omega_{n,4}^{(2,4)} + \Omega_{n,2}^{(2,4)} + \Omega_{n,2}^{(2,4)} \right\} \chi_{\frac{n^2}{4}}(q) \\ &= \sum_{n=0}^{\infty} (2n+1)\, \chi_{\frac{(2n)^2}{4}}(q) \\ &= \eta^{-1}(q) \sum_{\mathcal{S}\in\mathbb{Z}} q^{\mathcal{S}^2} . \end{aligned} \tag{2.40}$$

This is in precise agreement with the result found by Saleur and Bauer [50]. Their result is found as a limiting case of a Bethe ansatz analysis based on mapping the general Q-state Potts model (1.13) with $Q < 4$ onto the XXZ spin chain.

On the other hand, our interpretation of Baake *et al.* [2], yields the partition function

$$\begin{aligned} \mathcal{Z}^{(\widehat{D}_4;1,1)}_{\substack{\text{Baake}\\ \text{et al.}}}(q) &= \sum_{n=0}^{\infty}(3n+1)\,\chi_{\frac{(2n)^2}{4}}(q) \\ &= \eta^{-1}(q)\left\{\sum_{\mathcal{S}\in\mathbb{Z}} q^{\mathcal{S}^2} + \sum_{\mathcal{S}=1}^{\infty} q^{\mathcal{S}^2}\right\}. \end{aligned} \tag{2.41}$$

This result was found partially through a numerical study.

As explicit q-series, the results are

$$\mathcal{Z}^{(\widehat{D}_4;1,1)}(q) = q^{-1/24}(1 + 3\,q + 4\,q^2 + 7\,q^3 + 13\,q^4 + \mathcal{O}(q^5)) \tag{2.42}$$

and $$\mathcal{Z}^{(\widehat{D}_4;1,1)}_{\substack{\text{Baake}\\ \text{et al.}}}(q) = q^{-1/24}(1 + 4\,q + 5\,q^2 + 9\,q^3 + 17\,q^4 + \mathcal{O}(q^5)) \tag{2.43}$$

respectively. Hence a numerical investigation of the degeneracies will distinguish between these two alternatives very quickly. We find degeneracies in excellent agreement with (2.42), verifying both our theoretical result and that of Saleur and Bauer. We also find agreement with our theoretical predictions for a number of other models. The investigation is discussed in chapter 3.

2.5 Generating Functions

To further analyse the results for the partition functions it will be useful to rewrite the $\Omega_{n,\varepsilon}^{(a_1,\cdots,a_m)}$ in terms of their generating functions:

$$\begin{aligned}\Omega_{\varepsilon}^{(a_1,\cdots,a_m)}(x) &\equiv \sum_{n=0}^{\infty} \Omega_{n,\varepsilon}^{(a_1,\cdots,a_m)}\, x^n \\ &= x^{\varepsilon} \prod_{m'=1}^{m} \frac{1}{(1-x^{a_{m'}})}\,.\end{aligned} \tag{2.44}$$

So that in particular,

$$\begin{aligned}\Omega_{n,\varepsilon}^{(r)} &= \frac{1}{n!}\frac{\mathrm{d}^n}{\mathrm{d}x^n}\bigg|_{x=0} \Omega_{\varepsilon}^{(r)}(x) \\ &= \frac{1}{n!}\frac{\mathrm{d}^n}{\mathrm{d}x^n}\bigg|_{x=0} \frac{x^{\varepsilon}}{(1-x^r)}\end{aligned} \tag{2.45}$$

and

$$\begin{aligned}\Omega_{n,\varepsilon}^{(r,s)} &= \frac{1}{n!}\frac{\mathrm{d}^n}{\mathrm{d}x^n}\bigg|_{x=0} \Omega_{\varepsilon}^{(r,s)}(x) \\ &= \frac{1}{n!}\frac{\mathrm{d}^n}{\mathrm{d}x^n}\bigg|_{x=0} \frac{x^{\varepsilon}}{(1-x^r)(1-x^s)}\,.\end{aligned} \tag{2.46}$$

Using the latter together with result (2.35), the partition function of the $\widehat{A}_{[2h]}$ models may be written as

$$\mathcal{Z}^{(\widehat{A}_{[2h]};0,\varepsilon)}(q) = \sum_{n=0}^{\infty} \chi_{\frac{n^2}{4}}(q) \frac{1}{n!}\frac{\mathrm{d}^n}{\mathrm{d}x^n}\bigg|_{x=0} \frac{x^{\varepsilon}+x^{2h-\varepsilon}}{(1-x^2)(1-x^{2h})}\,. \tag{2.47}$$

Hence, using the fact demonstrated that any affine partition function may be expressed as a sum of $\widehat{A}$ partition functions (2.15), we see that for any affine model

$$\mathcal{Z}^{(\mathcal{G}_{[h]};a,b)}(q) = \sum_{n=0}^{\infty} \chi_{\frac{n^2}{4}}(q) \frac{1}{n!}\frac{\mathrm{d}^n}{\mathrm{d}x^n}\bigg|_{x=0} \frac{\mathsf{P}^{(\mathcal{G}_{[h]};a,b)}(x)}{(1-x^2)(1-x^{2h})}\,, \tag{2.48}$$

with $\mathsf{P}^{(\mathcal{G}_{[h]};a,b)}(x)$ a $2h$-reciprocal polynomial in x (i.e. $x^{2h}\,\mathsf{P}(x^{-1}) = \mathsf{P}(x)$). The polynomials $\mathsf{P}(x)$ may be deduced by examining directly the $\mathcal{G} \longrightarrow \widehat{A}$ decompositions (2.15). However, in general, the coefficients of this polynomial will not be positive (see equation (2.22) as an example). Just as we are able to write $\mathsf{P}(x)$ for the model $(\widehat{A};a,b)$ as a

polynomial with positive coefficients, it would be preferable to be able to do the same for the $\widehat{D}$ and $\widehat{E}$ models. If we can do this while only modifying the powers in the denominators then we will again see that the coefficients of the $\chi_{\frac{n^2}{4}}(q)$ are positive integers. In other words, we wish to write

$$\mathcal{Z}^{(\mathcal{G}_{[h]};a,b)}(q) = \sum_{n=0}^{\infty} \chi_{\frac{n^2}{4}}(q) \frac{1}{n!} \frac{\mathrm{d}^n}{\mathrm{d}x^n}\bigg|_{x=0} \frac{\mathsf{Q}^{(\mathcal{G}_{[h]};a,b)}(x)}{(1-x^r)(1-x^s)} \; ; \tag{2.49}$$

with $\mathsf{Q}(x)$, the "*generating polynomial*", a polynomial with positive integer coefficients. r, s and $\sup\deg \mathsf{Q}(x)$ all constant for a given model. Furthermore, the form (2.49) together with the reciprocity properties of $\mathsf{Q}(x)$ which the $\widehat{A}$ models already satisfy (as demonstrated by (2.47)), are suggestive of a possible relationship with the McKay correspondence [41] which will be explored later in this thesis (chapter 5).

For the $\widehat{D}$ models, it is easiest to compute $\mathsf{Q}(x)$ from (2.39), (2.45) and (2.46) rather than directly from $\mathsf{P}(x)$. The results for the fork nodes of (2.39) suggest that one of the numbers r or s is 4. This is indeed the case as a simple calculation shows that the $\widehat{D}$ models may be placed in the form (2.49) with $r = 4$ and $s = h$. In each case, the polynomial $\mathsf{Q}(x)$ is of degree less than or equal to $h+2$ and is $(h+2)$-reciprocal. The polynomials $\mathsf{Q}^{(\widehat{D}_{[h]};a,b)}(x)$ are listed as part of table 2.2 (page 76).

For the exceptional, $\widehat{E}_n$, cases, we calculate $\mathsf{P}(x)$ from the partition function. From this, we check for each individual boundary condition that we may rewrite the partition function in the form of (2.49) with appropriate integers r and s. For each model, suitable integers were found. Furthermore, the polynomials were again all found to be positive-integer valued and were q-reciprocal for some integer q, with q also the maximal degree of the polynomials. The values of r, s and q being dependent upon the choice of model alone.

The results for r, s and q for all ($\mathbb{Z}_2$-colourable) models are given in table 2.1 (page 75); and the results for the polynomials $\mathsf{Q}(x)$ for the $\widehat{E}_6$, $\widehat{E}_7$ and $\widehat{E}_8$ models appear as tables 2.3, 2.4 and 2.5 respectively (page 77 onwards).

2.6 Comments

2.6.1 Boundary Condition Parity

We remark on the importance of the parity of the boundary conditions (a, b). As observed in section 2.1, a model with an even (odd) boundary condition may expressed in terms of $\widehat{A}$ models with strictly even (odd) boundary conditions. The fact that the Coxeter number h is always even for the models considered and the result (2.30) for the model A_∞ ensures that this property is reflected in the partition functions expressed as Virasoro characters. A model with even (odd) boundary conditions has therefore an expansion (2.25) in terms of Virasoro characters of highest weights $\frac{n^2}{4}$, with n even (odd).

2.6.2 The General Decomposition Coefficients

The coefficients (2.17) are the analogues of the classical intertwiners (1.67). They possess a similar algebraic form and play a similar role. They differ immediately chiefly in that they relate a model with affine Coxeter number h to a model with affine Coxeter number $2h$ and even interrelate $\widehat{A}_n$ models. In contrast, intertwiners interrelate classical models with the Coxeter number preserved in the relation.

It is certainly tempting, given the form A.1 for the eigenvectors $\underset{\sim}{\phi}^{(\mu)}$ of the $\widehat{A}_{[2h]}$ graph, to identify the coefficients (2.17) with the classical intertwiners. Denote by square-parentheses the Coxeter number of the graph to which a vector refers. Then, naïvely

$$\frac{\phi^{(2\mu)}_{[2h]\lambda}}{\phi^{(2\mu)}_{[2h]0}} \equiv \frac{\phi^{(\mu)}_{[h]\lambda}}{\phi^{(\mu)}_{[h]0}} \,. \tag{2.50}$$

However the terms on the right-hand side of this equality are not defined unless μ is even (i.e. an exponent of the $\widehat{A}$ graph); the more general summation over the full exponent set of the graph $\mathcal{G}$ ensures that this is not always the case.

The results of section 2.2.1 manifest most clearly the difference between the classical intertwiners and the new "*affine intertwiners*" (2.17). The classical intertwiners take strictly non-negative integer values; but equations (2.20–2.23) lead us to conjecture that the affine intertwiners (2.17) are half-integers and may have either positive or negative sign. Note that, as seen, this does not contradict the appearance of positive integer multiplicities

in (2.25).

2.6.3 The Partition Functions, Paths and Graph Topology

We note that the results for the A_∞ and $\widehat{A}$ models permit the following interpretation: the quantity $\Omega^{(2)}_{n,\varepsilon}$ may be interpreted as the number of *topologically distinct paths* between the nodes 0 and ε on the graph A_∞; i.e. 1 or 0 depending on the parity of the path between the two nodes. The result $\Omega^{(2,2h)}_{n,\varepsilon} + \Omega^{(2,2h)}_{n,2h-\varepsilon}$ for the graph $\widehat{A}_{[2h]}$ also has this interpretation. Indeed, the cyclicity $2h$ of the graph introduces two sets of topologically distinct paths between any two nodes: we may travel between the two nodes 0 and ε either the "long" (negative) or the "short" (positive) way and we may also loop around the graph an arbitrary number of times inducing a winding number (and thereby producing topologically distinct paths). The two parts of the $\widehat{A}$ result thus correspond to the positive and negative windings about the $\widehat{A}$ graph.

Generalising this interpretation to the $\widehat{D}_{[h]}$ cases is complicated. The cases where the boundary conditions do not involve both boundary nodes on the same fork of the $\widehat{D}$ graph have again this topological interpretation once we count a visit to one of the end nodes as equivalent to crossing to the other half of a circle. The cases $(\widehat{D}; X, {}^{(}\overline{X}{}^{)})$ do not generalise so trivially as in each case one half of the zeroth winding sector disappears.

In particular, in all cases including the exceptional $\widehat{E}$ models, the first Virasoro character to appear in the expansion (2.25) is $\chi_{\frac{\mathbb{K}^2}{4}}(q)$ where $\mathbb{K} \equiv \mathbb{K}_{ab}$ is the length of the shortest path on $\mathcal{G}$ between a and b. Thus, the highest weight of the lowest energy level of any given model is $h_{(a,b)} = \mathbb{K}^2/4$ (recall the discussion of section 1.2.5).

2.6.4 Model Equivalences

In any case it is interesting to note that the result (2.35) for the model $(\widehat{A}_{[h]}; 0, \varepsilon)$ (i.e. with even h substituted for $2h$) and the result (2.39) for the model $(\widehat{D}_{[h]}; X, \varepsilon)$ (i.e. with the boundary conditions set up so that the value at one end is a fork node, X, and taking $\varepsilon \equiv a$) indicate that these two models (on the cylinder) are entirely equivalent, at least in the continuum limit.

2.6.5 The Models and the Virasoro Algebra

We note that the Virasoro characters appearing in equation (2.25) are degenerate $c = 1$ characters. All the affine $\widehat{A}\widehat{D}\widehat{E}$ models may now be written in this form, demonstrating as promised, that each of these models provides a (typically reducible) representation of the $c = 1$ Virasoro algebra.

Model	h	$\overline{h}$	r	s	$\mathsf{q} \equiv \sup\deg \mathrm{Q}(x)$
$\widehat{A}_{2n-1}$	$2n$	$2n$	2	$2n$	$2n$
$\widehat{D}_{n+2}$	$2n$	$2n+2$	4	$2n$	$2n+2$
$\widehat{E}_6$	6	12	6	8	12
$\widehat{E}_7$	12	18	8	12	18
$\widehat{E}_8$	30	30	12	20	30

Table 2.1: Results for r and s appearing in (2.49) and $\mathsf{q} \equiv \sup\deg \mathrm{Q}(x)$ for each of the affine models (except $\widehat{A}_{2n}$). We note in each case that the polynomial $\mathrm{Q}(x)$ has positive integer coefficients and is q-reciprocal (i.e. $x^{\mathsf{q}}\,\mathrm{Q}(x^{-1}) = \mathrm{Q}(x)$). The affine Coxeter number h is also stated for each model $\widehat{X}_n$ together with the Coxeter number $\overline{h}$ of the related classical algebra X_n.

Model $(\mathcal{G}; a, b)$	Coefficient $\Lambda_n^{(\mathcal{G};a,b)}$ of $\chi_{\frac{n^2}{4}}(q)$ Generating Polynomial $\mathrm{Q}^{(\mathcal{G};a,b)}(x)$
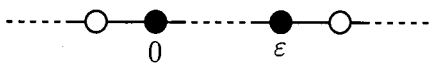	$\Omega^{(2)}_{n,\varepsilon}$ ———
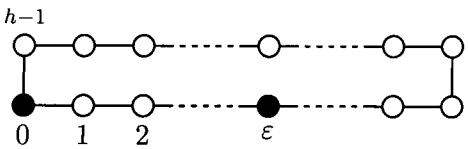	$\Omega^{(2,h)}_{n,\varepsilon} + \Omega^{(2,h)}_{n,h-\varepsilon}$ $x^{\varepsilon} + x^{h-\varepsilon}$
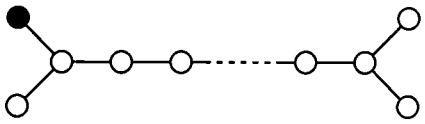	$\Omega^{(2,h)}_{n,h} + \Omega^{(4)}_{n,0}$ $1 + x^{h+2}$
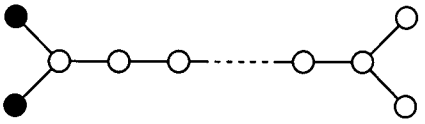	$\Omega^{(2,h)}_{n,h} + \Omega^{(4)}_{n,2}$ $x^2 + x^h$
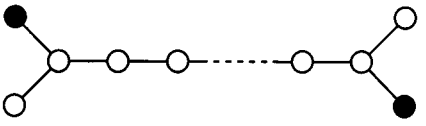	$\Omega^{(2,h)}_{n,\frac{h}{2}}$ $x^{\frac{h}{2}} + x^{\frac{h}{2}+2}$
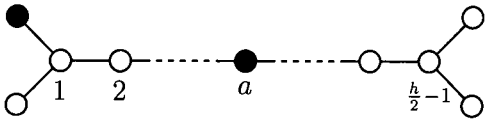	$\Omega^{(2,h)}_{n,a} + \Omega^{(2,h)}_{n,h-a}$ $x^a + x^{a+2} + x^{h-a} + x^{h-a+2}$
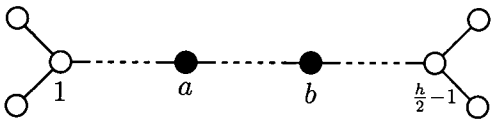	$\Omega^{(2,h)}_{n,\lvert a-b\rvert} + \Omega^{(2,h)}_{n,h-\lvert a-b\rvert} + \Omega^{(2,h)}_{n,\lvert a+b\rvert} + \Omega^{(2,h)}_{n,h-\lvert a+b\rvert}$ $x^{\lvert a-b\rvert} + x^{\lvert a-b\rvert+2} + x^{\lvert a+b\rvert} + x^{\lvert a+b\rvert+2} +$ $x^{h-\lvert a-b\rvert} + x^{h+2-\lvert a-b\rvert} + x^{h-\lvert a+b\rvert} + x^{h+2-\lvert a+b\rvert}$

Table 2.2: Coefficients $\Lambda_n^{(\mathcal{G};a,b)}$ in the expansion (2.25) and the generating polynomial $\mathrm{Q}^{(\mathcal{G};a,b)}(x)$ in the expression (2.49), for the partition functions of the A_∞, $\widehat{A}_{[h]}$ and $\widehat{D}_{[h]}$ based models. The graph $\mathcal{G}$ is indicated graphically, the boundary conditions a, b are indicated by coloured nodes.

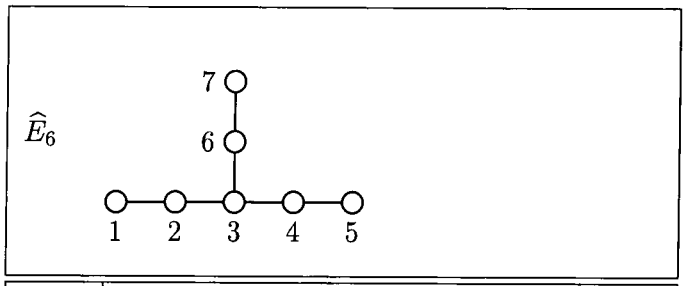

(a,b)	$Q^{(\widehat{E}_6;a,b)}(x)$
$(1,1)$	$1+x^{12}$
$(1,2)$	$x+x^5+x^7+x^{11}$
$(1,3)$	$x^2+x^4+2\,x^6+x^8+x^{10}$
$(1,4)$	$x^3+x^5+x^7+x^9$
$(1,5)$	x^4+x^8
$(2,2)$	$1+x^2+x^4+2\,x^6+x^8+x^{10}+x^{12}$
$(2,3)$	$x+2\,x^3+3\,x^5+3\,x^7+2\,x^9+x^{11}$
$(2,4)$	$x^2+2\,x^4+2\,x^6+2\,x^8+x^{10}$
$(3,3)$	$1+2\,x^2+4\,x^4+4\,x^6+4\,x^8+2\,x^{10}+x^{12}$

Table 2.3: Generating polynomial $Q^{(\widehat{E}_6;a,b)}(x)$ in the expression (2.49) for the partition functions of the 9 independent $\widehat{E}_6$ based models.

$\widehat{E}_7$

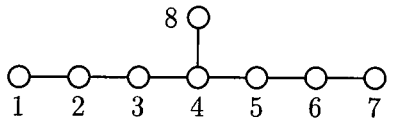

(a,b)	$Q^{(\widehat{E}_7;a,b)}(x)$
$(1,1)$	$1+x^{18}$
$(1,2)$	$x+x^{7}+x^{11}+x^{17}$
$(1,3)$	$x^{2}+x^{6}+x^{8}+x^{10}+x^{12}+x^{16}$
$(1,4)$	$x^{3}+x^{5}+x^{7}+2\,x^{9}+x^{11}+x^{13}+x^{15}$
$(1,5)$	$x^{4}+x^{6}+x^{8}+x^{10}+x^{12}+x^{14}$
$(1,6)$	$x^{5}+x^{7}+x^{11}+x^{13}$
$(1,7)$	$x^{6}+x^{12}$
$(2,2)$	$1+x^{2}+x^{6}+x^{8}+x^{10}+x^{12}+x^{16}+x^{18}$
$(2,3)$	$x+x^{3}+x^{5}+2\,x^{7}+2\,x^{9}+2\,x^{11}+x^{13}+x^{15}+x^{17}$
$(2,4)$	$x^{2}+2\,x^{4}+2\,x^{6}+3\,x^{8}+3\,x^{10}+2\,x^{12}+2\,x^{14}+x^{16}$
$(2,5)$	$x^{3}+2\,x^{5}+2\,x^{7}+2\,x^{9}+2\,x^{11}+2\,x^{13}+x^{15}$
$(2,6)$	$x^{4}+2\,x^{6}+x^{8}+x^{10}+2\,x^{12}+x^{14}$
$(3,3)$	$1+x^{2}+2\,x^{4}+2\,x^{6}+3\,x^{8}+3\,x^{10}+2\,x^{12}+2\,x^{14}+x^{16}+x^{18}$
$(3,4)$	$x+2\,x^{3}+3\,x^{5}+4\,x^{7}+4\,x^{9}+4\,x^{11}+3\,x^{13}+2\,x^{15}+x^{17}$
$(3,5)$	$x^{2}+2\,x^{4}+3\,x^{6}+3\,x^{8}+3\,x^{10}+3\,x^{12}+2\,x^{14}+x^{16}$
$(4,4)$	$1+2\,x^{2}+3\,x^{4}+5\,x^{6}+5\,x^{8}+5\,x^{10}+5\,x^{12}+3\,x^{14}+2\,x^{16}+x^{18}$
$(1,8)$	$x^{4}+x^{8}+x^{10}+x^{14}$
$(2,8)$	$x^{3}+x^{5}+x^{7}+2\,x^{9}+x^{11}+x^{13}+x^{15}$
$(3,8)$	$x^{2}+x^{4}+2\,x^{6}+2\,x^{8}+2\,x^{10}+2\,x^{12}+x^{14}+x^{16}$
$(4,8)$	$x+x^{3}+2\,x^{5}+3\,x^{7}+2\,x^{9}+3\,x^{11}+2\,x^{13}+x^{15}+x^{17}$
$(8,8)$	$1+x^{4}+x^{6}+x^{8}+x^{10}+x^{12}+x^{14}+x^{18}$

Table 2.4: Generating polynomial $Q^{(\widehat{E}_7;a,b)}(x)$ in the expression (2.49) for the partition functions of the 21 independent $\widehat{E}_7$ based models.

$\widehat{E}_8$

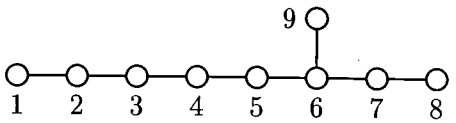

(a,b)	$\mathrm{Q}^{(\widehat{E}_8;a,b)}(x)$
$(1,1)$	$1 + x^{30}$
$(1,2)$	$x + x^{11} + x^{19} + x^{29}$
$(1,3)$	$x^2 + x^{10} + x^{12} + x^{18} + x^{20} + x^{28}$
$(1,4)$	$x^3 + x^9 + x^{11} + x^{13} + x^{17} + x^{19} + x^{21} + x^{27}$
$(1,5)$	$x^4 + x^8 + x^{10} + x^{12} + x^{14} + x^{16} + x^{18} + x^{20} + x^{22} + x^{26}$
$(1,6)$	$x^5 + x^7 + x^9 + x^{11} + x^{13} + 2\,x^{15} + x^{17} + x^{19} + x^{21} + x^{23} + x^{25}$
$(1,7)$	$x^6 + x^8 + x^{12} + x^{14} + x^{16} + x^{18} + x^{22} + x^{24}$
$(1,8)$	$x^7 + x^{13} + x^{17} + x^{23}$
$(1,9)$	$x^6 + x^{10} + x^{14} + x^{16} + x^{20} + x^{24}$
$(2,2)$	$1 + x^2 + x^{10} + x^{12} + x^{18} + x^{20} + x^{28} + x^{30}$
$(2,3)$	$x + x^3 + x^9 + 2\,x^{11} + x^{13} + x^{17} + 2\,x^{19} + x^{21} \ + x^{27} + x^{29}$
$(2,4)$	$x^2 + x^4 + x^8 + 2\,x^{10} + 2\,x^{12} + x^{14} + x^{16} + 2\,x^{18} + 2\,x^{20} + x^{22} + x^{26} + x^{28}$

Continued overleaf . . .

Continued from preceding page.

(a,b)	$Q^{(\widehat{E}_8;a,b)}(x)$
$(2,5)$	$x^3+x^5+x^7+2x^9+2x^{11}+2x^{13}+2x^{15}+2x^{17}+2x^{19}+2x^{21}+x^{23}+x^{25}+x^{27}$
$(2,6)$	$x^4+2x^6+2x^8+2x^{10}+2x^{12}+3x^{14}+3x^{16}+2x^{18}+2x^{20}+2x^{22}+2x^{24}+x^{26}$
$(2,7)$	$x^5+2x^7+x^9+x^{11}+2x^{13}+2x^{15}+2x^{17}+x^{19}+x^{21}+2x^{23}+x^{25}$
$(2,8)$	$x^6+x^8+x^{12}+x^{14}+x^{16}+x^{18}+x^{22}+x^{24}$
$(2,9)$	$x^5+x^7+x^9+x^{11}+x^{13}+2x^{15}+x^{17}+x^{19}+x^{21}+x^{23}+x^{25}$
$(3,3)$	$1+x^2+x^4+x^8+2x^{10}+2x^{12}+x^{14}+x^{16}+2x^{18}+2x^{20}+x^{22}+x^{26}+x^{28}+x^{30}$
$(3,4)$	$x+x^3+x^5+x^7+2x^9+3x^{11}+2x^{13}+2x^{15}+2x^{17}+3x^{19}+2x^{21}+x^{23}+x^{25}+x^{27}+x^{29}$
$(3,5)$	$x^2+x^4+2x^6+2x^8+3x^{10}+3x^{12}+3x^{14}+3x^{16}+3x^{18}+3x^{20}+2x^{22}+2x^{24}+x^{26}+x^{28}$
$(3,6)$	$x^3+2x^5+3x^7+3x^9+3x^{11}+4x^{13}+4x^{15}+4x^{17}+3x^{19}+3x^{21}+3x^{23}+2x^{25}+x^{27}$
$(3,7)$	$x^4+2x^6+2x^8+2x^{10}+2x^{12}+3x^{14}+3x^{16}+2x^{18}+2x^{20}+2x^{22}+2x^{24}+x^{26}$
$(3,8)$	$x^5+x^7+x^9+x^{11}+x^{13}+2x^{15}+x^{17}+x^{19}+x^{21}+x^{23}+x^{25}$
$(3,9)$	$x^4+x^6+2x^8+x^{10}+2x^{12}+2x^{14}+2x^{16}+2x^{18}+x^{20}+2x^{22}+x^{24}+x^{26}$
$(4,4)$	$1+x^2+x^4+2x^6+2x^8+3x^{10}+3x^{12}+3x^{14}+3x^{16}+3x^{18}+3x^{20}+2x^{22}+2x^{24}+x^{26}+x^{28}+x^{30}$
$(4,5)$	$x+x^3+2x^5+3x^7+3x^9+4x^{11}+4x^{13}+4x^{15}+4x^{17}+4x^{19}+3x^{21}+3x^{23}+2x^{25}+x^{27}+x^{29}$
$(4,6)$	$x^2+2x^4+3x^6+4x^8+4x^{10}+5x^{12}+5x^{14}+5x^{16}+5x^{18}+4x^{20}+4x^{22}+3x^{24}+2x^{26}+x^{28}$

Continued overleaf . . .

Continued from preceding page.

(a,b)	$\mathrm{Q}^{(\widehat{E}_8;a,b)}(x)$
$(4,7)$	$x^3+2x^5+2x^7+3x^9+3x^{11}+3x^{13}+4x^{15}+3x^{17}+3x^{19}+3x^{21}+2x^{23}+2x^{25}+x^{27}$
$(4,8)$	$x^4+x^6+x^8+2x^{10}+x^{12}+2x^{14}+2x^{16}+x^{18}+2x^{20}+x^{22}+x^{24}+x^{26}$
$(4,9)$	$x^3+x^5+2x^7+2x^9+2x^{11}+3x^{13}+2x^{15}+3x^{17}+2x^{19}+2x^{21}+2x^{23}+x^{25}+x^{27}$
$(5,5)$	$1+x^2+2x^4+3x^6+4x^8+4x^{10}+5x^{12}+5x^{14}+5x^{16}+5x^{18}+4x^{20}+4x^{22}+3x^{24}+2x^{26}+x^{28}+x^{30}$
$(5,6)$	$x+2x^3+3x^5+4x^7+5x^9+6x^{11}+6x^{13}+6x^{15}+6x^{17}+6x^{19}+5x^{21}+4x^{23}+3x^{25}+2x^{27}+x^{29}$
$(5,7)$	$x^2+2x^4+2x^6+3x^8+4x^{10}+4x^{12}+4x^{14}+4x^{16}+4x^{18}+4x^{20}+3x^{22}+2x^{24}+2x^{26}+x^{28}$
$(5,8)$	$x^3+x^5+x^7+2x^9+2x^{11}+2x^{13}+2x^{15}+2x^{17}+2x^{19}+2x^{21}+x^{23}+x^{25}+x^{27}$
$(5,9)$	$x^2+x^4+2x^6+2x^8+3x^{10}+3x^{12}+3x^{14}+3x^{16}+3x^{18}+3x^{20}+2x^{22}+2x^{24}+x^{26}+x^{28}$
$(6,6)$	$1+2x^2+3x^4+4x^6+5x^8+7x^{10}+7x^{12}+7x^{14}+7x^{16}+7x^{18}+7x^{20}+5x^{22}+4x^{24}+3x^{26}+2x^{28}+x^{30}$
$(6,7)$	$x+2x^3+2x^5+3x^7+4x^9+5x^{11}+5x^{13}+4x^{15}+5x^{17}+5x^{19}+4x^{21}+3x^{23}+2x^{25}+2x^{27}+x^{29}$
$(6,8)$	$x^2+x^4+x^6+2x^8+2x^{10}+3x^{12}+2x^{14}+2x^{16}+3x^{18}+2x^{20}+2x^{22}+x^{24}+x^{26}+x^{28}$
$(6,9)$	$x+x^3+2x^5+2x^7+3x^9+4x^{11}+3x^{13}+4x^{15}+3x^{17}+4x^{19}+3x^{21}+2x^{23}+2x^{25}+x^{27}+x^{29}$
$(7,7)$	$1+x^2+x^4+2x^6+2x^8+3x^{10}+3x^{12}+3x^{14}+3x^{16}+3x^{18}+3x^{20}+2x^{22}+2x^{24}+x^{26}+x^{28}+x^{30}$
$(7,8)$	$x+x^5+x^7+x^9+2x^{11}+x^{13}+2x^{15}+x^{17}+2x^{19}+x^{21}+x^{23}+x^{25}+x^{29}$
$(7,9)$	$x^2+x^4+x^6+2x^8+2x^{10}+3x^{12}+2x^{14}+2x^{16}+3x^{18}+2x^{20}+2x^{22}+x^{24}+x^{26}+x^{28}$

Continued overleaf . . .

Continued from preceding page.

(a,b)	$\mathrm{Q}^{(\widehat{E}_8;a,b)}(x)$
$(8,8)$	$1+x^6+x^{10}+x^{14}+x^{16}+x^{20}+x^{24}+x^{30}$
$(8,9)$	$x^3+x^7+x^9+x^{11}+2\,x^{13}+2\,x^{17}+x^{19}+x^{21}+x^{23}+x^{27}$
$(9,9)$	$1+x^4+x^6+x^8+2\,x^{10}+x^{12}+2\,x^{14}+2\,x^{16}+x^{18}+2\,x^{20}+x^{22}+x^{24}+x^{26}+x^{30}$

Table 2.5: Generating polynomial $\mathrm{Q}^{(\widehat{E}_8;a,b)}(x)$ in the expression (2.49) for the partition functions of the 45 independent $\widehat{E}_8$ based models.

Chapter 3

Numerical Verification

In this chapter, we discuss the numerical analysis carried out on the results, displayed as tables 2.1–2.5, for a subset of these affine models. It was considered necessary to carry out such a study as there is a lack of known results for affine Pasquier models currently existing in the literature. As already mentioned in section 2.4, we know of only two results, both for the 4-state Potts model with free boundary conditions on either end of the cylinder. The first of these results, that of Saleur and Bauer [50] is summarised by equation (2.42); and the second, that of Baake *et al.* [2] by (2.43). These results do not agree. The former does, however, agree with our own theoretical result as discussed in section 2.4. The purpose of the numerical study described here is, therefore, both to corroborate generally the results found for the models in chapter 2 and to refute our interpretation of the result of [2], i.e. (2.43).

We make use of the theory of finite-size scaling discussed in section 1.2.6. By examining the spectrum of the Hamiltonian or transfer matrix for lattice approximations of different lengths to a given model, we observe the degeneracies $\{N_n\}$ of the energy levels, the scaling dimensions $\{x_n\}$ and by examining specifically the ground state, we attempt to infer the value of the central charge c.

In section 3.1 we discuss the algorithm used to calculate and diagonalise the transfer matrices of the models examined. This consists of a review of the algorithm (except for the interpretation, not in itself original), a discussion of modifications to this algorithm made by us (original) and notes specific to our implementation. Finally, in section 3.2, we

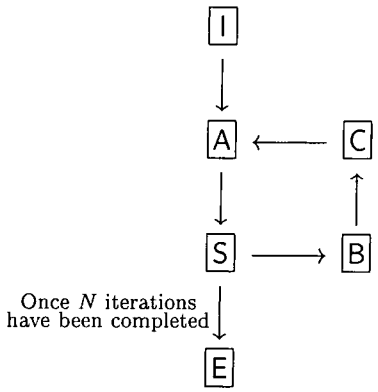

Figure 3.1: Schematic diagram of the power method algorithm.

state our results and conclusions (original).

3.1 Algorithm and Implementation

The eigenvalues of the Hamiltonian for a model based on a cylinder of length L are found by first diagonalising the transfer matrix T. As the Hilbert space of states $\mathcal{H}$ is typically quite large even for small cylinder lengths, it is impractical to diagonalise T entirely. Instead we choose to find only the first few eigenvalues using a *power method algorithm* (see [32]). This algorithm begins with a set of vectors $\{v_i\}$, the number of which is much smaller than the dimension, $\dim \mathcal{H}$, of the Hilbert space and for a matrix with strictly positive eigenvalues such as T, iteratively brings them to approximates of the eigenvectors with greatest eigenvalues. The procedure is illustrated schematically in figure 3.1. The individual steps [I], [A], [S], [B], [C] and [E] are:

[I] Initialise a set of (distinct) vectors $\left\{ \underset{\sim}{v_i} \mid 0 \leq i < n \right\}$.

[A] Multiply each vector $\underset{\sim}{v_i}$ by the transfer matrix T; i.e. $\underset{\sim}{v_i} \mapsto T \underset{\sim}{v_i}$.

[S] This step is not present in the basic algorithm (i.e. it does nothing). However we found it necessary to introduce some modifications to the algorithm at this point. These will be discussed later in the text.

[B] Subtract out the overlap that each vector now has with the preceding vectors;

i.e.

$$\underset{\sim}{v_j} \mapsto \underset{\sim}{v_j} - \sum_{i<j} (\underset{\sim}{v_j} \cdot \underset{\sim}{\widehat{v}_i})\, \underset{\sim}{\widehat{v}_i} \, .$$

The vector $\underset{\sim}{v_0}$ is invariant.

C Renormalise the vectors so that each is of unit length; i.e.

$$\underset{\sim}{v_j} \mapsto \underset{\sim}{\widehat{v}_j} \equiv \frac{\underset{\sim}{v_j}}{|\underset{\sim}{v_j}|} \, .$$

E End of procedure. We estimate the first n eigenvalues, λ_i, $0 \leq i \leq n$, of the transfer matrix by again multiplying each vector $\underset{\sim}{v_i}$ by T. The associated eigenvalue is given by the length of this new vector; i.e.

$$\lambda_i \approx |T\, \underset{\sim}{\widehat{v}_i}| \quad \text{for each } 0 \leq i \leq n.$$

The steps in the main loop: A, S, B and C are carried out in sequence some number, N, times before executing step E.

The repeated application of T and subtraction off of the lower eigenvectors, eventually stretches each vector $\underset{\sim}{v_i}$ in the direction of the eigenvector $\underset{\sim}{e_i}$. Indeed, consider the vector $\underset{\sim}{v_i}$ expressed in terms of the true eigenvectors $\{\underset{\sim}{e_j}\}$, ordered so that the associated eigenvalues satisfy $\lambda_j \geq \lambda_i$, for all $j < i$; i.e.

$$\underset{\sim}{v_i} \equiv \sum_j v_i^j \, \underset{\sim}{e_j} \, ; \tag{3.1}$$

then, upon multiplication by T,

$$v_i^j \mapsto \lambda_j \, v_i^j \, . \tag{3.2}$$

Repeated multiplications increase the power of λ_j so that $\underset{\sim}{v_i}$ becomes dominated by the component in the direction of the eigenvector with the largest eigenvalue, namely $\underset{\sim}{e_0}$. If the components in the directions of the first i eigenvectors (i.e. the eigenvectors with the

highest i eigenvalues) are subtracted out at each step, then $\underset{\sim}{v_i}$ will be instead dominated by the component in the direction of $\underset{\sim}{e_i}$. The best estimate of $\underset{\sim}{e_j}$ at any time is $\underset{\sim}{v_j}$, so in step [B], the $\{\underset{\sim}{v_i}\}$ are used to perform this subtraction. Typically, one obtains good estimates of the 'highest lying' eigenvectors and their eigenvalues by performing the loop [A]-[S]-[B]-[C], $N \sim 200$ times.

The exact manner of the initialisation, step [I], is not critical provided the vectors chosen have a significant overlap with the eigenvectors they are supposed eventually to approximate. We chose the first n unit basis vectors w.r.t. the basis provided for the Hilbert space by the paths on $\mathcal{G}$ of length L between a and b. Such a choice has the added advantage that the vectors are orthonormal from the outset. Any such randomly chosen vectors will, more than likely, overlap the 'highest eigenvectors' to some degree. With the exception of numerical rounding errors, therefore, we do not expect there to be any problem in finding the corresponding eigenvalues with the correct degeneracies. Experiments with alternative choices of initial vectors demonstrated that the chances of choosing a bad initial set are indeed negligible.

The algorithm was implemented using the C programming language. Given the adjacency matrix $\mathcal{G}$, Perron-Frobenius eigenvector $\underset{\sim}{\psi}$ and boundary conditions a and b for a model on a cylinder of fixed length L (or equivalently, on an infinite strip of width L); the Boltzmann weights and transfer matrix $T \equiv T(L)$ for the model are calculated. A set $\{ v_i \mid 0 \leq i \leq n \}$ of vectors is initialised and the first n eigenvalues are found using the algorithm as described. For each model $(\mathcal{G}; a, b)$ examined, this was repeated for a number of cylinder lengths. As L is finite, for given boundary conditions a and b, the parity of L and the parity of the paths between a and b must match. Hence L is incremented in jumps of 2.

We performed a number of tests on the program as implemented using models with results appearing elsewhere in the literature, for example the models of [50] and also the periodic (toroidal) versions of the Ising and 3-state Potts models (circumference L). We are able to reproduce data in agreement with theoretical predictions. This serves as a check on the correctness of the implementation.

It was discovered in the new affine cases, that eigenvalues were initially often found with incorrect degeneracies. There appeared to be some roughly periodic instability in the convergence towards the correct eigenvalues as examinations of the eigenvalues found after successive iterations of the main loop demonstrated (for high N). This was suggestive of there being some rotation of the approximate eigenvectors associated with a degenerate eigenspace taking place from iteration to iteration. This would interfere with the subtraction of step [B]. Empirically, it was discovered that this instability is removed by modifying the basic algorithm by estimating the eigenvalues, as in step [E], and sorting the eigenvectors v_i into order so that $\lambda_i \geq \lambda_j$ whenever $i < j$. A simple bubble sort is used for this and implemented as step [S] (refer to figure 3.1). The reason this is required is unclear. It might be the case that the choice of initial vectors at step [I] is somehow more important than supposed. However, using different initial choices of $\{\underset{\sim}{v_n}\}$ does not improve the results. Also examining when the sort algorithm is invoked it is seen that the eigenvectors are still being sorted even when the number of iterations N is large. The fact that it is not necessary to perform the sort in order to verify the results of [50] or of the periodic Ising and 3-state Potts models, suggests that the extra symmetries of the affine graphs are perhaps, somehow, the root cause.

3.2 Results, Analysis and Conclusions

We examined the energy levels (i.e. the eigenvalues of the Hamiltonian) produced for the models based upon the $\widehat{A}_3$, $\widehat{A}_5$, $\widehat{D}_4$ and $\widehat{D}_5$ graphs. These graphs are generally small enough so that $\dim\mathcal{H}$ is in turn small enough at a given cylinder-length L so as to allow sufficient data to be gathered for analysis.

Typically, we examined the behaviour of the first $n \sim 30$ levels for a range of values of L with L ranging from 5 to 14; the upper limit being determined by the dimension of the resulting Hilbert space of paths between the cylinder ends and the limitations of the computing facilities available. We were able to diagonalise transfer matrices of order 7000×7000 without problem. At each value of L we diagonalised using $N \sim 1000$ iterations of the loop A-S-B-C even though the eigenvalues appeared to converge much faster than this.

3.2.1 Scaling Dimensions and Degeneracies

The first analysis consists of examining the scaling dimensions and their degeneracies and comparing the results with the theoretical predictions read off from the partition functions using equation (1.136) or more properly (1.138). The scaling dimensions of the operators present in the theory are related to the gaps in the energy levels by equation (1.137). Thus

$$\frac{L\,\Delta E_n}{\pi} \sim \Delta x_n \,. \tag{3.3}$$

So that the general trend of the scaling dimensions as $L \to \infty$ may be examined by plotting a graph of $L\,\Delta E_n/\pi$ against $1/L$. This general trend combined with direct examination of the numerical data is used to determine the degeneracies.

This procedure was carried out for each of the boundary conditions on the models stated above. Unfortunately, little information on the scaling dimensions can be inferred from the data as the higher energy levels are found to converge slowly as $L \to \infty$. This is a property of finite-size scaling alone and not an artifact of the diagonalisation scheme used. However, the next-to-ground state of most models is seen to tend to $\Delta x_1 = 1$ as expected. A typical example is provided by the model $(\widehat{D}_5; X, \overline{X})$ in figure 3.3. Exceptions are the models

$(\widehat{D}_5; X, X)$, $(\widehat{D}_6; X, X)$ and $(\widehat{D}_5; 1, 2)$. In the first two cases, this is entirely reassuring as in fact, as can be seen from the list of partition functions in table 3.1, this energy state has zero-multiplicity. It is not possible to tell if the next state, ΔE_2, converges properly to the expected $\Delta x_2 = 2$, as may be seen in figure 3.6, as the convergence is too slow. In the last case, $(\widehat{D}_5; 1, 2)$, it appears that a numerical artifact has corrupted the scaling data (refer to figure 3.5). This will also be discussed below in regard to the degeneracies.

The degeneracies, to the degree to which they are clearly defined in the data, are given in table 3.1. The quality of the numerical data is generally quite good in that degeneracies are typically well defined for at least the first three levels. The degeneracies are determined: first by estimating them by qualitatively examining the general trend of the energy levels and the numerical data directly; then the data is re-examined more quantitatively to ensure that the degenerate energy levels all lie within a certain percentage of the mean value for that level. This percentage is no more than 12% in any case but is typically around 5% or less. Where the gap does not exceed 25% of the value of the higher of two supposed levels, we assume that the two levels cannot be resolved and we do not state these levels here*.

Generally speaking, the results obtained are quite good with the degeneracies, so far as they can be determined, in agreement with the theoretical predictions of the preceding chapter.

An example of a particularly good result is that of the 4-state Potts model with free boundary conditions (i.e. $(\widehat{D}_4; 1, 1)$ in the notation of appendix A). The graph of $L\,\Delta E_n/\pi$ against $1/L$ for this model appears as figure 3.2. The lines appear closely bunched together with well defined degeneracies for the first five levels. The observed degeneracies, '$1, 3, 4, 6, 13, \ldots$', compare exceptionally well with the prediction of equation (2.42), i.e. '$1, 3, 4, 7, 13, \ldots$'. There is a slight discrepancy in the fourth degeneracy, however this may be accounted for by the fact that the Hilbert space at $L = 12$ is a poor approximation to the Hilbert space of the continuum model. Our interpretation (2.43) of the result found by Baake *et al.* [2] is, however, conclusively refuted. We also observe the trend towards

*We are grateful to Robert Weston for suggesting this quantitative definition of the degeneracies.

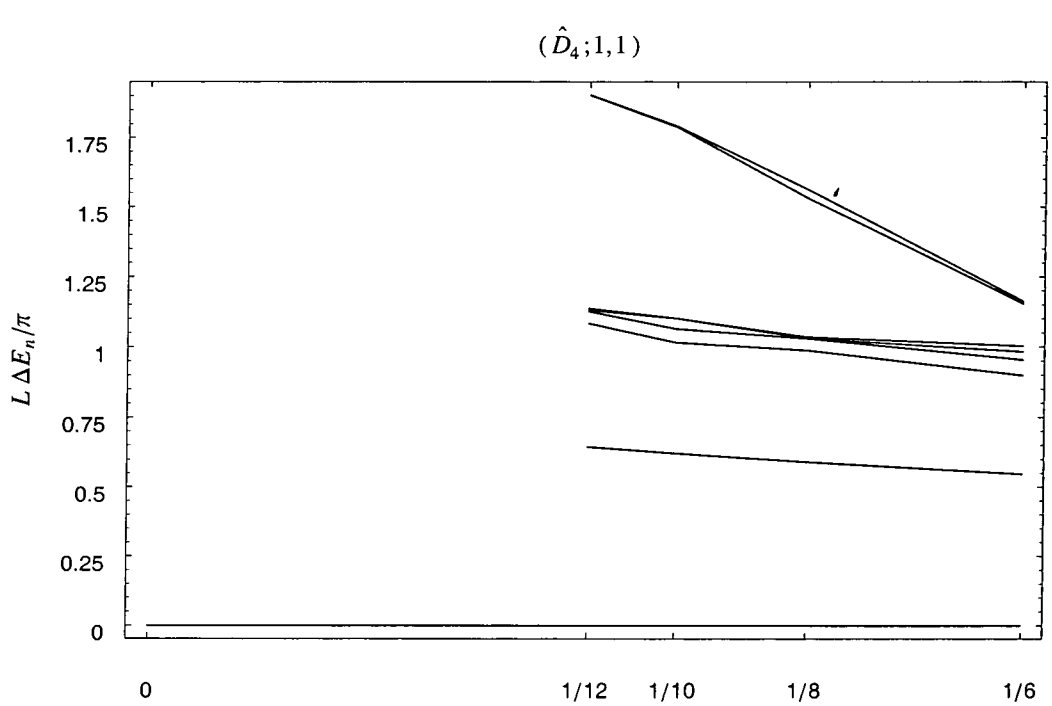

Figure 3.2: Scaled energy gap, $L\,\Delta E_n/\pi$, vs. inverse length, $1/L$, for the 4-state Potts model with free boundary conditions. The degeneracies are clearly defined, and for each group of lines are: '$1, 3, 4, 6, 13, \ldots$', in good agreement with the exact degeneracies, '$1, 3, 4, 7, 13, \ldots$'. The next-to-ground state also appears to tend to $\Delta x_1 = 1$. Only the first 10 levels are shown above.

the predicted integer scaling dimension $\Delta x_1 = 1$ as $L \to \infty$. Other results of this quality are found for the models $(\widehat{A}_3; 0, 2)$ and $(\widehat{A}_5; 0, 3)$. These models are peculiar in that there is a doubling in the degeneracies (the degeneracies are all divisible by 2) due to the existence of an energy-preserving involution on the paths between either end of the cylinder $(a \leftrightarrow h - a)$ and hence on the configurations of the model.

Typically we are able to extract clear degeneracies for only the first three levels. Figure 3.3 shows the graph of $L\,\Delta E_n/\pi$ vs. inverse length, $1/L$, for the model $(\widehat{D}_5; X, \overline{X})$. This data is typical, with degeneracies and the trend towards the predicted scaling dimension $\Delta x_1 = 1$ clearly visible.

Less well-defined degeneracies are produced for the $(\widehat{A}_3; 0, 1)$, $(\widehat{A}_5; 0, 1)$ and $(\widehat{D}_4; X, 1)$ models. The first couple of degeneracies are correct, however the graph of $L\,\Delta E_n/\pi$ vs.

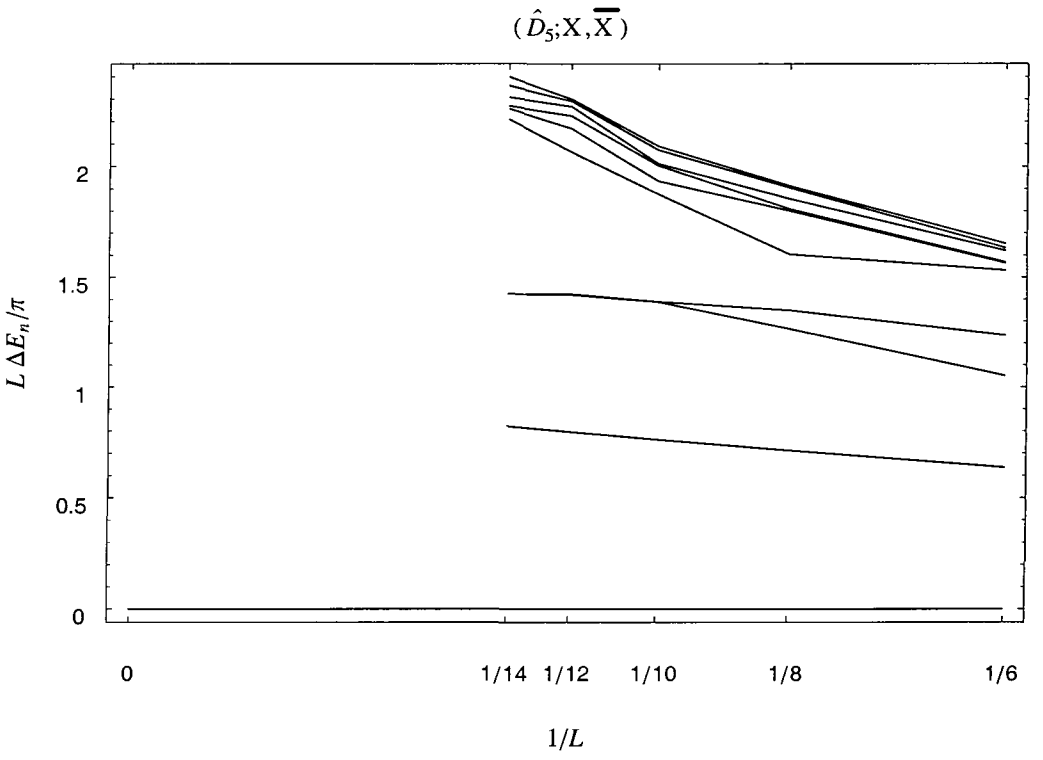

Figure 3.3: Scaled energy gap, $L\,\Delta E_n/\pi$, vs. inverse length, $1/L$, for the model $(\widehat{D}_5; X, \overline{X})$. The observed degeneracies are: '$1, 1, 2, \ldots$'. This graph is typical of the results obtained for most models. The lines are clearly bunched together giving well-defined degeneracies for the first three levels. The trend towards $\Delta x_1 \to 1$ as $L \to \infty$ is clear.

$1/L$ for $(\widehat{A}_5; 0, 1)$ (figure 3.4) demonstrates how in these cases the next two degeneracies have grouped together; these higher levels have not yet clearly split away from each other. We observe degeneracies of '$1, 1, 5, \ldots$' which look likely to eventually split to give '$1, 1, 2, 3, \ldots$'. These results are not inconsistent with the theory as the predicted degeneracies do look likely to develop as L is increased.

There were a small number of models for which the data does not at first glance appear to be as expected or displays peculiarities. These require comment:

The data for $(\widehat{D}_5; 1, 2)$ appears in figure 3.5 and shows how perhaps numerical errors of some kind have corrupted the data. The data behaves roughly as expected until the final calculation ($L = 11$) regathers the lines together. This appears to be a numerical artifact as we find approximately the degeneracies we are looking for once this final set of data is

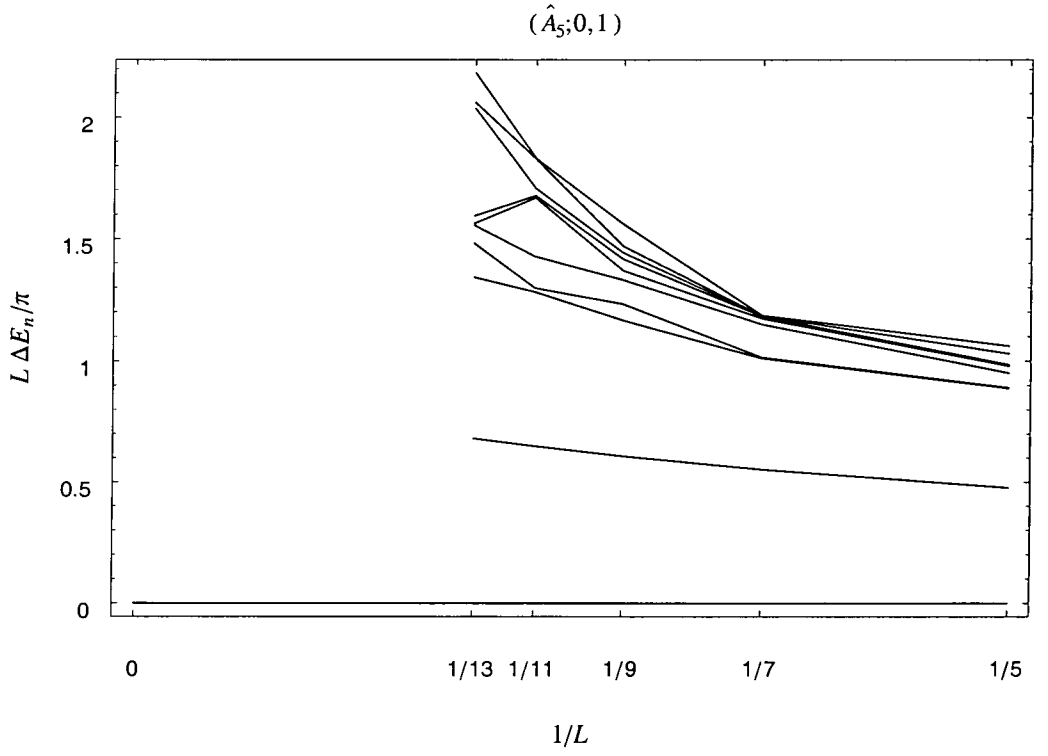

Figure 3.4: Scaled energy gap, $L\,\Delta E_n/\pi$, vs. inverse length, $1/L$, for the model $(\widehat{A}_5;0,1)$. The lines are bunched together with degeneracies '$1,1,5,\ldots$'; however it appears that the third group may yet split to yield degeneracies '$1,1,2,3,\ldots$'. Furthermore, $\Delta x_1 \to 1$ appears likely as $L \to \infty$.

ignored.

Only the first two degeneracies are clearly defined for the $(\widehat{D}_4;X,X)$ and $(\widehat{D}_5;X,X)$ models. This is explained by the fact that in both cases the (theoretical) partition functions behave as

$$q^{-1/24}\,(1+0\,q+q^2+q^3+\mathcal{O}(q^4))\;; \tag{3.4}$$

i.e. the 'second' degeneracy is zero. We are in fact observing degeneracies '$1,0,1,\ldots$'. Unfortunately as the graph (figure 3.6) for $(\widehat{D}_4;X,X)$ shows, the poor convergence of the higher energy levels means it is not yet clear that the lowest non-ground state line is necessarily tending towards $\Delta x_2 = 2$. This is also the case for the model $(\widehat{D}_5;X,X)$.

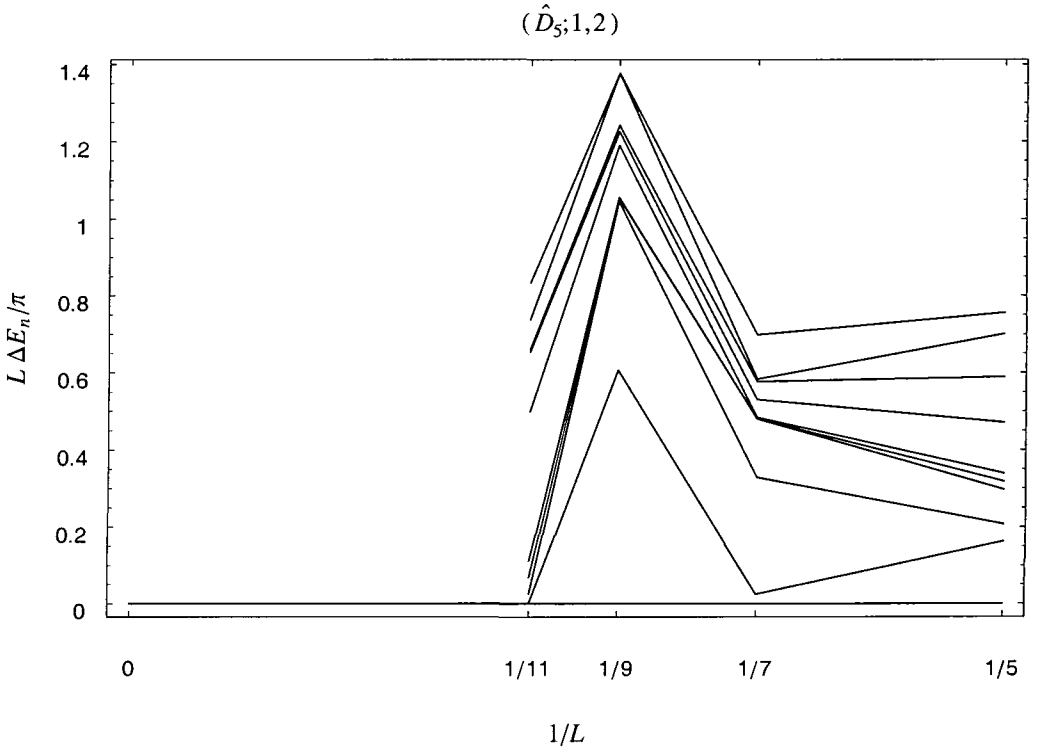

Figure 3.5: Scaled energy gap, $L\,\Delta E_n/\pi$, vs. inverse length, $1/L$, for the model $(\widehat{D}_5;1,2)$. Once the data for the final value, $L = 11$, is ignored, we observe the degeneracies '$1,1,3,5,\ldots$' which compares well with the theoretical '$1,1,4,5,\ldots$'. Unfortunately, little can be said of the general trend of Δx_1.

Finally the degeneracies found for the model $(\widehat{D}_5;X,1)$ appear to be wholly incorrect. An explanation for this is difficult to provide. Examining the graph, figure 3.7, we find that the first 2 degeneracies are correct until again there is a regathering at the largest cylinder length ($L = 13$). This looks again to be a numerical artifact. Unfortunately the higher degeneracies do not come out as expected even ignoring the final $L = 13$ data. It might be supposed that there is a missing level caused by a bad choice of initial vectors $\{v_n\}$ combined with rounding errors. However, we experimented by choosing alternative initial vectors at step $\boxed{\text{I}}$ and this did not produce any affect. This is the only result found to be inconsistent with the theoretical predictions.

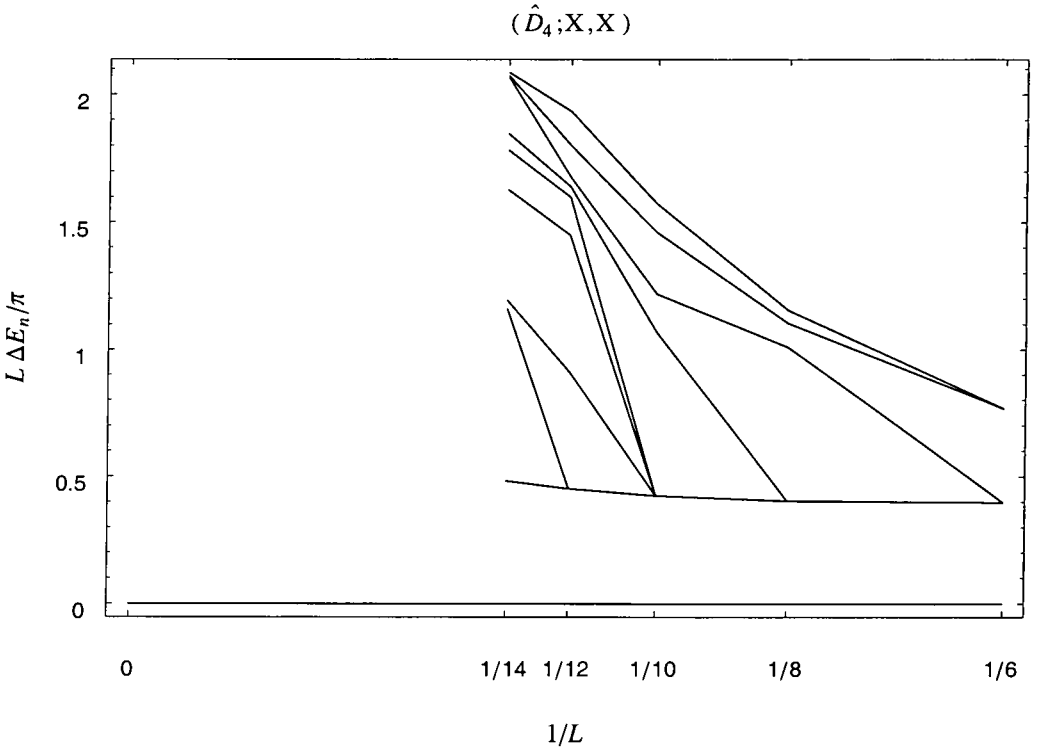

Figure 3.6: Scaled energy gap, $L\,\Delta E_n/\pi$, vs. inverse length, $1/L$, for the model $(\widehat{D}_4; X, X)$. The observed degeneracies are: '$1, 1, \ldots$' which agree with the theoretical '$1, 0, 1, \ldots$' (see text). The poor convergence (with scaling) of the higher energy levels means that it is unclear that the next-to-ground state level is in fact $\Delta x_2 = 2$.

3.2.2 The Central Charge

The second analysis carried out was the examination of the scaling of the ground state energy $E_0(L)$ in an attempt to determine the central charge c of the models. A number of examinations of the scaling data based on the expression (1.143) (or (1.144)) were tried. As mentioned in section 1.2.6, at the critical point the Hamiltonian differs from the renormalisation group fixed-point Hamiltonian by terms involving irrelevant operators. Hence it is expected (see [3], [12] and [14]) that there are corrections to (1.143). Furthermore, for the models we examine, these corrections can be logarithmic in form. For example, it is known [14] that for the toroidal geometry, equation (1.143) becomes

$$E_0(L) = f_\infty L + \frac{\pi}{L}\left\{-\frac{c}{6} + \frac{A_3}{(\ln L)^3} + \mathcal{O}(\frac{1}{(\ln L)^4})\right\} . \tag{3.5}$$

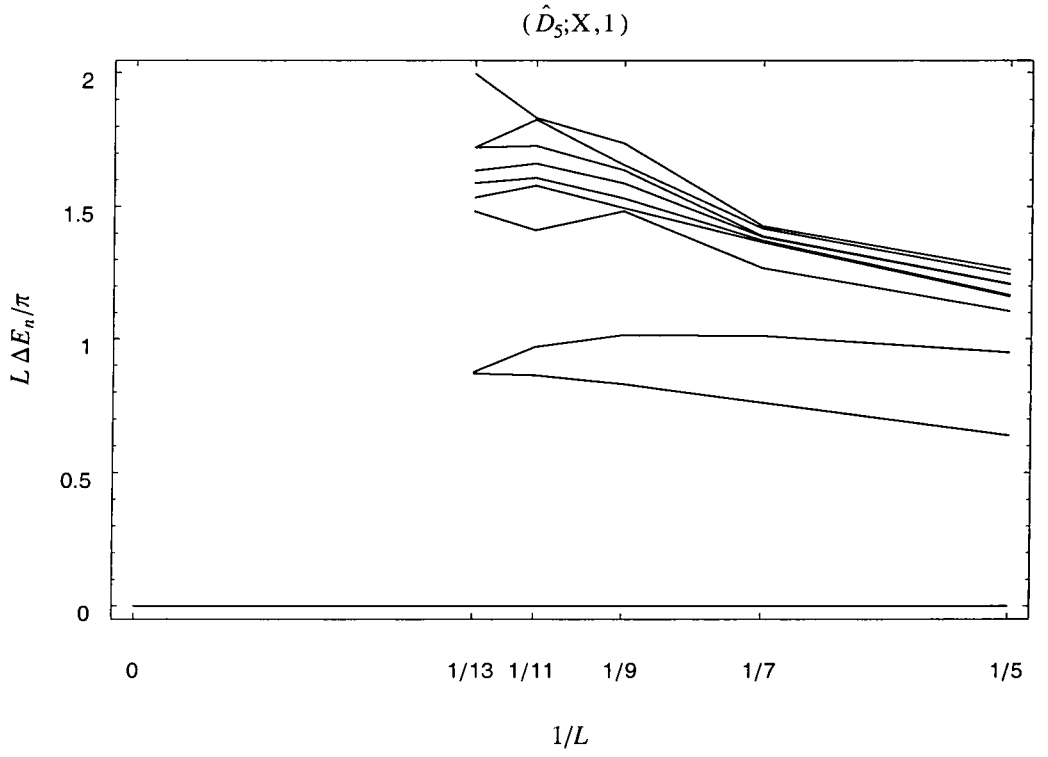

Figure 3.7: Scaled energy gap, $L\,\Delta E_n/\pi$, vs. inverse length, $1/L$ for the model $(\widehat{D}_5; X, 1)$. The observed degeneracies are: '$1, 2, 6, \ldots$' which compares badly with the expected '$1, 1, 2, 3, 5, \ldots$'. This is the only result obtained inconsistent with expectations.

(This is essentially (1.143) with $f^{(\alpha,\beta)} \equiv 0$ as there are no surface terms, the factor $1/24$ introduced earlier by the Schwartzian derivative is replaced by a factor $1/6$ in the periodic case and there are now also additional logarithmic corrections present.) It is clear, that for the cylinder lengths we consider, such logarithmic corrections can be large. Unfortunately, for any given cylinder length L, the Hilbert space of a toroidal model can be quite large (typically 4 or 5 times that of a similar cylinder model). Hence, we were unable to generate enough useful scaling data for the toroidal versions of the models under examination to make any use of (3.5). We remark that such logarithmic corrections are not expected to affect the degeneracies of the model in any way.

For the cylinder cases of interest to us, we considered on empirical grounds and by analogy

with (3.5), that

$$E_0(L) = f_\infty L + f^{(\alpha,\beta)} + \frac{\pi}{L}\left\{h_{(\alpha,\beta)} - \frac{c}{24} + \frac{A_1}{\ln L} + \frac{A_3}{(\ln L)^3} + \frac{A_4}{(\ln L)^4}\right\}. \tag{3.6}$$

This form for the ground state energy is found to fit the data quite well provided A_1 is not restricted to be zero. In all cases, the bulk energy f_∞ is found to be independent of the boundary conditions and, in fact, independent of the precise model concerned also. For the models where the shortest path length $\mathbb{K}$ between the boundary nodes a and b is zero, (3.6) yields a value of c typically around 0·9. However, it must be stressed that for the narrow range of cylinder lengths available to us, the main $1/(\ln L)$ correction is very large and in fact dominates the contribution to $E_0(L)$. Because of this and the fact that so little data is available, we do not consider such results reliable and therefore do not repeat them here.

3.2.3 Conclusions

Overall, whilst the results of the numerical analysis are not absolutely conclusive, they are strongly suggestive of the validity of the partition functions given as tables 2.2–2.5. In most cases, the next-to-ground state of the model is observed to have scaling dimension $\Delta x_1 \sim 1$ indicating, at least, that there are no operators of scaling dimension x with $h_{(a,b)} < x < h_{(a,b)} + 1$, which is a severe constraint on the models. With the exception of the model $(\widehat{D}_5; X, 1)$, the observed degeneracies match our theoretical predictions extremely well. In particular, the observed degeneracies of the 4-state Potts model with free boundary conditions favour the predictions given by both us and by Saleur and Bauer and not (our interpretation of) the prediction of Baake *et al.* (see also section 2.4). The $(\widehat{D}_5; X, 1)$ case may be no more than due to the peculiarities of the finite-sized approximation or a numerical artifact.

Currently, duplicate data is being generated using a different technique for diagonalising the transfer matrix. It is hoped that these calculations, being carried out using the computing facilities of the INFN Bologna, Italy[†], will permit an examination of the scaling at much greater cylinder lengths $L > 15$. This should allow more detailed degeneracies

[†]We are grateful to Gabor Takacs for his assistance in running these calculations on our behalf.

and scaling dimensions for each of the models to be found. In particular, the anomalous case $(\widehat{D}_5; X, 1)$ can now and will be re-examined. The additional data should also allow a more in-depth study of the logarithmic corrections and a proper determination of the value(s) of the central charge c of each of the models. Unfortunately, we do not have any reason to suppose that our ansatz (3.6) is indeed the correct way in which the ground state scales. A precise understanding of what this is, is an involved problem in its own right and beyond the scope of this thesis.

Model $(\mathcal{G};a,b)$	Theoretical Partition Function $\mathcal{Z}^{(\mathcal{G};a,b)}(q)$	Observed Degeneracies
$(\widehat{A}_3;0,0)$	$q^{-1/24}\,(\,1+q+2\,q^2+3\,q^3+7\,q^4+\mathcal{O}(q^5)\,)$	$1,1,2,\ldots$
$(\widehat{A}_3;0,1)$	$q^{5/24}\,(\,1+q+3\,q^2+4\,q^3+7\,q^4+\mathcal{O}(q^5)\,)$	$1,1,3+4,\ldots$
$(\widehat{A}_3;0,2)$	$q^{23/24}\,(\,2+2\,q+4\,q^2+6\,q^3+10\,q^4+\mathcal{O}(q^5)\,)$	$2,2,4,6,10,\ldots$
$(\widehat{A}_5;0,0)$	$q^{-1/24}\,(\,1+q+2\,q^2+3\,q^3+5\,q^4+\mathcal{O}(q^5)\,)$	$1,1,2,\ldots$
$(\widehat{A}_5;0,1)$	$q^{5/24}\,(\,1+q+2\,q^2+3\,q^3+5\,q^4+\mathcal{O}(q^5)\,)$	$1,1,2+3,\ldots$
$(\widehat{A}_5;0,2)$	$q^{23/24}\,(\,1+q+2\,q^2+4\,q^3+6\,q^4+\mathcal{O}(q^5)\,)$	$1,1,2,\ldots$
$(\widehat{A}_5;0,3)$	$q^{53/24}\,(\,2+2\,q+4\,q^2+6\,q^3+8\,q^4+\mathcal{O}(q^5)\,)$	$2,2,4,6,\ldots$
$(\widehat{D}_4;X,X)$	$q^{-1/24}\,(\,1+q^2+q^3+4\,q^4+\mathcal{O}(q^5)\,)$	$1,1,\ldots$
$(\widehat{D}_4;X,1)$	$q^{5/24}\,(\,1+q+3\,q^2+4\,q^3+7\,q^4+\mathcal{O}(q^5)\,)$	$1,1,3+4,\ldots$
$(\widehat{D}_4;X,\overline{X})$	$q^{23/24}\,(\,1+q+2\,q^2+3\,q^3+5\,q^4+\mathcal{O}(q^5)\,)$	$1,1,2,\ldots$
$(\widehat{D}_4;1,1)$	$q^{-1/24}\,(\,1+3\,q+4\,q^2+7\,q^3+13\,q^4+\mathcal{O}(q^5)\,)$	$1,3,4,6,13,\ldots$
$(\widehat{D}_5;X,X)$	$q^{-1/24}\,(\,1+q^2+q^3+3\,q^4+\mathcal{O}(q^5)\,)$	$1,1,\ldots$
$(\widehat{D}_5;X,1)$	$q^{5/24}\,(\,1+q+2\,q^2+3\,q^3+5\,q^4+\mathcal{O}(q^5)\,)$	$1,2,6,\ldots$
$(\widehat{D}_5;X,\overline{X})$	$q^{23/24}\,(\,1+q+2\,q^2+2\,q^3+4\,q^4+\mathcal{O}(q^5)\,)$	$1,1,2,\ldots$
$(\widehat{D}_5;X,Y)$	$q^{53/24}\,(\,1+q+2\,q^2+3\,q^3+4\,q^4+\mathcal{O}(q^5)\,)$	$1,1,2,\ldots$
$(\widehat{D}_5;X,2)$	$q^{23/24}\,(\,1+q+2\,q^2+4\,q^3+6\,q^4+\mathcal{O}(q^5)\,)$	$1,1,2,\ldots$
$(\widehat{D}_5;1,2)$	$q^{5/24}\,(\,1+q+4\,q^2+5\,q^3+9\,q^4+\mathcal{O}(q^5)\,)$	$1,1,3,5,\ldots$
$(\widehat{D}_5;1,1)$	$q^{-1/24}\,(\,1+2\,q+3\,q^2+5\,q^3+9\,q^4+\mathcal{O}(q^5)\,)$	$1,2,3,\ldots$

Table 3.1: The theoretical partition functions and the observed degeneracies for a number of affine Pasquier models on the cylinder. The degeneracies are stated to the degree to which they are clearly visible in the numerical data (see text). The degeneracies stated in the form $y+z$ indicate that at this level, the individual degeneracies are not distinguishable but that several levels are grouped together. These may yet split further (see text).

Chapter 4

SU(2), Kac-Moody Algebras and the Coxeter Element

We introduce here the background material for the analysis conducted in Chapter 5. This material is not original.

4.1 Kac-Moody Algebras

We present a brief review of the untwisted affine Kac-Moody algebras. These may be thought of as generalisations of the simple Lie algebras. Many properties are common to both. It will be assumed that the reader is already familiar with the standard formalism of simple Lie algebras and the associated root systems and Weyl groups; reviews of such material may be found in [18] and [35] respectively. We choose to denote the scalar product of a simple or semisimple Lie algebra $\overline{\mathrm{g}}$ by $(\,,)$ and the associated root systems, weights, etc. by barred quantities whenever it is necessary to distinguish these quantities from those associated with the more general Kac-Moody algebras. In particular, we will denote by "$\overline{\alpha}$" ("$\overline{\rho}$") a typical root (weight) of $\overline{\mathrm{g}}$ and by $\overline{\theta}$ the highest root of $\overline{\mathrm{g}}$.

Much of this review follows [27], [28] and [38].

4.1.1 Classification

A Kac-Moody algebra is the Lie algebra of smooth mappings from the manifold S^1 to some finite Lie algebra $\overline{\mathrm{g}}$, allowing however, for a non-trivial central extension. A finite-

dimensional simple Lie algebra is completely characterised by the $3l$ generators

$$\{ E^i_\pm, H^i \mid i = 1, \ldots, l \} \; ; \tag{4.1}$$

obeying the Jacobi identity and the *Chevalley-Serre* relations:

$$\begin{aligned} &[H^i \, , \, H^j] = 0 \, , \\ &[H^i \, , \, E^j_\pm] = \pm \mathsf{C}^{ji} E^j_\pm \, , \\ &[E^i_+ \, , \, E^j_-] = \delta^{ij} H^j \, , \\ &(\mathrm{ad}_{E^i_\pm})^{1-\mathsf{C}^{ji}} E^j_\pm = 0 \quad \text{for } i \neq j \; ; \end{aligned} \tag{4.2}$$

together with the following requirements on the indecomposable *Cartan matrix* C:

$$\begin{aligned} &\mathsf{C}^{ii} = 2 \, , \\ &\mathsf{C}^{ij} \leq 0 \quad \text{for } i \neq j \, , \\ &\mathsf{C}^{ij} = 0 \quad \text{iff } \mathsf{C}^{ji} = 0 \, , \\ &\mathsf{C}^{ij} \in \mathbb{Z} \; ; \end{aligned} \tag{4.3}$$

and

$$\det \mathsf{C} > 0 \, . \tag{4.4}$$

In particular, $\mathrm{rank}\, \overline{\mathsf{g}} = l$. The *Kac-Moody algebras* are obtained by weakening the conditions on the matrix C. The most important subclass, the *affine algebras*, is obtained by replacing (4.4) with

$$\det \mathsf{C}_{\{i\}} > 0 \quad \forall \, i = 0, \ldots, l \; ; \tag{4.5}$$

where $\det \mathsf{C}_{\{i\}}$ denote the principal minors of C. As is conventional, we have changed our labelling of the Chevalley generators $E^i_\pm$, H^i to $i = 0, 1, \ldots, l$. With this prescription, the simple Lie algebras are those algebras with $\mathrm{rank}\, \mathsf{C} = l + 1$. The rank of the Cartan matrix leading to the affine Kac-Moody algebras is $\mathrm{rank}\, \mathsf{C} = l$.

Once the classification of the simple Lie algebras is known, the classification of the Kac-

Moody algebras proceeds Simarily [27] [38]. We obtain a number (seven) of infinite series augmented by a number of exceptional cases. For our purposes, we are interested only in the so-called *simply-laced untwisted* affine algebras: the infinite series $\widehat{A}_n$ and $\widehat{D}_n$ together with the exceptional cases $\widehat{E}_6$, $\widehat{E}_7$ and $\widehat{E}_8$. Just as the classification of the simple Lie algebras (the non-Abelian Lie algebras with no proper ideals) may be formulated by means of Coxeter-Dynkin diagrams, so too may the classification of the affine algebras. The diagrams of the $\widehat{A}$, $\widehat{D}$ and $\widehat{E}$ cases are exactly those of table 1.1.

Inspecting table 1.1, one observes that removing a certain node (indicated by the label "0"), known as the *affine node*, from the Coxeter-Dynkin diagram of the affine Kac-Moody algebra, "$\widehat{X}_n$" *say*, one obtains the corresponding diagram of the simple Lie algebra "X_n" of table 1.2.

4.1.2 Loop Algebras and Central Extensions

In contrast to simple Lie algebras, the affine Kac-Moody algebras $\widehat{A}\widehat{D}\widehat{E}$ possess a non-trivial centre. Indeed, if we denote by $\underset{\sim}{\mathsf{c}}$ the zero-eigenvector of C normalised so that $\mathsf{c}_0 = 1$ (i.e. the basis vector for the kernel of C); then for any constant $c \neq 0$, the element

$$K = c\sum_{i=0}^{l} \mathsf{c}_i H^i \tag{4.6}$$

is a non-trivial central element of the affine algebra $\widehat{\mathfrak{g}}$. K commutes with all the Chevalley generators of $\widehat{\mathfrak{g}}$: Clearly it commutes with the H^i. That it commutes with the $E^i_{\pm}$ follows from (4.2) and the kernel properties of $\underset{\sim}{\mathsf{c}}$.

If $\mathcal{G}$ denotes the adjacency matrix of the Coxeter-Dynkin diagram of $\widehat{\mathfrak{g}}$ then the Cartan matrix of $\widehat{\mathfrak{g}}$ is $\mathsf{C} = 2 - \mathcal{G}$. Thus $\underset{\sim}{\mathsf{c}}$ is a scalar multiple of the Perron-Frobenius eigenvector $\underset{\sim}{\psi}$ of $\mathcal{G}$. The components of the vector $\underset{\sim}{\mathsf{c}}$ are called the *dual Coxeter labels* (for the $\widehat{A}\widehat{D}\widehat{E}$ cases considered here these are also equivalent to the so-called *Coxeter labels*).

K is, up to scalar multiplication, the unique central element; as C has only one zero-eigenvector. For any given simple Lie algebra $\bar{\mathfrak{g}}$, we may construct an n-dimensional central extension. However it may be shown [27] that simple, and more generally semisimple, Lie

algebras (direct sums of simple Lie algebras) possess no non-trivial central extensions. Thus the possession of a central element distinguishes the non-simple affine algebras from the simple Lie algebras.

The close connection between the Coxeter-Dynkin diagrams of the affine algebras (table 1.1) and the diagrams of the simple Lie algebras (table 1.2) suggests that we may be able to obtain the affine Kac-Moody algebra $\widehat{\mathrm{g}}$ as some generalisation of some simple Lie algebra $\overline{\mathrm{g}}$ which would permit a non-trivial central extension. Indeed, we consider the vector space of analytic maps $\mathcal{S}^1 \to \overline{\mathrm{g}}$. Let $\{ T^a \mid a = 1, \ldots, d \}$ be a basis of $\overline{\mathrm{g}}$ and let $\mathcal{S}^1$ be considered as the unit circle in the complex plane $\mathbb{C}$ with coordinate z, then a basis of such a space is

$$\{ T^a_n \mid a = 1, \ldots, d; n \in \mathbb{Z} \} \ ; \tag{4.7}$$

with

$$T^a_n \equiv T^a \otimes z^n \ ; \tag{4.8}$$

where "$\otimes$" is a formal multiplication. This space becomes an infinite-dimensional Lie algebra, called the *loop algebra* g° *over* $\overline{\mathrm{g}}$, under the natural bracket operation

$$\begin{aligned} [T^a_m \, , \, T^b_n] &\equiv [T^a \otimes z^m \, , \, T^b \otimes z^n] \\ &\stackrel{\text{def}}{=} [T^a \, , \, T^b] \otimes z^{m+n} \ ; \end{aligned} \tag{4.9}$$

i.e.

$$[T^a_m \, , \, T^b_n] = \overline{f}^{ab}{}_c \, T^c \otimes z^{m+n} = \overline{f}^{ab}{}_c \, T^c_{m+n} \ ; \tag{4.10}$$

where the $\overline{f}^{ab}{}_c$ are the structure constants of $\overline{\mathrm{g}}$.

One may now look for central extensions of this loop algebra. It turns out [27] that there is a unique non-trivial central extension $\mathrm{g}^{\circledast}$ of g° characterised by the brackets

$$\begin{aligned} &[T^a_m \, , \, T^b_n] = \overline{f}^{ab}{}_c \, T^c_{m+n} + m \, \delta_{m+n,0} \, \overline{\kappa}^{ab} \, K \ , \\ &[K \, , \, T^a_n] = 0 \ ; \end{aligned} \tag{4.11}$$

where K denotes the new central element (the central extension is 1-dimensional) and $\overline{\kappa}$ is the Killing-form of $\overline{\mathrm{g}}$. The case where $\overline{\mathrm{g}}$ is a compact real Lie algebra is of most interest to us so that we may choose a basis with $\overline{\kappa}^{ab} = -\delta^{ab}$, thus

$$[T^a_m\,,\,T^b_n] = \overline{f}^{abc}\,T^c_{m+n} - m\,\delta_{m+n,0}\,\delta^{ab}\,K\;. \tag{4.12}$$

The *untwisted* affine Kac-Moody algebra $\widehat{\mathrm{g}}$ is obtained from $\mathrm{g}^{\circledast}$ by adding one further generator, the so-called *derivation* D which has Lie brackets

$$\begin{aligned}[D\,,\,T^a_m] &= -[T^a_m\,,\,D] = m\,T^a_m\;,\\ [D\,,\,K] &= 0\;.\end{aligned} \tag{4.13}$$

This is a particular choice amongst several possibilities and corresponds to the so-called *homogeneous gradation*. The centre of $\widehat{\mathrm{g}}$ so chosen is 1-dimensional and K here corresponds to the K of (4.6) with $c \equiv \frac{1}{2}\left(\overline{\theta}\,,\,\overline{\theta}\right)$. The above realisation of the affine Kac-Moody algebra indicates that such an algebra is infinite-dimensional. We remark that $\overline{\mathrm{g}}$ above is referred to as the *horizontal subalgebra* of $\widehat{\mathrm{g}}$ and it is generated as a subalgebra by the set $\left\{\,T^i_0 \mid i = 1,\ldots,l\,\right\}$. This also happens in these cases $(\widehat{A}\widehat{D}\widehat{E})$ to coincide with the so-called *zero-mode* subalgebra of $\widehat{\mathrm{g}}$.

4.1.3 The Root System

The analogue of the Cartan-Weyl basis for the untwisted Kac-Moody algebra $\widehat{\mathrm{g}}$ is constructed as follows: Clearly the maximal Abelian subalgebra $\widehat{\mathrm{h}}$ contains the Cartan subalgebra $\overline{\mathrm{h}}$ of $\overline{\mathrm{g}}$ generated by $\left\{\,H^i_0 \mid i = 1,\ldots,l\,\right\}$. It also contains the central generator K. As

$$[H^i_0\,,\,H^j_n] = [K\,,\,H^j_n] = [H^i_0\,,\,D] = [K\,,\,D] = 0\;, \tag{4.14}$$

it must contain yet one more generator. Choosing D, we see that it is the only one because

$$[D\,,\,H^j_n] \neq 0 \quad \text{for } n \neq 0\;. \tag{4.15}$$

Thus the Cartan subalgebra $\widehat{\mathsf{h}}$ of $\widehat{\mathsf{g}}$ is generated by

$$\{ K , D \} \cup \left\{ H_0^j \mid j = 1, \ldots , l \right\} . \tag{4.16}$$

Or equivalently

$$\{ D \} \cup \left\{ H_0^j \mid j = 0, 1, \ldots , l \right\} . \tag{4.17}$$

The roots w.r.t. $\widehat{\mathsf{h}}$ are found from the observation that for any root $\overline{\alpha}$ of $\overline{\mathsf{g}}$ and any $n \in \mathbb{Z}$,

$$[H_0^i , E_n^{\overline{\alpha}}] = \overline{\alpha}_i E_n^{\overline{\alpha}} , \quad [K , E_n^{\overline{\alpha}}] = 0 , \quad [D , E_n^{\overline{\alpha}}] = n E_n^{\overline{\alpha}} , \tag{4.18}$$

and

$$[H_0^i , H_n^j] = 0 , \quad [K , H_n^j] = 0 , \quad [D , H_n^j] = n H_n^j . \tag{4.19}$$

So that the roots w.r.t. (H, K, D) are

$$\underbrace{\{ \alpha = (\overline{\alpha} , 0 , n) \mid \overline{\alpha} \text{ a root of } \overline{\mathsf{g}}, n \in \mathbb{Z} \}}_{\text{(A)}} \cup \underbrace{\{ \alpha = (0 , 0 , n) \mid n \in \mathbb{Z} \setminus \{0\} \}}_{\text{(B)}} . \tag{4.20}$$

The roots of type (A) correspond to the generators $\{ E_n^{\overline{\alpha}} \}$ and are non-degenerate. The roots of type (B) correspond to the generators $\{ H_n^j \mid n \neq 0 \}$, and are l-fold degenerate as they do not depend upon the label j of H_n^j.

Denote the roots of $\widehat{\mathsf{g}}$ by $\widehat{\Phi}$. We identify a subset of $\widehat{\Phi}$ with the root system $\overline{\Phi}$ of $\overline{\mathsf{g}}$ by

$$(\overline{\alpha} , 0 , 0) \equiv \overline{\alpha} . \tag{4.21}$$

It is consistent to take the positive roots $\widehat{\Phi}^+$ of $\widehat{\mathsf{g}}$ to be

$$\widehat{\Phi}^+ \stackrel{\text{def}}{=} \left\{ \alpha = (\overline{\alpha} , 0 , n) \in \widehat{\Phi} \;\middle|\; n > 0 \text{ or } n = 0, \overline{\alpha} \in \overline{\Phi}^+ \right\} , \tag{4.22}$$

and the negative roots $\widehat{\Phi}^- \equiv \widehat{\Phi} \setminus \widehat{\Phi}^+$. We use the notation $\alpha > 0$ for positive roots and $\alpha < 0$ for negative roots.

Given the choice (4.22), *simple roots* exist and are

$$\alpha_i = (\,\overline{\alpha}_i\,,\,0\,,\,0\,) = \overline{\alpha}_i \quad \text{for } i = 1,\dots,l\,; \tag{4.23}$$

where $\overline{\Pi} \equiv \{\,\overline{\alpha}_a \mid a \in \mathcal{G} \setminus \{0\}\,\}$ are the simple roots of $\overline{\Phi}$; together with

$$\alpha_0 = \big(-\overline{\theta}\,,\,0\,,\,1\big) = \delta - \overline{\theta}\,. \tag{4.24}$$

$\overline{\theta}$ is the highest root of $\overline{\mathfrak{g}}$ and $\delta \equiv (\,0\,,\,0\,,\,1\,)$. We shall denote by $\widehat{\Pi}$ the set of simple roots of $\widehat{\Phi}$. The corresponding step operators are given by,

$$\begin{aligned} &E^i_+ = E_0^{\overline{\alpha}_i} \quad \text{for } i = 1,\dots,l\,, \\ \text{and} \quad &E^0_+ = E_1^{-\overline{\theta}}\,. \end{aligned} \tag{4.25}$$

We remark upon the important property of the simple roots, that if

$$\alpha = \sum_{i=0}^{l} a_i\,\alpha_i\,, \tag{4.26}$$

then

$$\begin{aligned} &\alpha > 0 \Leftrightarrow a_i \in \mathbb{Z}^+ \text{ for } i = 0,\dots,l\,, \\ &\alpha < 0 \Leftrightarrow a_i \in \mathbb{Z}^- \text{ for } i = 0,\dots,l\,; \end{aligned} \tag{4.27}$$

i.e. any root $\alpha \in \widehat{\Phi}$ may be expressed as a strictly non-negative or non-positive integer sum over the simple roots $\widehat{\Pi}$.

The analogue of the Killing form, as in the simple Lie algebraic case, is characterised by the properties of symmetry, bilinearity and associativity. (The property of *associativity* or *invariance* of the Killing form is that $\kappa([x\,,\,y],z) = \kappa(x,[y\,,\,z])$.) It is found to be (choosing a specific normalisation)

$$\kappa = \begin{pmatrix} \overline{\kappa}\,\delta_{m+n,0} & 0 & 0 \\ 0 & 0 & 1 \\ 0 & 1 & 0 \end{pmatrix} \tag{4.28}$$

w.r.t. the generators $(T^a_m\,,\ K\,,\ D)$. The restriction of κ to the Cartan subalgebra $\widehat{\mathsf{h}}$ yields a metric $\langle\,,\rangle$ for the root space $(\widehat{\mathsf{h}}^*)$ and its dual, the weight space $(\widehat{\mathsf{h}})$

$$G^{ij} = \begin{pmatrix} \overline{G}^{ij} & 0 & 0 \\ 0 & 0 & 1 \\ 0 & 1 & 0 \end{pmatrix}\,, \tag{4.29}$$

which is clearly of a Lorentzian nature. A scalar product allows one to identify the root space with its dual. Thus if $(\,,)$ is the scalar product on the root space $\overline{\mathsf{h}}^*$ of $\overline{\mathsf{g}}$ then the scalar product on $\widehat{\mathsf{h}}^*$ of $\lambda \equiv \left(\overline{\lambda}\,,\ k\,,\ d\right)$ and $\lambda' \equiv (\overline{\lambda}'\,,\ k'\,,\ d')$ is

$$\langle\lambda\,,\,\lambda'\rangle = \left(\overline{\lambda}\,,\,\overline{\lambda}'\right) + k\,d' + k'\,d\,. \tag{4.30}$$

In particular, for roots,

$$\langle\alpha\,,\,\alpha'\rangle = (\overline{\alpha}\,,\,\overline{\alpha}')\ . \tag{4.31}$$

Also, the non-degenerate roots of (4.20) have the property

$$\langle\alpha\,,\,\alpha\rangle > 0 \quad \text{for } \overline{\alpha} \in \overline{\Phi}\,, \tag{4.32}$$

and are termed the *real roots* $\widehat{\Phi}_{\mathrm{R}}$; whilst the degenerate roots have

$$\langle\alpha\,,\,\alpha\rangle = 0 \quad \text{for } \alpha = n\delta,\ n \neq 0\,, \tag{4.33}$$

and are termed *lightlike* (or *imaginary*) *roots* $\widehat{\Phi}_{\mathrm{I}}$.

For any real root α, the *coroot* is defined as

$$\alpha^\vee \stackrel{\text{def}}{=} \frac{2}{\langle\alpha\,,\,\alpha\rangle}\,\alpha\,. \tag{4.34}$$

The *(affine) Cartan matrix* is constructed as

$$\mathsf{C}^{ab} \stackrel{\text{def}}{=} \langle\alpha_a\,,\,\alpha_b^\vee\rangle\ , \tag{4.35}$$

with $a, b = 0, 1, \ldots, l$. We remark that in the cases of interest to us (the $\widehat{A}\widehat{D}\widehat{E}$ algebras), C is symmetric and the roots and coroots may be identified by choosing the normalisation

$$\left|\alpha_a\right|^2 \equiv \langle \alpha_a \, , \, \alpha_a \rangle = 2 \quad \forall \; a = 0, \ldots, l. \tag{4.36}$$

Nonetheless, we will continue to use the concept of coroot in our notation unless we specify otherwise. The Cartan matrix C here, is identified with the matrix C of (4.2). We remark that just as with the Cartan matrix of a simple Lie algebra, $\mathcal{G} = 2 - \mathsf{C}$ is the adjacency matrix of the Coxeter-Dynkin diagram of $\widehat{\mathfrak{g}}$.

The *fundamental weights* $\{ \rho_a \mid a = 0, 1, \ldots, l \}$ are defined to be dual to the simple coroots (i.e. the coroots of the simple roots); i.e.

$$\left\langle \rho_a \, , \, \alpha_b^\vee \right\rangle = \delta_{ab} \quad \forall \; a, b = 0, 1, \ldots, l \, , \tag{4.37}$$

and are found, in terms of the weights $\{ \overline{\rho}_b \mid b = 1, \ldots, l \}$ of the horizontal subalgebra $\overline{\mathfrak{g}}$, to be

$$\rho_a = \left(\overline{\rho}_a \, , \, \tfrac{1}{2} \langle \overline{\theta} \, , \, \overline{\theta} \rangle \, \mathsf{c}_a \, , \, 0 \right) \; ; \tag{4.38}$$

where $\overline{\rho}_0$ is defined as $\overline{\rho}_0 \equiv 0$.

We mention as an aside that the Coxeter number of $\overline{\mathfrak{g}}$ is

$$\overline{h} \equiv \sum_{a \in \mathcal{G}} \mathsf{c}_a \, , \tag{4.39}$$

and the highest root

$$\overline{\theta} \equiv \sum_{a \in \mathcal{G} \setminus \{0\}} \mathsf{c}_a \, \alpha_a \, . \tag{4.40}$$

4.1.4 The Weyl Group

In analogy to simple Lie algebras, the *Weyl reflection* σ_α w.r.t. the real root α is defined by

$$\lambda \mapsto \sigma_\alpha \lambda \stackrel{\text{def}}{=} \lambda - \langle \lambda \, , \, \alpha^\vee \rangle \, \alpha \, . \tag{4.41}$$

The group generated by these reflections is known as the *affine Weyl group* $\widehat{W}$. Now

$$\langle \sigma_\alpha \lambda \, , \, \alpha^\vee \rangle = - \langle \lambda \, , \, \alpha^\vee \rangle \, , \tag{4.42}$$

so that (4.41) defines a reflection through the hyperplane perpendicular to α. From a purely Euclidean point of view, we note that this hyperplane for a real root $\alpha \equiv (\, \overline{\alpha} \, , \, 0 \, , \, n \,)$ is given by

$$H_{(\overline{\alpha}\,,0\,,n)} = \left\{ \, \lambda \equiv (\, \overline{\lambda} \, , \, k \, , \, d \,) \in \widehat{\mathsf{h}}^* \; \middle| \; (\frac{1}{k} \overline{\lambda} \, , \, \overline{\alpha}^\vee) = -n \right\} \, , \tag{4.43}$$

so that the hyperplane H_α may be regarded as no longer through the origin but is instead (parallel) shifted by $-\frac{n}{2} \overline{\alpha}$ (see also [35]).

Most properties of the affine Weyl group are the same as those of the ordinary Weyl group $\overline{W}$ associated with $\overline{\mathsf{g}}$ [35]. $\widehat{W}$ is generated by the reflections $\{ \, \sigma_a \equiv \sigma_{\alpha_a} \mid a = 0, 1, \ldots , l \, \}$ w.r.t. the simple roots. There are however several new properties arising from the existence of the lightlike roots. For example, $\sigma_a(n\,\delta) = n\,\delta$, $\forall \; n \in \mathbb{Z} \setminus \{0\}$; the lightlike roots are pointwise invariant under the action of the affine Weyl group. The most important new property is the existence within the Weyl group $\widehat{W}$ of translations. Indeed it is this very property which gives the affine Weyl group and affine algebras their name. We define the '*translation*'

$$\mathsf{t} \stackrel{\text{def}}{=} \sigma_0 \, \sigma_{\overline{\theta}} \, . \tag{4.44}$$

The action of t on any $\lambda \equiv (\, \overline{\lambda} \, , \, k \, , \, d \,)$ is

$$\mathsf{t} \lambda = \left(\, \overline{\lambda} - k \, \overline{\theta}^\vee \, , \, k \, , \, d - (\overline{\lambda} \, , \, \overline{\theta}^\vee) - \frac{2}{(\overline{\theta} \, , \, \overline{\theta})} k \right) \, ; \tag{4.45}$$

and in particular, for any root $\alpha \equiv (\overline{\alpha}\,,\,0\,,\,n)$,

$$\begin{aligned} \mathrm{t}\,\alpha &= (\,\overline{\alpha}\,,\,0\,,\,n - (\overline{\alpha}\,,\,\overline{\theta}^{\vee})\,) \\ &= \alpha - (\overline{\alpha}\,,\,\overline{\theta}^{\vee})\,\delta\,; \end{aligned} \tag{4.46}$$

i.e. it 'translates' any real root by $-(\overline{\alpha}\,,\,\overline{\theta}^{\vee})$ in the lightlike direction. As $\sigma_0 = \mathrm{t}\,\sigma_{\overline{\theta}}$ we may regard $\widehat{W}$ as being generated by the set

$$\{\mathrm{t}\} \cup \{\,\sigma_a \mid a = 1, \ldots, l\,\}\ . \tag{4.47}$$

$\widehat{W}$ is the smallest group containing both the (classical) Weyl group $\overline{W}$ of $\overline{\mathrm{g}}$ and the affine translation t.

We remark that the behaviour of the weights under Weyl reflections is given by

$$\sigma_a \rho_b = \rho_b - \delta_{ab}\,\alpha_b\ . \tag{4.48}$$

This useful fact follows directly from the duality (4.37) of the weights and the simple coroots.

Finally, we note the important property of *normality* of the scalar product $\langle\,,\rangle$. Using the definition (4.41) of the Weyl reflection, it is an easy exercise to see

$$\langle \eta\lambda\,,\,\eta\lambda'\rangle = \langle \lambda\,,\,\lambda'\rangle \quad \forall\ \eta \in \widehat{W};\ \lambda, \lambda' \in \widehat{\mathrm{h}}^*\ . \tag{4.49}$$

This is indeed the case even when $\eta \equiv \mathrm{t}$.

For further details of Weyl groups, we refer the reader to reference [35].

4.2 The Affine Coxeter Element

A *Coxeter element* or *Coxeter transformation* of a Weyl group, be the group affine or not, is defined as any product of (all) the reflections associated to the simple roots. As these reflections do not in general commute, any such element ω will depend upon both the choice of simple roots and the way (i.e. the order) in which one chooses to form the product. Thus typically there are a number of distinct Coxeter elements within any given Weyl group.

In spite of this, certain properties are held in common amongst all these elements. The Coxeter elements associated to any fixed classical algebra, all have the same order $\overline{h}$; indeed this is one definition of the Coxeter number $\overline{h}$ of a given ADE algebra [35]. Simarily, all the Coxeter elements belonging to an affine Weyl group have infinite order [6], [17]. (The true 'Coxeter number' in these cases is therefore infinite. However, a finite number, the *affine Coxeter number* h, does play the analogous role to the ordinary Coxeter number where it appears in expressions for eigenvectors and eigenvalues.) The Coxeter elements associated to a classical algebra are known to be mutually conjugate (within $\overline{W}$) and so possess identical spectra [35]. Dorey [19], [20] and [21] demonstrated the role such an element has within the partition functions of Pasquier models and S-matrices associated with the classical ADE graphs of table 1.2. In particular, he choose a fixed ordering of the simple roots, first investigated by Steinberg [52], to define the Coxeter element. It is our intention to extend this relationship to include the affine Pasquier models also. Thus we are most interested in the natural affine generalisation of this choice of Coxeter element. This form in the classical case has been well studied (see for example [39]) and we can therefore generalise many useful results easily.

The question of conjugacy of the affine Coxeter elements was addressed by Berman *et al.* [6] and also by Coleman [17]. In the case of the affine tree graphs, i.e. the $\widehat{D}$ and $\widehat{E}$ cases, it can be proved that all Coxeter elements are conjugate (see also [35]). Since there is no special choice of Coxeter element, we choose the most convenient example to manipulate. However, in the case of the cycles, the $\widehat{A}$ graphs, the Coxeter elements do fall into a number of distinct spectral classes. Indeed, the Coxeter elements associated with the graph $\widehat{A}_{n-1}$ fall into $[n/2]$ spectral classes. In particular they do not belong all to a single

conjugacy class. Regardless, we will find the affine generalisation of the Steinberg-ordered Coxeter element to be the most useful even in this case. It possesses the property of being a representative of the largest spectral class. When n is even, this largest spectral class is unique and might be taken to define a natural choice of sorts (in fact, coincidentally, we will ignore the odd cycles $\widehat{A}_{2n}$), although we do not make use of this property. In any case, we remark that any Coxeter element and its inverse, both belong to the same spectral class.

We discuss the Steinberg ordering and the properties of the associated Coxeter element now.

4.2.1 The Steinberg Ordering

Let $\widehat{P}$ be the set of integers $0, 1, \ldots, l$ and let $\overline{P}$ be the set with 0 removed. Then it follows from the $\mathbb{Z}_2$-colourability of the Coxeter-Dynkin diagram $\mathcal{G}$ of $\widehat{\mathfrak{g}}$ that we may uniquely partition $\overline{P}$ as a disjoint union $\overline{P} = \overline{P}_1 \cup \overline{P}_2$; so that for $j = 1, 2$ the set $\overline{\Pi}_j \stackrel{\text{def}}{=} \{ \alpha_i \mid i \in \overline{P}_j \}$ consists of mutually orthogonal roots. In particular, the affine node α_0 is orthogonal to all the elements in either $\overline{\Pi}_1$ or $\overline{\Pi}_2$. We fix the notation by requiring that α_0 is orthogonal to the roots of $\overline{\Pi}_2$. Let:

$$\begin{aligned} \widehat{\Pi}_2 &\stackrel{\text{def}}{=} \overline{\Pi}_2 \cup \{\alpha_0\} \,, \\ \widehat{\Pi}_1 &\stackrel{\text{def}}{=} \overline{\Pi}_1 \,, \\ \widehat{P}_2 &\stackrel{\text{def}}{=} \overline{P}_2 \cup \{0\} \\ \text{and} \quad \widehat{P}_1 &\stackrel{\text{def}}{=} \overline{P}_1 \,; \end{aligned} \tag{4.50}$$

and we note:

$$\begin{aligned} \overline{\Pi} &\stackrel{\text{def}}{=} \overline{\Pi}_1 \cup \overline{\Pi}_2 \\ \text{and} \quad \widehat{\Pi} &\stackrel{\text{def}}{=} \widehat{\Pi}_1 \cup \widehat{\Pi}_2 \,; \end{aligned} \tag{4.51}$$

the sets of simple roots of $\overline{\Phi}$ and $\widehat{\Phi}$ respectively. Note also that $\widehat{P} \cong \mathcal{G}$; i.e. there is a one-to-one correspondence between the two sets. We will often use these symbols interchangeably.

For convenience, we additionally define

$$P(a) \stackrel{\text{def}}{=} \begin{cases} 1 & ; \text{if } a \in \widehat{P}_1. \\ 2 & ; \text{if } a \in \widehat{P}_2. \end{cases} . \tag{4.52}$$

Define the involutions

$$\begin{aligned} \omega_1 &\stackrel{\text{def}}{=} \prod_{a \in \widehat{P}_1} \sigma_a \\ \text{and} \quad \omega_2 &\stackrel{\text{def}}{=} \prod_{a \in \widehat{P}_2} \sigma_a \, . \end{aligned} \tag{4.53}$$

The "*Steinberg-ordered*" Coxeter element of the affine Weyl group $\widehat{W}$ is

$$\omega \equiv \omega_2 \, \omega_1 \, . \tag{4.54}$$

Note that none of ω_1, ω_2 or ω depend upon the exact labelling of the elements within the sets $\widehat{P}_1$ or $\widehat{P}_2$ as the corresponding reflections commute. As the choice depends only upon the choice of $\mathbb{Z}_2$-colouring, the definition of the Steinberg-ordered Coxeter element is *unique* up to inverse. In particular, ω and ω^{-1} are conjugate within $\widehat{W}$:

$$\omega^{-1} = \omega_1 \, \omega_2 = \omega_2^{-1} \, (\omega_2 \, \omega_1) \, \omega_2 = \omega_2^{-1} \, \omega \, \omega_2 \, . \tag{4.55}$$

The Steinberg-ordered Coxeter element $\overline{\omega}$ of the classical Weyl group $\overline{W}$ is defined essentially identically [52]. One notes that $\overline{\theta}$ is orthogonal to the roots of $\overline{\Pi}_2$. The operators $\overline{\omega}_1$ and $\overline{\omega}_2$ are defined by substituting $\overline{\Pi}_i$ for $\widehat{\Pi}_i$ $(i = 1, 2)$ in (4.53). Finally $\overline{\omega} \stackrel{\text{def}}{=} \overline{\omega}_2 \, \overline{\omega}_1$. Note that

$$\omega \equiv \sigma_0 \, \overline{\omega} \, . \tag{4.56}$$

4.2.2 The Coxeter Orbits

Consider the action of ω on the set of roots $\widehat{\Phi}$. Given any two roots α, $\beta \in \widehat{\Phi}$; define the relation $\sim$ by

$$\alpha \sim \beta \Leftrightarrow \omega^p \alpha = \beta \quad \text{for some } p \in \mathbb{Z}. \tag{4.57}$$

Clearly $\sim$ is an equivalence relation. The equivalence classes of $\sim$ are called the *Coxeter orbits* (w.r.t. ω). We denote by $\langle\omega\rangle$ the group generated by ω and by $\langle\omega\rangle\alpha$ the Coxeter orbit of the root α.

In order to study these orbits, one requires a representative from each distinct orbit. Such a set of representatives is *not* generally afforded by the simple roots. One may however generalise [36] the orbit representatives of Kostant [39] for the classical Coxeter element $\overline{\omega}$. The representatives comprise the set $\widehat{\mathsf{R}} \equiv \{\, \phi_a \mid a \in \mathcal{G} \,\}$ with

$$\phi_a \stackrel{\text{def}}{=} (1 - \omega^{-1})\rho_a \,, \tag{4.58}$$

or equivalently, by (4.48) and (4.54),

$$\phi_a = \begin{cases} \alpha_a & ;\, \text{if } a \in \widehat{P}_1. \\ \omega_1 \alpha_a & ;\, \text{if } a \in \widehat{P}_2. \end{cases} \,. \tag{4.59}$$

It follows from the linear independence [39] of the subset $\{\, \phi_a \equiv \overline{\phi}_a \mid a \in 1, 2, \ldots, l \,\}$ viewed as orbit representatives of a classical Coxeter element $\overline{\omega}$ of $\overline{\mathsf{g}}$ that these elements are linearly independent. Furthermore, their orbits are distinct; indeed as Dorey's argument shows [20], if one supposes that ϕ_b lies in the Coxeter orbit of another: i.e. $\omega^p \phi_a = \phi_b$ for some values of a, b and p; then, by (4.58),

$$\omega^p \rho_a = \rho_b \,. \tag{4.60}$$

This *cannot* be true as all fundamental weights are dominant highest weights and are therefore *not* related to each other by any Weyl element [34].

These elements may be *uniquely* characterised as those positive roots of $\widehat{\Phi}$ which are

mapped into negative roots under the action of ω [35]. It is easily seen that $\widehat{\mathsf{R}} \subseteq \widehat{\Phi}^+$, $\omega\widehat{\mathsf{R}} \subseteq \widehat{\Phi}^-$ and that the *length* $\mathfrak{L}(\omega)$ of ω is $l+1 = |\widehat{\mathsf{R}}|$.

4.2.3 The Euclidean Coxeter Element

A useful means of examining the Coxeter element is provided by factoring out the translation t. Define $\check{\omega}_2$ by the requirement

$$\omega_2 = \mathsf{t}\check{\omega}_2 = \check{\omega}_2\mathsf{t}^{-1}\,, \tag{4.61}$$

so that

$$\check{\omega}_2 = \sigma_{\overline{\theta}}\sigma_{z_1}\ldots\sigma_{z_k}\;; \tag{4.62}$$

where $\overline{P}_2 = \{z_1,\ldots,z_k\}$ say. $\check{\omega}_2$ is simply ω_2 with the reflection σ_0 replaced with $\sigma_{\overline{\theta}}$. Note that $\sigma_{\overline{\theta}}$ commutes with all the reflections of $\overline{\Pi}_2$. Define

$$\begin{aligned} \check{\omega}_1 &\stackrel{\text{def}}{=} \omega_1 \\ \text{and}\quad \check{\omega} &\stackrel{\text{def}}{=} \check{\omega}_2\check{\omega}_1\;; \end{aligned} \tag{4.63}$$

so that $\omega \equiv \mathsf{t}\check{\omega}$. Note in particular that $\check{\omega}$, $\check{\omega}_1$ and $\check{\omega}_2$ are all elements of the Weyl group $\overline{W}$ of the horizontal subalgebra $\overline{\mathfrak{g}}$ and are therefore constrained to be of *finite* order. We call $\check{\omega}$ the "*Euclidean Coxeter element*".

Let $\sharp$ denote the "*forknode*" of $\mathcal{G}$: for the cases $\widehat{D}_n$ and $\widehat{E}_{6,7,8}$, this is the unique node with 3 links once one has excluded links to the affine node 0; in the case $\widehat{A}_{2n-1}$ this is chosen to be the n^{th} node. Denote by $\mathcal{G}_\sharp \stackrel{\text{def}}{=} \mathcal{G}\setminus\{\sharp\}$ the Coxeter-Dynkin diagram of $\mathcal{G}$ with the node $\sharp$ removed. Let $\overline{\omega}_\sharp$ denote the Coxeter element associated with $\mathcal{G}_\sharp$ (preserving the same colours). Then, following Steinberg [53] (see [6] also), one can show that $\check{\omega}$ is conjugate to $\overline{\omega}_\sharp$; i.e.

$$\overline{\omega}_\sharp = \eta\check{\omega}\eta^{-1}\;; \tag{4.64}$$

where $\eta \in \overline{W}$, $\eta\overline{\theta} = -\alpha_\sharp$. Clearly, $\overline{\omega}_\sharp$ has a finite order, as it is the Coxeter element of a

collection of disconnected A_n type graphs. In fact it, and hence $\check{\omega}$, has period h, where h is the *affine Coxeter number* associated with $\widehat{\mathrm{g}}$. (Note that this number is not in general equal to the *Coxeter number* $\overline{h}$ of $\overline{\mathrm{g}}$.)

4.3 The Finite Subgroups of SU(2)

In this section, we review the McKay correspondence. This important result relates the finite subgroups of SU(2) and the affine Kac-Moody algebras discussed in section 4.1. We also examine the problem of finding how irreducible representations of SU(2), when restricted to a finite subgroup of SU(2), decompose over the irreducible representations of that subgroup. The analysis follows that of Kostant [40] and [41].

4.3.1 The McKay Correspondence

Let us introduce some notation: Let Γ be a non-trivial (i.e. $|\Gamma| > 1$) subgroup of SU(2). For any such subgroup, denote by Γ^* the *unitary dual* (i.e. the set of irreducible representations) of Γ and by $\gamma_a \in \Gamma^*$ the irreducible representation labelled a. Let γ_0 denote the trivial representation of Γ and γ the given 2-dimensional (fundamental) representation $\Gamma \to \mathrm{SU}(2)$, i.e. $\pi_1|_\Gamma$ (which may be reducible). Define the matrix $\mathcal{G}(\Gamma)$ by

$$\gamma_a \otimes \gamma = \sum_b \mathcal{G}(\Gamma)_{ab}\, \gamma_b \,. \tag{4.65}$$

The coefficients of this matrix are clearly non-negative integers so that $\mathcal{G}(\Gamma)$ has a graph representation; hence we shall term this matrix the "*graph*" of the subgroup Γ.

Theorem 4.1 (The McKay Correspondence) Let Γ be a non-trivial subgroup of SU(2); then there exists an affine Kac-Moody algebra $\widehat{\mathfrak{g}}$ of $\widehat{A}\widehat{D}\widehat{E}$ type of rank $l+1$ with adjacency matrix $\mathcal{G} \equiv 2\mathbb{1} - \mathsf{C}$ such that for a suitable ordering of the simple roots $\widehat{\Pi} \equiv \{\, \alpha_a \mid a \in \mathcal{G} \,\}$ of $\widehat{\mathfrak{g}}$ there is a bijection

$$\begin{aligned} \mu : \Gamma^* &\to \widehat{\Pi}\,, \\ \gamma_0 &\mapsto \alpha_0\,, \\ \gamma_a &\mapsto \alpha_a\,; \end{aligned} \tag{4.66}$$

with

$$\mathcal{G}(\Gamma) = \mathcal{G}\,. \tag{4.67}$$

The bijection μ is called *the McKay correspondence.* □

Proof A classification-free proof of this result may be found in [53]. ■

We abuse notation and write by $\mu(\Gamma)$ the affine Kac-Moody algebra $\widehat{\mathfrak{g}}$ for which (4.67) holds.

We remark that as a consequence of (4.65) and theorem 4.1, the vector $\dim \underset{\sim}{\gamma} \equiv \{\dim \gamma_a\}_a$ of dimensions of the representations γ_a, is an eigenvector of $\mathcal{G}$ with eigenvalue 2. Given that $\dim \gamma_0 = 1$, we identify the vector $\dim \underset{\sim}{\gamma}$ with $\underset{\sim}{\mathsf{c}}$ defined in section 4.1.2. We also note that $\gamma_\sharp \equiv \mu^{-1}(\alpha_\sharp)$ is the irreducible representation of Γ with maximal dimension, uniquely so in the cases $\mu(\Gamma) = \widehat{E}_{6,7,8}$.

4.3.2 The Finite Subgroups

Now to the subgroups of SU(2). Consider first the finite subgroups of SO(3). The following is well known:

Theorem 4.2 Only the following non-trivial finite groups F admit a faithful embedding in SO(3):

	$\mathbb{Z}_n$	The cyclic subgroups of order n,
	$\mathbb{D}_n$	The dihedral subgroups of order $2n$,
	$\mathbb{A}_4$	The alternating group on 4 objects,
	$\mathbb{S}_4$	The symmetric group on 4 objects,
and	$\mathbb{A}_5$	The alternating group on 5 objects.

□

Let

$$\Delta : \mathsf{SU}(2) \to \mathsf{SO}(3) \tag{4.68}$$

be the double covering of SO(3). One can use this to find the finite subgroups of SU(2). If F is a finite subgroup of SO(3) then denote by $\Delta^{-1}(F)$ its inverse image under Δ so that $|\Delta^{-1}(F)| = 2|F|$. With the exception of one special family, all the subgroups of SU(2) are of the form $\Delta^{-1}(F)$ for $F \subseteq \mathsf{SO}(3)$:

Proposition 4.3 Let $\Gamma \subseteq \mathsf{SU}(2)$ be a finite subgroup; then $\Gamma = \Delta^{-1}(F)$ for some unique $F \subseteq \mathsf{SO}(3)$ iff Γ is not a cyclic group of odd order. □

We remark that the graphs of the subgroups $\{ \mathbb{Z}_{2n+1} \mid n \in \mathbb{Z}^+ \}$ are cycles with an odd number of nodes and as such the graphs of $\{ \mu(\mathbb{Z}_{2n+1}) \mid n \in \mathbb{Z}^+ \}$ (i.e. the graphs of $\widehat{A}_{2n}$ type) are not $\mathbb{Z}_2$-colourable. Hence the only subgroups in which we will be interested, together with their images under the McKay correspondence, are as listed in table 4.1.

Γ	$\Delta^{-1}(\mathbb{Z}_n)$	$\Delta^{-1}(\mathbb{D}_n)$	$\Delta^{-1}(\mathbb{A}_4)$	$\Delta^{-1}(\mathbb{S}_4)$	$\Delta^{-1}(\mathbb{A}_5)$
$\mu(\Gamma)$	$\widehat{A}_{2n-1}$	$\widehat{D}_{n+2}$	$\widehat{E}_6$	$\widehat{E}_7$	$\widehat{E}_8$

Table 4.1: The subgroups of SU(2) with $\mathbb{Z}_2$-colourable graphs and their images under the McKay correspondence μ.

4.3.3 Tensor Products of SU(2) Representations

Consider the following problem: Denote by π_n the irreducible representation of SU(2) of dimension $n+1$ and let $\mathsf{SU}(2)^* \equiv \{ \pi_n \mid n \in \mathbb{Z}^+ \}$ be the unitary dual of SU(2). Let Γ be a non-trivial finite subgroup of SU(2). We wish to find how the restriction of a specific representation $\pi_n|_\Gamma$ to the finite subgroup Γ decomposes as irreducible representations of Γ; i.e. one wishes to determine the integers $m_a(n)$, $a = 0, 1, \ldots, l$, so that

$$\pi_n|_\Gamma = \bigoplus_{a=0}^{l} m_a(n)\, \gamma_a \,, \quad \text{with } \gamma_a \in \Gamma^* \ \forall a \,. \tag{4.69}$$

Kostant [41] deals with this question by considering instead the corresponding vector v_n in the root space of $\widehat{\mathfrak{g}} \equiv \mu(\Gamma)$ defined as

$$v_n = \sum_{a=0}^{l} m_a(n)\, \alpha_a \ ; \tag{4.70}$$

where $\gamma_a \mapsto \alpha_a$ under the McKay correspondence μ.

We remark that $\mathcal{G}$ may be regarded as an operator on the root space $\widehat{\mathfrak{h}}^*$ of $\widehat{\mathfrak{g}}$. Indeed let $\mathcal{G}$ also denote the operator whose matrix is $\mathcal{G}$ w.r.t. the simple roots $\widehat{\Pi}$; i.e.

$$\begin{aligned} &\mathcal{G} : \widehat{\mathfrak{h}}^* \to \widehat{\mathfrak{h}}^* \ , \\ &\alpha_a \mapsto \sum_{b \in \mathcal{G}} \mathcal{G}_{ab}\, \alpha_b \ . \end{aligned} \tag{4.71}$$

The Clebsch-Gordon formula for SU(2) is

$$\pi_n \otimes \pi_1 = \pi_{n+1} + \pi_{n-1} \ ; \tag{4.72}$$

where π_{-1} denotes the zero-representation. Restricting these representations to the finite subgroup Γ and using the McKay correspondence, one sees that

$$\mathcal{G}\, v_n = v_{n+1} + v_{n-1} \ . \tag{4.73}$$

Using the same $\mathbb{Z}_2$-colouring as in section 4.2.1, which is found to be related to whether or not γ_a may be considered a representation of the SO(3) subgroup $F \equiv \Delta(\Gamma)$ [41], it is found that

Proposition 4.4 (Kostant [41])

$$m_a(n) = 0 \quad \forall\ a \in \widehat{P}_{(n \pmod 2)+1} \ . \tag{4.74}$$

In other words, a and n must be of the same parity, or else $m_a(n) = 0$. □

Another, very useful result which derives from (4.71) is:

Lemma 4.5 (Kostant [41]) The action of $\mathcal{G}$ regarded as an operator on $\widehat{\mathfrak{h}}^*$ is

$$\mathcal{G} = \omega_1 + \omega_2 \; ; \tag{4.75}$$

where ω_1 and ω_2 are the involutions (4.53). □

Taking (4.73) as the starting point, together with $v_0 = \alpha_0$ (which itself is a consequence of Schur's lemma [18]), lemma 4.5 allows one to re-express v_n in terms of the affine Coxeter element and α_0. From a study of the affine Coxeter element ω defined in section 4.2.1 and its classical horizontal 'partner' (i.e.. $\overline{\omega}$ defined by (4.56)), Kostant [41] determined the generating function for the vectors $\{ v_n \mid n \in \mathbb{Z}^+ \}$ to be

$$\begin{aligned} P_\Gamma(x) &\equiv \sum_{n=0}^{\infty} v_n \, x^n \\ &= \frac{z(x)}{(1-x^r)(1-x^s)} \; , \end{aligned} \tag{4.76}$$

with

$$z(x) \equiv \sum_{i=0}^{\overline{h}} z_i \, x^i \tag{4.77}$$

a polynomial in x with coefficients in the root system $\widehat{\Phi}$ of $\widehat{\mathfrak{g}}$. Note that the Coxeter element of section 4.2.1 is defined in terms of a $\mathbb{Z}_2$-colouring, it is for this reason that we have excluded from interest the non-$\mathbb{Z}_2$-colourable $\widehat{A}_{2n}$-series of graphs. The integers r and s are subgroup-dependent. They satisfy $r + s = \overline{h} + 2$, where $\overline{h}$ is the Coxeter number of the horizontal subalgebra of $\mu(\Gamma)$, and $rs = |\Gamma|$. They are listed in table 4.2. We remark that the horizontal subalgebras of the McKay images of all the subgroups with which we are concerned all have even Coxeter number $\overline{h}$. We define the integer $g \stackrel{\text{def}}{=} \overline{h}/2$.

Define

$$\overline{\omega}_n = \begin{cases} \overline{\omega}_1 & ; \text{ if } n \text{ is odd.} \\ \overline{\omega}_2 & ; \text{ if } n \text{ is even.} \end{cases} \; . \tag{4.78}$$

Let $\overline{\omega}^{(n)} = \overline{\omega}_n \, \overline{\omega}_{n-1} \, \ldots \, \overline{\omega}_1$ with $\overline{\omega}^{(0)} = \mathbb{1}$ and also let $\overline{\omega}^{[n]} = \overline{\omega}_{g+n} \, \overline{\omega}_{g+n-1} \, \ldots \, \overline{\omega}_{g+1}$.

Γ	$\mu(\Gamma)$	h	$\overline{h}$	r	s
$\Delta^{-1}(\mathbb{Z}_n)$	$\widehat{A}_{2n-1}$	$2n$	$2n$	2	$2n$
$\Delta^{-1}(\mathbb{D}_n)$	$\widehat{D}_{n+2}$	$2n$	$2n+2$	4	$2n$
$\Delta^{-1}(\mathbb{A}_4)$	$\widehat{E}_6$	6	12	6	8
$\Delta^{-1}(\mathbb{S}_4)$	$\widehat{E}_7$	12	18	8	12
$\Delta^{-1}(\mathbb{A}_5)$	$\widehat{E}_8$	30	30	12	20

Table 4.2: The integers r and s for each of the $\mathbb{Z}_2$-colourable finite subgroups Γ of SU(2). The affine Coxeter number h of $\mu(\Gamma)$ together with the Coxeter number of its horizontal subalgebra are also indicated; in all cases, h and $\overline{h}$ are even. Note the similarity between this table and table 2.1.

Kostant [41] determined the coefficients $z_i \in \widehat{\Phi}$ to be:

$$\begin{aligned} z_h &= z_0 = \alpha_0 \ , \\ z_n &= \left(\overline{\omega}^{(n)} - \overline{\omega}^{(n-1)}\right) \overline{\theta} \quad \text{for } 1 \leq n \leq h-1 \ ; \end{aligned} \tag{4.79}$$

or equivalently, in terms of the forknode of $\mathcal{G}$:

$$\begin{aligned} z_h &= z_0 = \alpha_0 \ , \\ z_g &= 2\,\alpha_\sharp \ , \\ z_{g-n} &= z_{g+n} = \left(\overline{\omega}^{[n]} - \overline{\omega}^{[n-1]}\right) \alpha_\sharp \quad \text{for } 1 \leq n \leq g-1 \ . \end{aligned} \tag{4.80}$$

In a basis of the simple roots $\widehat{\Pi}$, this last enables a very simple calculation of the z_n.

The Poincaré series $P_\Gamma(x)_a$ for the individual representation γ_a is obviously obtained by considering only the a^{th} coefficient of the vectors v_n; i.e.

$$\begin{aligned} P_\Gamma(x)_a &= \langle \rho_a \, , \, P_\Gamma(x) \rangle \\ &= \frac{K_a(x)}{(1-x^r)(1-x^s)} \ ; \end{aligned} \tag{4.81}$$

with $K_a(x) \equiv \langle \rho_a \, , \, z(x) \rangle$.

In particular, from (4.80),

$$\begin{aligned} K_0(x) &= 1 + x^{\overline{h}} \,, \\ K_\sharp(x) &= \sum_{n=0}^{r/2-1} \left(x^{g-2n} + x^{g+2n} \right) \,, \end{aligned} \tag{4.82}$$

and the $K_a(x)$ (for all a) are $\overline{h}$-reciprocal polynomials.

4.4 The Chebychev Polynomials

An important tool in the analysis of the next chapter will be the Chebychev polynomials of the second kind. The *Chebychev polynomial* $\mathcal{U}^{(n)}(x)$ of degree n over the indeterminate x is defined by the recursion relation

$$\mathcal{U}^{(n)}(x) = x\,\mathcal{U}^{(n-1)}(x) - \mathcal{U}^{(n-2)}(x)\ ; \tag{4.83}$$

together with two 'initial conditions': the values of two subsequent polynomials in the series. For our purposes we will be concerned only with the series of polynomials generated by the initial conditions:

$$\mathcal{U}^{(0)}(x) = 1\ , \qquad \mathcal{U}^{(1)}(x) = x\ ; \tag{4.84}$$

and we note that this implies that $\mathcal{U}^{(-1)}(x) = 0$.

This series, which we shall denote $\mathfrak{H}^2$, is generated by the function

$$\begin{aligned} \mathfrak{C}_2(p|x) &\equiv \sum_{m=0}^{\infty} \mathcal{U}^{(m)}(x)\,p^m \\ &= \frac{1}{1 - p\,x + p^2}\ . \end{aligned} \tag{4.85}$$

It possesses the important property that each polynomial in the series is a strictly odd or strictly even function depending upon the oddness or evenness of its degree; i.e. there exists a $\mathbb{Z}_2$-colouring:

$$\begin{aligned} &\tau_2 : \mathfrak{H}^2 \to \mathbb{Z}_2\ , \\ &\mathcal{U}^{(n)}(x) \mapsto n \pmod 2\ , \end{aligned} \tag{4.86}$$

with

$$\mathcal{U}^{(n)}(-x) = (-1)^{\tau_2(\mathcal{U}^{(n)}(x))}\,\mathcal{U}^{(n)}(x)\ . \tag{4.87}$$

As an example, we note that the intertwiners (1.67) satisfy both (4.83) and (4.84). Choos-

ing $\alpha = 1$, equation (1.68) may be rewritten [25] as

$$V^{\lambda+1} = V^{\lambda}\mathcal{G} - V^{\lambda-1} \quad \text{for } \lambda = 2, 3, \ldots, n-1. \tag{4.88}$$

The initial conditions are given by considering one end of the A_n graph, and are

$$V^1 = \mathbb{1}\,, \qquad V^2 = \mathcal{G}\,. \tag{4.89}$$

The definition of V^{λ} may be extended to any λ as examination of the A_n graph implies $V^n = \mathbb{1}$, so defining $V^{mn} = 0$ for all integers m yields a consistent series of polynomials. Thus,

$$V^{\lambda}_{ab} \equiv \mathcal{U}^{(\lambda-1)}_{ab}(\mathcal{G})\,. \tag{4.90}$$

We note that this last implies that the intertwiners (1.67) are integer valued.

Chapter 5

The Role of the Coxeter Element

In his paper [21], Dorey demonstrated the role that the classical Coxeter element plays in the partition functions, and hence in the physics, of the classical Pasquier models. In this chapter we will discuss the role that the affine analogue of the Coxeter element (i.e. the affine Coxeter element) plays in the partition functions of the affine models. In so doing, we will also provide an alternative derivation of Dorey's classical result. Before arriving at our main geometric result, it proves both useful and interesting in its own right to establish a simple closed expression for the partition functions in terms of Chebychev polynomials of the second kind. This brings into light the important connection between the affine Pasquier models and the representation theory of SU(2) already observed for the classical Pasquier models (see [24] and [21]). To do this we first examine the results of chapter 2 and attempt to make a connection with the work of Kostant discussed in the preceding chapter.

5.1 Preliminary Observations

As seen in section 2.5, we were able to express the partition function of a given model, $(\mathcal{G}; a, b)$, in terms of a reciprocal polynomial, namely the $\mathsf{P}^{(\mathcal{G};a,b)}(x)$ of equation (2.48). This equation (2.48) could in turn be re-expressed in terms of a simpler polynomial $\mathsf{Q}^{(\mathcal{G};a,b)}(x)$ whose coefficients were positive integers as equation (2.49). Apart from manifesting the positivity of the coefficients of the $\chi_{\frac{n^2}{4}}(q)$, the form of the Poincaré series appearing in (2.49) was chosen because it coincides with the general form (4.81) of the $P_{\Gamma}(x)_a$; where the $K_a(x)$ there are q-reciprocal polynomials in the indeterminate x with positive-integer

coefficients; and r and s integers with q, r and s the same numbers given for particular models in table 2.1. Furthermore, we observe that the polynomials $\mathsf{P}^{(\mathcal{G};a,b)}(x)$, $\mathsf{Q}^{(\mathcal{G};a,b)}(x)$ and $K_n(x)$ all have well defined parities (this last result comes from proposition 4.4); i.e. they are strictly-odd or strictly-even polynomials. This striking similarity in form suggests immediately that there is some direct connection between the representation theory of SU(2) and the affine partition functions.

It is tempting at this point to see if the polynomials $\mathsf{Q}^{(\mathcal{G};a,b)}(x)$ permit a decomposition onto the set $\{ K_i(x) \mid i \in \mathcal{G} \}$. This was observed on a case-by-case basis using Mathematica. Indeed not only does it appear that such a decomposition is allowed but that the decomposition is positive and integer-valued; i.e. we observe that

$$\mathsf{Q}^{(\mathcal{G};a,b)}(x) = \sum_{n \in \mathcal{G}} R^n_{ab} K_n(x) \; ; \tag{5.1}$$

where $R^n_{ab} \in \mathbb{Z}^+$. Moreover, we note from the discussions of the preceding chapter, that associated to each node $a \in \mathcal{G}$ there is an irreducible representation γ_a of a fixed subgroup $\Gamma \equiv \widehat{\mu}^{-1}(\mathcal{G}) \subset \mathsf{SU}(2)$. To this in turn we may associate the polynomial $K_a(x)$ which describes how the entire set of (SU(2)-irreducible but Γ-reducible) representations $\{ \pi_i|_\Gamma \mid i \in \mathbb{Z}^+ \}$ decomposes onto the representation γ_a (section 4.3.3). Examining, again on a case-by-case basis using Mathematica, we observe (empirically) that

$$\dim \gamma_a \; \dim \gamma_b = \sum_{n \in \mathcal{G}} R^n_{ab} \dim \gamma_n \; . \tag{5.2}$$

This observation shadows a Clebsch-Gordon decomposition: the model $(\mathcal{G}; a, b)$ being associated with the (typically reducible) representation $\gamma_a \otimes \gamma_b$ of the subgroup $\Gamma \equiv \widehat{\mu}^{-1}(\mathcal{G})$. We remark also that the partition function $\mathcal{Z}^{(\mathcal{G};a,b)}(q)$ obeys the graph symmetries w.r.t. a and b, in particular it is a symmetric function in a and b as is this tensor product representation. In addition it may be observed that the $\{K_n(x)\}$ also obey graph symmetries so that the connection between the partition function $\mathcal{Z}^{(\mathcal{G};a,b)}(q)$ and the tensor product $\gamma_a \otimes \gamma_b$ does indeed appear more than merely plausible.

It must be emphasised that all these observations are (so far) purely *empirical* and were observed with the aid of a computer using an appropriate Mathematica script.

5.2 SU(2) and the Partition Functions

We shall for now *assume* that the partition function $\mathcal{Z}^{(\mathcal{G};a,b)}(q)$ is related to the decomposition of the tensor product $\gamma_a \otimes \gamma_b$ in terms of Γ-irreducibles ($\Gamma \equiv \widehat{\mu}^{-1}(\mathcal{G})$) and see what such an assumption implies.

Define the symbols $\bigoplus^{(2)}$ and $\sum^{(2)}$ by

$$\bigoplus_{c=a}^{b\,(2)} F(c) \equiv \bigoplus_{c'=0}^{\frac{b-a}{2}} F(a+2c') \,, \tag{5.3}$$

and

$$\sum_{c=a}^{b\,(2)} F(c) \equiv \sum_{c'=0}^{\frac{b-a}{2}} F(a+2c') \tag{5.4}$$

i.e. just 'summing in twos'. As a trivial exercise with Young-tableaux shows, the Clebsch-Gordon decomposition for irreducible representations of SU(2) is

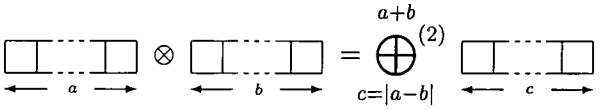

$$= \bigoplus_{c=|a-b|}^{a+b\,(2)} \,, \tag{5.5}$$

i.e.,

$$\pi_a \otimes \pi_b = \bigoplus_{c=|a-b|}^{a+b\,(2)} \pi_c \tag{5.6}$$

Restricting these representations to the finite subgroup $\Gamma \subset \mathrm{SU}(2)$ we have

$$\pi_a|_\Gamma \otimes \pi_b|_\Gamma = \bigoplus_{c=|a-b|}^{a+b\,(2)} \pi_c|_\Gamma \,. \tag{5.7}$$

Each of the restricted SU(2) representations decomposes into irreducible representations of the finite subgroup Γ according to equation (4.69). Define the matrices $\left\{ B^k_{(j)i} \,\middle|\, j \in \mathcal{G} \right\}$ by the decomposition of the tensor product of two irreducible representations of Γ as

$$\gamma_i \otimes \gamma_j = \bigoplus_{k \in \mathcal{G}} B^k_{(j)i}\, \gamma_k \; ; \tag{5.8}$$

then (5.7) yields

$$\bigoplus_{i,j,k \in \mathcal{G}} m_i(a)\, m_j(b)\, B^k_{(j)i}\, \gamma_k = \bigoplus_{c=|a-b|}^{a+b\,(2)} \bigoplus_{k \in \mathcal{G}} m_k(c)\, \gamma_k \; . \tag{5.9}$$

In analogy with Kostant [41], we replace each irreducible representation γ_k of Γ with the corresponding root α_k in the Kac-Moody algebra $\widehat{\mathfrak{g}} \equiv \widehat{\mu}(\Gamma)$ under the McKay correspondence (theorem 4.1). We get

$$\sum_{i,j,k \in \mathcal{G}} m_i(a)\, m_j(b)\, B^k_{(j)i}\, \alpha_k = \sum_{c=|a-b|}^{a+b\,(2)} \sum_{k \in \mathcal{G}} m_k(c)\, \alpha_k \; ; \tag{5.10}$$

where the matrices $\left\{ B^k_{(j)i} \,\middle|\, j \in \mathcal{G} \right\}$ are now defined to operate on the vectors $\left\{ \alpha_k \,\middle|\, k \in \mathcal{G} \right\}$. Thus we may rewrite this as

$$\sum_{i,j,k \in \mathcal{G}} \left\langle \rho_k \, , \, m_j(b)\, B_{(j)}\, m_i(a)\, \alpha_i^\vee \right\rangle \, \alpha_k = \sum_{c=|a-b|}^{a+b\,(2)} m_k(c)\, \alpha_k \; . \tag{5.11}$$

Writing $\mathcal{G}^{(b)} \equiv \sum_j m_j(b)\, B_{(j)}$ and using (4.70), this reduces to

$$\mathcal{G}^{(b)}\, v_a = \sum_{c=|a-b|}^{a+b\,(2)} v_c \; . \tag{5.12}$$

From this, it follows easily by induction that

$$\mathcal{G}^{(b)} \equiv \mathcal{U}^{(b)}(\mathcal{G}) \; ; \tag{5.13}$$

where $\mathcal{G}$ is the adjacency matrix of $\widehat{\mathfrak{g}} \equiv \widehat{\mu}(\Gamma)$ and $\mathcal{U}^{(n)}(x)$ is the n^{th} *Chebychev polynomial of the second kind* (see section 4.4) with $\mathcal{U}^{(0)}(\mathcal{G}) = \mathbb{1}$ and $\mathcal{U}^{(1)}(\mathcal{G}) = \mathcal{G}$. It is also consistent

to write $\mathcal{U}^{(-1)}(\mathcal{G}) = 0$. Equation (5.13) now tells us that

$$\sum_{j\in\mathcal{G}} m_j(b)\, B_{(j)} = \mathcal{U}^{(b)}(\mathcal{G})\ . \tag{5.14}$$

Multiply both sides by x^b and sum over $b \in \mathbb{Z}^+$ to get

$$\sum_{j\in\mathcal{G}} B_{(j)}\, P_\Gamma(x)_j = \sum_{b\in\mathbb{Z}^+} \mathcal{U}^{(b)}(\mathcal{G})\, x^b\ ; \tag{5.15}$$

where $P_\Gamma(x)_j$ was introduced in section 4.3.3. Substituting in expression (4.81) for $P_\Gamma(x)_j$, we have

$$\sum_{j\in\mathcal{G}} B_{(j)}\, K_j(x)\, \frac{1}{(1-x^r)(1-x^s)} = \sum_{b\in\mathbb{Z}^+} \mathcal{U}^{(b)}(\mathcal{G})\, x^b\ . \tag{5.16}$$

We note that the components of the matrices $B_{(j)}$ are, by definition, positive integers, so that the sum $\sum_j B_{(j)}\, K_j(x)$ is a positive integer sum over the "*Kostant polynomials*" $K_j(x)$ of (4.81). As remarked upon in the preceding section, this is exactly the property exhibited by the generating polynomial $\mathsf{Q}(x)$ of the affine partition functions introduced in section 2.5; indeed we may identify the $B_{(j)_{ab}}$ appearing here with R^j_{ab} in equation (5.1). Thus we *conjecture* that

$$\mathsf{Q}^{(\mathcal{G};a,b)}(x) \equiv \sum_{j\in\mathcal{G}} B_{(j)}\, K_j(x)\ . \tag{5.17}$$

If we assume that this is true, then equation (2.49) becomes

$$\boxed{\mathcal{Z}^{(\mathcal{G};a,b)}(q) = \sum_{n=0}^{\infty} \chi_{\frac{n^2}{4}}(q)\, \mathcal{U}^{(n)}_{ab}(\mathcal{G})}\ . \tag{5.18}$$

This is a very simple expression and is very easy to compute for a given adjacency matrix $\mathcal{G}$. Furthermore, as is shown later, the "Chebychev form" that this expression has will allow us to make the connection with the underlying geometry of the affine Weyl group $\widehat{W}$ of the algebra $\widehat{\mathfrak{g}}$.

Equation (5.18) is in fact correct; as we demonstrate now.

5.3 Proof of the Chebychev Form

We possess (5.18), a candidate general expression for the partition functions. We construct a simple proof. We begin by examining the $\widehat{A}$ cases.

Lemma 5.1 The coefficient $\Lambda_n^\varepsilon \equiv \Lambda_n^{(\widehat{A}_{[2h]};0,\varepsilon)}$ of $\chi_{\frac{n^2}{4}}(q)$ in the expansion (2.25) of the partition function of the model $(\widehat{A}_{[2h]};0,\varepsilon)$ is given by

$$\Lambda_n^\varepsilon = \mathcal{U}_{0\varepsilon}^{(n)}(\widehat{A}_{[2h]}) \,. \tag{5.19}$$

In other words, it is given by the n^{th}-Chebychev polynomial of the second kind satisfying $\mathcal{U}^{(0)}(\widehat{A}) = \mathbb{I}$ and $\mathcal{U}^{(1)}(\widehat{A}) = \widehat{A}$. □

Proof The proof is by induction on the variable n.

We first establish that the initial conditions (4.84) for the Chebychev recursion relation are satisfied. We observe, directly from (2.35), that

$$\Lambda_0^\varepsilon = \delta_0^\varepsilon = \mathcal{U}_{0\varepsilon}^{(0)}(\widehat{A}_{[2h]}) \tag{5.20}$$

and

$$\Lambda_1^\varepsilon = \delta_1^\varepsilon + \delta_{2h-1}^\varepsilon = \mathcal{U}_{0\varepsilon}^{(1)}(\widehat{A}_{[2h]}) \tag{5.21}$$

as required.

Having established that the initial conditions are satisfied, we now examine the recursion relation (4.83). Assume that $\exists\ N \in \mathbb{Z}^+$ such that $\forall\ 2 \leq n < N$ that (5.19) holds. Then

$$\begin{aligned}\left[\mathcal{U}^{(N-1)}(\widehat{A}_{[2h]})\,\widehat{A}_{[2h]} - \mathcal{U}^{(N-2)}(\widehat{A}_{[2h]})\right]_{0\varepsilon} &= \sum_{\lambda\in\widehat{A}_{[2h]}} \Lambda_{N-1}^\lambda\,\widehat{A}_{\lambda\varepsilon} - \Lambda_{N-2}^\varepsilon \\ &= \Lambda_{N-1}^{\varepsilon-1} + \Lambda_{N-1}^{\varepsilon+1} - \Lambda_{N-2}^\varepsilon\end{aligned} \tag{5.22}$$

using the induction hypothesis. Note that, as mentioned in section 2.3.2, the Λ_n^ε have a period $2h$ in the variable ε, so that addition and subtraction in this variable (such as in (5.22)) are understood to be taken *modulo* $2h$.

The righthand side of (5.22) will be equal to the required $\Lambda^{\varepsilon}_{N}$ iff

$$\Lambda^{\varepsilon-1}_{N-1} + \Lambda^{\varepsilon+1}_{N-1} = \Lambda^{\varepsilon}_{N} + \Lambda^{\varepsilon}_{N-2} \,. \tag{5.23}$$

This equation is identically true $\forall$ N replaced with $n > 2$ as a detailed analysis of the coefficients $\Lambda^{\varepsilon}_{n}$ shows. If we examine a typical grid of values $\Lambda^{\varepsilon}_{n}$ (given by equation (2.35)), as in table 5.1. Fixing arbitrarily, the values of ε and n we see that $\Lambda^{\varepsilon}_{n}$ takes the value,

ε	n														
	0	1	2	3	4	5	**6**	7	8	9	10	11	**12**	13	14
4	**0**		1		**2**		**2**		3		**4**		**4**		5
5		1		1		**2**		3		3		**4**		5	
0	1		1		1		3		3		3		5		5
1		1		1		**2**		3		3		**4**		5	
2	**0**		1		**2**		**2**		3		**4**		**4**		5
3		**0**		**2**		**2**		**2**		**4**		**4**		**4**	
4	**0**		1		**2**		**2**		3		**4**		**4**		5
5		1		1		**2**		3		3		**4**		5	
0	1		1		1		3		3		3		5		5
1		1		1		**2**		3		3		**4**		5	

Table 5.1: The coefficients $\Lambda_{n,\varepsilon}$ for the model $\widehat{A}_5$. The multiples of $n = h \equiv 6$ are highlighted in bold. Due to 'parity constraints', every second value is automatically zero and these values have been left blank for clarity. The values in the table are 'coloured' alternatively bold and normal to emphasise the "embedded-diamond"-like pattern of the numbers. Note that the table is periodic in the variable ε and that n takes values from 0 to ∞. This same basic pattern of numbers occurs for each of the $\mathbb{Z}_2$-colourable $\widehat{A}$ models.

m say, with coordinates ε and n in the grid, $\Lambda^{\varepsilon}_{n-2}$ takes the values two spaces to the left (or 'west') of this value, $\Lambda^{\varepsilon-1}_{n-1}$ takes the value 'northwest' and $\Lambda^{\varepsilon+1}_{n-1}$ the value 'southwest'. Due to the periodicity of the variable ε and the "embedded-diamond"-like pattern the

numbers Λ_n^ε follow (for any value of even h) one of the following is *always* the case:

$$\Lambda_n^\varepsilon = \Lambda_{n-2}^\varepsilon = \Lambda_{n-1}^{\varepsilon-1} = \Lambda_{n-1}^{\varepsilon+1} = m \; ; \tag{i}$$

$$\Lambda_n^\varepsilon = \Lambda_{n-1}^{\varepsilon-1} = m, \quad \Lambda_{n-1}^{\varepsilon+1} = \Lambda_{n-2}^\varepsilon = m-1 \; ; \tag{ii}$$

$$\Lambda_n^\varepsilon = \Lambda_{n-1}^{\varepsilon+1} = m, \quad \Lambda_{n-1}^{\varepsilon-1} = \Lambda_{n-2}^\varepsilon = m-1 \; ; \tag{iii}$$

$$\Lambda_n^\varepsilon = m, \quad \Lambda_{n-2}^\varepsilon = m-2, \quad \Lambda_{n-1}^{\varepsilon-1} = \Lambda_{n-1}^{\varepsilon+1} = m-1 \; ; \tag{iv}$$

with m some positive integer and in each such case, the identity (5.23) holds.

This concludes the proof. ■

Thus equation (5.18) is established for the ($\mathbb{Z}_2$-colourable) $\widehat{A}$ models. We may now proceed to establish this result also for the other affine models by making use of the intertwining relationship (2.15).

We note the following property of the eigenvalues of the $\widehat{A}\widehat{D}\widehat{E}$ adjacency matrices: If we denote by $\beta_{[h]}^{(\mu)}$ the eigenvalue with exponent μ of any model $\mathcal{G}$ with Coxeter number h; then

$$\beta_{[2h]}^{(2\mu)} = \beta_{[h]}^{(\mu)} \; . \tag{5.24}$$

This is very useful given the form (2.15) interrelating the $\widehat{A}\widehat{D}\widehat{E}$ models and we make use of it in the following theorem (theorem 5.2).

Note that, as in equation (2.15), we will assume from now on that the eigenvectors

$$\left\{ \underset{\sim}{\psi}^{(\mu)} \;\middle|\; \mu \in \mathrm{v}^*(\mathcal{G}) \right\} \tag{5.25}$$

provide an *orthonormal* eigenbasis of $\mathcal{G}$.

Theorem 5.2 The coefficients of the Virasoro characters in the expansion (2.25) are given by the Chebychev polynomials of equation (5.18). In other words

$$\sum_{\substack{\mu\in \mathrm{v}^*(\mathcal{G}) \\ \varepsilon\in \widehat{A}_{[2h]}}} \frac{\phi_\varepsilon^{(2\mu)}}{\phi_0^{(2\mu)}}\, \psi_a^{(\mu)*}\, \psi_b^{(\mu)}\, \Lambda_n^\varepsilon = \mathcal{U}_{ab}^{(n)}(\mathcal{G})\ . \tag{5.26}$$

Here $\mathcal{U}^{(n)}(\mathcal{G})$ denotes the Chebychev polynomial of the second kind satisfying: $\mathcal{U}^{(0)}(\mathcal{G}) = \mathbb{I}$ and $\mathcal{U}^{(1)}(\mathcal{G}) = \mathcal{G}$ and Λ_n^ε again denotes the coefficient $\Lambda_n^{(\widehat{A}_{[2h]};0,\varepsilon)}$. □

Proof (by induction on n).

We first establish that the initial conditions (4.84) are satisfied:

$$\begin{aligned}
\sum_{\mu,\varepsilon} \frac{\phi_\varepsilon^{(2\mu)}}{\phi_0^{(2\mu)}}\, \psi_a^{(\mu)*}\, \psi_b^{(\mu)}\, \Lambda_0^\varepsilon &= \sum_{\mu,\varepsilon} \frac{\phi_\varepsilon^{(2\mu)}}{\phi_0^{(2\mu)}}\, \psi_a^{(\mu)*}\, \psi_b^{(\mu)}\, \delta_n^\varepsilon \\
&= \sum_{\mu} \psi_a^{(\mu)*}\, \psi_b^{(\mu)} \\
&= \delta_{ab} \\
&= \mathcal{U}_{ab}^{(0)}(\mathcal{G})
\end{aligned} \tag{5.27}$$

and

$$\begin{aligned}
\sum_{\mu,\varepsilon} \frac{\phi_\varepsilon^{(2\mu)}}{\phi_0^{(2\mu)}}\, \psi_a^{(\mu)*}\, \psi_b^{(\mu)}\, \Lambda_1^\varepsilon &= \sum_{\mu,\varepsilon} \frac{\phi_\varepsilon^{(2\mu)}}{\phi_0^{(2\mu)}}\, \psi_a^{(\mu)*}\, \psi_b^{(\mu)}\, \left(\delta_1^\varepsilon + \delta_{2h-1}^\varepsilon\right) \\
&= \sum_{\mu,\varepsilon} \frac{\phi_{2h-1}^{(2\mu)} + \phi_1^{(2\mu)}}{\phi_0^{(2\mu)}}\, \psi_a^{(\mu)*}\, \psi_b^{(\mu)} \\
&= \sum_{\mu} \beta_{[2h]}^{(2\mu)}\, \psi_a^{(\mu)*}\, \psi_b^{(\mu)} \\
&= \mathcal{G}_{ab} \\
&= \mathcal{U}_{ab}^{(1)}(\mathcal{G})
\end{aligned} \tag{5.28}$$

as required.

It remains to show that the Chebychev recursion relation (4.83) holds. Assume that $\exists\ N \in \mathbb{Z}^+$ such that $\forall\ 2 \leq n < N$ that (5.26) is true. Then

$$\begin{aligned}\sum_c \mathcal{U}_{ac}^{(N-1)}(\mathcal{G})\,\mathcal{G}_{cb} - \mathcal{U}_{ab}^{(N-2)}(\mathcal{G}) &= \sum_c \sum_{\mu,\varepsilon} \frac{\phi_\varepsilon^{(2\mu)}}{\phi_0^{(2\mu)}}\,\psi_a^{(\mu)*}\,\psi_c^{(\mu)}\,\Lambda_{N-1}^{\varepsilon}\,\mathcal{G}_{cb} \\ &\qquad - \sum_{\mu,\varepsilon} \frac{\phi_\varepsilon^{(2\mu)}}{\phi_0^{(2\mu)}}\,\psi_a^{(\mu)*}\,\psi_b^{(\mu)}\,\Lambda_{N-2}^{\varepsilon} \\ &= \sum_{\mu,\varepsilon} \frac{\phi_\varepsilon^{(2\mu)}}{\phi_0^{(2\mu)}}\,\psi_a^{(\mu)*}\,\psi_b^{(\mu)}\left(\beta_{[h]}^{(\mu)}\Lambda_{N-1}^{\varepsilon} - \Lambda_{N-2}^{\varepsilon}\right) \\ &= \sum_{\mu,\varepsilon} \frac{\phi_\varepsilon^{(2\mu)}}{\phi_0^{(2\mu)}}\,\psi_a^{(\mu)*}\,\psi_b^{(\mu)}\left(\beta_{[2h]}^{(2\mu)}\Lambda_{N-1}^{\varepsilon} - \Lambda_{N-2}^{\varepsilon}\right).\end{aligned} \tag{5.29}$$

We have used the eigenvector properties of the $\underset{\sim}{\psi}^{(\mu)}$ and the eigenvalue property $\beta_{[2h]}^{(2\mu)} = \beta_{[h]}^{(\mu)}$. Now we note that for any function F,

$$\begin{aligned}\sum_\mu \beta_{[2h]}^{(2\mu)}\,\phi_{[2h]\varepsilon}^{(2\mu)}\,F(\varepsilon) &= \sum_{\mu,\lambda}\left(\widehat{A}_{[2h]}\right)_{\varepsilon\lambda}\phi_{[2h]\varepsilon}^{(2\mu)}\,F(\varepsilon) \\ &= \phi_{[2h]\varepsilon}^{(2\mu)}\left\{F(\varepsilon-1 \pmod{2h}) + F(\varepsilon+1 \pmod{2h})\right\}.\end{aligned} \tag{5.30}$$

Thus, as a direct consequence of lemma 5.1, the calculation (5.29) continues as

$$\begin{aligned}\sum_c \mathcal{U}_{ac}^{(N-1)}(\mathcal{G})\,\mathcal{G}_{cb} - \mathcal{U}_{ab}^{(N-2)}(\mathcal{G}) &= \sum_{\mu,\varepsilon} \frac{\phi_\varepsilon^{(2\mu)}}{\phi_0^{(2\mu)}}\,\psi_a^{(\mu)*}\,\psi_b^{(\mu)}\left(\Lambda_{N-1}^{\varepsilon-1} + \Lambda_{N-1}^{\varepsilon+1} - \Lambda_{N-2}^{\varepsilon}\right) \\ &= \sum_{\mu,\varepsilon} \frac{\phi_\varepsilon^{(2\mu)}}{\phi_0^{(2\mu)}}\,\psi_a^{(\mu)*}\,\psi_b^{(\mu)}\,\Lambda_N^{\varepsilon} \\ &= \mathcal{U}_{ab}^{(N)}(\mathcal{G})\end{aligned} \tag{5.31}$$

as required. Hence equation (5.26) is valid for all values $n \in \mathbb{Z}^+$.

This concludes the proof. ■

We remark here that as the relationship (2.15) is valid also for the odd cycles $\widehat{A}_{2p}$ so that the expression (5.18) in fact applies for all affine $\widehat{A}\widehat{D}\widehat{E}$ models.

Importantly, the form (5.18) easily makes manifest the *graph symmetry* of the partition functions. A bijection $\zeta \in \operatorname{aut}\mathcal{G}$,

$$\zeta : \mathcal{G} \to \mathcal{G} \,, \tag{5.32}$$

is a symmetry of the graph $\mathcal{G}$ iff

$$\left({}^{\zeta}G\right)_{ab} \equiv \mathcal{G}_{\zeta^{-1}(a)\,\zeta^{-1}(b)} = \mathcal{G}_{ab} \quad \forall\, a, b \in \mathcal{G} \,. \tag{5.33}$$

Given such a symmetry ζ, it is easily established that $({}^{\zeta}\mathcal{G})^n = \mathcal{G}^n \;\forall\, n \in \mathbb{Z}^+$ from which the result $\mathcal{U}^{(n)}({}^{\zeta}\mathcal{G}) = \mathcal{U}^{(n)}(\mathcal{G}) \;\forall\, n \in \mathbb{Z}^+$ follows. Hence the boundary condition dependence of the partition function $\mathcal{Z}^{(\mathcal{G};a,b)}(q)$ is only upon the relative positions of a and b on the graph $\mathcal{G}$. Given the original physical specification of the models, this is entirely as one would expect.

5.4 The Affine Coxeter Element

In this section we establish the role played by the affine Coxeter element in the partition functions of the affine models. The role played by the classical analogue was first investigated by Dorey [21].

Before proving the main result, it will be useful to establish a useful property of the action of the matrix operator $\mathcal{G}$ on the set of affine Coxeter orbit representatives $\widehat{\mathsf{R}}$.

Proposition 5.3 The action of the operator $\mathcal{G}$ (see equation (4.71)) on the orbit representatives $\widehat{\mathsf{R}}$, is given by

$$\sum_{c\in\mathcal{G}} \phi_c \, \mathcal{G}_{cb} = \begin{cases} (1+\omega^{-1})\,\phi_b & ;\text{ if } b \in \widehat{P}_1. \\ (1+\omega)\,\phi_b & ;\text{ if } b \in \widehat{P}_2. \end{cases} \tag{5.34}$$

□

Proof We proceed by simple calculation:

$$\begin{aligned} \sum_c \phi_c \, \mathcal{G}_{cb} &= \sum_c (1-\omega^{-1})\,\rho_c \, \mathcal{G}_{cb} \\ &= (1-\omega^{-1})\,(\omega_1+\omega_2)\,\rho_b \;; \end{aligned} \tag{5.35}$$

where we use (4.58) and lemma 4.5.

If $b \in \widehat{P}_1$ then we may 'premultiply' ρ_b by ω_2 as $\omega_2\,\rho_b = \rho_b$ in this case (by (4.48)). Thus, for $b \in \widehat{P}_1$ we have,

$$\begin{aligned} \sum_c \phi_c \, \mathcal{G}_{cb} &= (1-\omega^{-1})\,(\omega^{-1}+1)\,\rho_b \\ &= (1+\omega^{-1})\,\phi_b \end{aligned} \tag{5.36}$$

as required.

If $b \in \widehat{P}_2$ then we may premultiply ρ_b by ω_1 as now $\omega_1 \rho_b = \rho_b$. Thus (5.35) becomes

$$\begin{aligned} \sum_c \phi_c \mathcal{G}_{cb} &= (1-\omega^{-1})(1+\omega)\rho_b \\ &= (1+\omega)\phi_b \end{aligned} \tag{5.37}$$

as required. ■

In analogy with [21], we introduce the function

$$v_a \equiv \begin{cases} 0 & ; \text{if } a \in \widehat{P}_2. \\ 1 & ; \text{if } a \in \widehat{P}_1. \end{cases} ; \tag{5.38}$$

and define $v_{ab} \equiv v_a - v_b$.

We now demonstrate the connection between the Chebychev polynomials and the affine Coxeter element. Dorey [21] demonstrated using explicit forms for the eigenvectors in the intertwiners (1.67) that the partition functions of the *classical* Pasquier models could be expressed as

$$\mathcal{Z}^{(\mathcal{G};a,b)}(q) = \sum_{\overline{\omega}^{-p}\overline{\phi}_b \in \overline{\Phi}^+} \chi^c_{1,2p+1+v_{ab}}(q) \left(\overline{\rho}_a\,,\, \overline{\omega}^{-p}\overline{\phi}_b^{\vee}\right) . \tag{5.39}$$

The quantities $\overline{\rho}_a$, $\overline{\omega}$ and $\overline{\phi}_b$ refer to the root system and Weyl group of a classical Lie algebra $\overline{\mathfrak{g}}$ with adjacency matrix $\mathcal{G}$; the scalar product $(\,,\,)$ is the usual Euclidean bilinear form and the Virasoro characters $\chi^c_{a,b}(q)$ refer to representations of the conformal algebra with central charge $c = 1 - \frac{6}{\overline{h}(\overline{h}-1)} < 1$. As demonstrated earlier (equation (4.90)), (classical) intertwiners and the Chebychev polynomials are related. Thus we are led to conjecture a similar form for the affine partition functions by equating the natural *affine* generalisation of the inner product appearing in (5.39) to the Chebychev polynomials of the affine adjacency matrices.

Theorem 5.4 Let v_{ab} be defined as above. If $\mathcal{G}$ is the Coxeter-Dynkin diagram of the Kac-Moody algebra $\widehat{\mathfrak{g}}$ and $\langle , \rangle$ the *affine* bilinear form (scalar product) on the maximal Cartan subalgebra $\widehat{\mathfrak{h}}$ of $\widehat{\mathfrak{g}}$; then

$$\mathcal{U}_{ab}^{(2p+v_{ab})}(\mathcal{G}) = \left\langle \rho_a \, , \, \omega^{-p} \phi_b^\vee \right\rangle \; ; \tag{5.40}$$

ω denotes the (Steinberg-ordered affine) Coxeter element defined in equation (4.54). □

Proof The proof is by induction on the variable N in $\mathcal{U}^{(N)}(\mathcal{G})$. We first check that the form $\langle \rho_a \, , \, \omega^{-p} \phi_b^\vee \rangle$ reproduces the correct initial conditions (4.83), i.e. $\mathcal{U}^{(0)}(\mathcal{G}) = \mathbb{I}$ and $\mathcal{U}^{(1)}(\mathcal{G}) = \mathcal{G}$. We check each of the four possibilities for assigning a and b to the sets $\widehat{P}_2$ and $\widehat{P}_1$ separately. We make use of the properties of normality of the affine scalar product, the duality between the roots and the weights, the properties particular to the affine Coxeter element defined in section 4.2.1 and of its orbit representatives.

$\underline{a, b \in \widehat{P}_2}$: $v_a = v_b = 0 \Rightarrow v_{ab} = 0$; so:

$$\begin{aligned} \left\langle \rho_a \, , \, \phi_b^\vee \right\rangle &= \left\langle \rho_a \, , \, \omega_1 \alpha_b^\vee \right\rangle \\ &= \left\langle \omega_1 \rho_a \, , \, \alpha_b^\vee \right\rangle \\ &= \left\langle \rho_a \, , \, \alpha_b^\vee \right\rangle \\ &= \delta_{ab} \\ &= \mathcal{U}_{ab}^{(2(0)+0)}(\mathcal{G}) \\ &= \mathcal{U}_{ab}^{(2(0)+v_{ab})}(\mathcal{G}) \, . \end{aligned} \tag{5.41}$$

Where the third line is obtained from the second using the normal property (4.49) of the scalar product.

$\underline{a, b \in \widehat{P}_1}$: $v_a = v_b = 1 \Rightarrow v_{ab} = 0$.

$$\begin{aligned} \left\langle \rho_a \, , \, \phi_b^\vee \right\rangle &= \left\langle \rho_a \, , \, \alpha_b^\vee \right\rangle \\ &= \delta_{ab} \\ &= \mathcal{U}_{ab}^{(2(0)+0)}(\mathcal{G}) \\ &= \mathcal{U}_{ab}^{(2(0)+v_{ab})}(\mathcal{G}) \, . \end{aligned} \tag{5.42}$$

$\underline{a \in \widehat{P}_1,\ b \in \widehat{P}_2}$: $v_a = 1,\ v_b = 0 \Rightarrow v_{ab} = 1$.

$$\begin{aligned}
\langle \rho_a\,,\, \phi_b^\vee \rangle &= \langle \rho_a\,,\, \omega_1 \alpha_b^\vee \rangle \\
&= \langle \omega_1 \rho_a\,,\, \alpha_b^\vee \rangle \\
&= \langle \sigma_a \rho_a\,,\, \alpha_b^\vee \rangle \\
&= \langle (\rho_a - \alpha_a)\,,\, \alpha_b^\vee \rangle \\
&= \langle \rho_a\,,\, \alpha_b^\vee \rangle - \langle \alpha_a\,,\, \alpha_b^\vee \rangle \\
&= 0 - \mathsf{C}_{ab} \\
&= \mathcal{G}_{ab} \\
&= \mathcal{U}_{ab}^{(2(0)+1)}(\mathcal{G}) \\
&= \mathcal{U}_{ab}^{(2(0)+v_{ab})}(\mathcal{G})\,.
\end{aligned} \tag{5.43}$$

We obtain the adjacency matrix from the Cartan matrix C, by noting that $\mathcal{G} = 2 - \mathsf{C}$ so that when $a \neq b$: $\mathcal{G}_{ab} = -\mathsf{C}_{ab}$.

$\underline{a \in \widehat{P}_2,\ b \in \widehat{P}_1}$: $v_a = 0$ and $v_b = 1$ so that $v_{ab} = -1$. Now:

$$\begin{aligned}
\langle \rho_a\,,\, \omega^{-1} \phi_b^\vee \rangle &= \langle \rho_a\,,\, \omega_1 \omega_2 \alpha_b^\vee \rangle \\
&= \langle \omega_2 \omega_1 \rho_a\,,\, \alpha_b^\vee \rangle \\
&= \langle \omega_2 \rho_a\,,\, \alpha_b^\vee \rangle \\
&= \langle \sigma_a \rho_a\,,\, \alpha_b^\vee \rangle \\
&= \langle (\rho_a - \alpha_a)\,,\, \alpha_b^\vee \rangle \\
&= \langle \rho_a\,,\, \alpha_b^\vee \rangle - \langle \alpha_a\,,\, \alpha_b^\vee \rangle \\
&= 0 - \mathsf{C}_{ab} \\
&= \mathcal{G}_{ab} \\
&= \mathcal{U}_{ab}^{(2(1)-1)}(\mathcal{G}) \\
&= \mathcal{U}_{ab}^{(2(1)+v_{ab})}(\mathcal{G})\,.
\end{aligned} \tag{5.44}$$

Thus we see that $\mathcal{U}^{(0)}(\mathcal{G}) = \mathbb{1}$ and $\mathcal{U}^{(1)}(\mathcal{G}) = \mathcal{G}$.

Assume that $\exists\, N \in \mathbb{Z}^+$ with $2p + v_{ab} = N$ where a and b denote, as before, the boundary

conditions; such that $\forall\, n < N$ that equation (5.40) holds. We wish to show that (5.40) holds for N also and hence is valid $\forall\, n \in \mathbb{Z}^+$ by induction. The proof again splits into the four possible arrangements of a and b amongst the sets $\widehat{P}_1$ and $\widehat{P}_2$. In the first two cases, the number N is even, in the last two, N is odd. Our method makes repeated use of proposition 5.3.

$\underline{a, b \in \widehat{P}_2}$: As $b \in \widehat{P}_2$, the non-zero components of $\mathcal{G}_{cb}$ may occur only for $c \in \widehat{P}_1$. Thus $v_{ab} = 0 - 0 = 0$ and $v_{ac} = 0 - 1 = -1$. Hence

$$\begin{aligned}
\mathcal{U}_{ac}^{(2p-1)}(\mathcal{G})\,\mathcal{G}_{cb} - \mathcal{U}_{ab}^{(2p-2)}(\mathcal{G}) &= \mathcal{U}_{ac}^{(2p+v_{ac})}(\mathcal{G})\,\mathcal{G}_{cb} - \mathcal{U}_{ab}^{(2(p-1)+v_{ab})}(\mathcal{G}) \\
&= \left\langle \rho_a\,,\, (\omega^{-p}\mathcal{G}_{cb} - \omega^{-(p-1)}\delta_{cb})\,\phi_c^\vee \right\rangle \\
&= \left\langle \rho_a\,,\, (\omega^{-p}(1+\omega) - \omega^{-(p-1)})\,\phi_b^\vee \right\rangle \\
&= \left\langle \rho_a\,,\, \omega^{-p}\phi_b^\vee \right\rangle \\
&= \mathcal{U}_{ab}^{(2p+v_{ab})}(\mathcal{G}) \\
&= \mathcal{U}_{ab}^{(2p)}(\mathcal{G})
\end{aligned} \tag{5.45}$$

as required.

$\underline{a, b \in \widehat{P}_1}$: Now $b \in \widehat{P}_1$, so that the non-zero components of $\mathcal{G}_{cb}$ occur when $c \in \widehat{P}_2$. Thus we see that $v_{ab} = 1 - 1 = 0$ and $v_{ac} = 1 - 0 = 1$. Now:

$$\begin{aligned}
\mathcal{U}_{ac}^{(2p-1)}(\mathcal{G})\,\mathcal{G}_{cb} - \mathcal{U}_{ab}^{(2p-2)}(\mathcal{G}) &= \mathcal{U}_{ac}^{(2(p-1)+v_{ac})}(\mathcal{G})\,\mathcal{G}_{cb} - \mathcal{U}_{ab}^{(2(p-1)+v_{ab})}(\mathcal{G}) \\
&= \left\langle \rho_a\,,\, (\omega^{-(p-1)}\mathcal{G}_{cb} - \omega^{-(p-1)}\delta_{cb})\,\phi_c^\vee \right\rangle \\
&= \left\langle \rho_a\,,\, (\omega^{-(p-1)}(1+\omega^{-1}) - \omega^{-(p-1)})\,\phi_b^\vee \right\rangle \\
&= \left\langle \rho_a\,,\, \omega^{-p}\phi_b^\vee \right\rangle \\
&= \mathcal{U}_{ab}^{(2p+v_{ab})}(\mathcal{G}) \\
&= \mathcal{U}_{ab}^{(2p)}(\mathcal{G})
\end{aligned} \tag{5.46}$$

as required.

$\underline{a \in \widehat{P}_1,\, b \in \widehat{P}_2}$: $b \in \widehat{P}_2$ so that the non-zero components of $\mathcal{G}_{cb}$ are when $c \in \widehat{P}_1$. Thus $v_{ab} = 1 - 0 = 1$ and $v_{ac} = 1 - 1 = 0$. Again:

$$\begin{aligned}
\mathcal{U}_{ac}^{(2p)}(\mathcal{G})\,\mathcal{G}_{cb} - \mathcal{U}_{ab}^{(2p-1)}(\mathcal{G}) &= \mathcal{U}_{ac}^{(2p+v_{ac})}(\mathcal{G})\,\mathcal{G}_{cb} - \mathcal{U}_{ab}^{(2(p-1)+v_{ab})}(\mathcal{G}) \\
&= \left\langle \rho_a\,,\, (\omega^{-p}\mathcal{G}_{cb} - \omega^{-(p-1)}\delta_{cb})\,\phi_c^\vee \right\rangle \\
&= \left\langle \rho_a\,,\, (\omega^{-p}(1+\omega) - \omega^{-(p-1)})\,\phi_b^\vee \right\rangle \\
&= \left\langle \rho_a\,,\, \omega^{-p}\phi_b^\vee \right\rangle \\
&= \mathcal{U}_{ab}^{(2p+v_{ab})}(\mathcal{G}) \\
&= \mathcal{U}_{ab}^{(2p+1)}(\mathcal{G})
\end{aligned} \tag{5.47}$$

as required.

$\underline{a \in \widehat{P}_2,\, b \in \widehat{P}_1}$: Finally, in this case, $b \in \widehat{P}_1$ so that the non-zero components of $\mathcal{G}_{cb}$ are when $c \in \widehat{P}_2$. Thus $v_{ab} = 0 - 1 = -1$ and $v_{ac} = 0 - 0 = 0$. So:

$$\begin{aligned}
\mathcal{U}_{ac}^{(2p)}(\mathcal{G})\,\mathcal{G}_{cb} - \mathcal{U}_{ab}^{(2p-1)}(\mathcal{G}) &= \mathcal{U}_{ac}^{(2p+v_{ac})}(\mathcal{G})\,\mathcal{G}_{cb} - \mathcal{U}_{ab}^{(2p+v_{ab})}(\mathcal{G}) \\
&= \left\langle \rho_a\,,\, (\omega^{-p}\mathcal{G}_{cb} - \omega^{-p}\delta_{cb})\,\phi_c^\vee \right\rangle \\
&= \left\langle \rho_a\,,\, (\omega^{-p}(1+\omega^{-1}) - \omega^{-p})\,\phi_b^\vee \right\rangle \\
&= \left\langle \rho_a\,,\, \omega^{-(p+1)}\phi_b^\vee \right\rangle \\
&= \mathcal{U}_{ab}^{(2p+v_{ab})}(\mathcal{G}) \\
&= \mathcal{U}_{ab}^{(2p+1)}(\mathcal{G})
\end{aligned} \tag{5.48}$$

as required.

This completes the proof. Equation (5.40) follows by induction. ■

Thus we rewrite equation (5.18) as

$$\boxed{\mathcal{Z}^{(\mathcal{G};a,b)} = \sum_{p=p'}^{\infty} \chi_{\frac{(2p+v_{ab})^2}{4}}(q) \left\langle \rho_a \, , \, \omega^{-p} \phi_b^\vee \right\rangle} \tag{5.49}$$

with:

$$p' = \begin{cases} 0 & ; \text{ if } v_{ab} = 0 \text{ or } 1. \\ 1 & ; \text{ if } v_{ab} = -1. \end{cases} . \tag{5.50}$$

This expresses the affine partition functions in terms of the affine Coxeter element. Note that the summation automatically excludes those terms which are zero due to the requirement that $|a-b|$ and n (now replaced by $2p+v_{ab}$) be both even or both odd.

We remark that [21] demonstrated the form (5.39) for the *classical* models by an entirely different method. We duplicate his result using the method just described by recalling that the intertwiner V_{ab}^{λ} relating the $\mathcal{G} = D, E$ models to an A model is equivalent to a Chebychev polynomial by equation (4.90). Theorem 5.4 holds in the classical case also once one replaces the affine scalar product $\langle \, , \rangle$ with the usual one $(\, ,)$ and the affine Coxeter transformation, weights and orbit representatives with their classical analogues. Thus we may equate the intertwiner with a geometric expression. The result (5.39) follows directly from [50]

$$\mathcal{Z}^{(\mathcal{G};a,b)}(q) = \sum_{\lambda=1}^{h-1} \chi_{1,\lambda}^{c}(q) \, V_{ab}^{\lambda} \, . \tag{5.51}$$

5.5 Geometrical Consequences

In analogy with [21], we may attempt to construct invariant subspaces under the action of ω as follows:

Define

$$\alpha_i^{(\mu)} \stackrel{\text{def}}{=} \sum_{a \in \widehat{P}_i} \psi_a^{(\mu)} \alpha_a \quad \text{for } i = 1, 2. \tag{5.52}$$

These vectors would appear to possess the properties:

$$\begin{aligned} \omega_i \alpha_i^{(\mu)} &= -\alpha_i^{(\mu)} \,, \\ \omega_j \alpha_i^{(\mu)} &= \alpha_i^{(\mu)} + \beta^{(\mu)} \alpha_j^{(\mu)} \quad \text{for } i \neq j. \end{aligned} \tag{5.53}$$

So that $V^{(\mu)} \stackrel{\text{def}}{=} \text{span}\{\alpha_1^{(\mu)}, \alpha_2^{(\mu)}\}$ is closed.

Unfortunately, for some values of μ and i, such vectors (5.52) may be identically zero; this can be verified by explicit calculation. However, for $\mu = 0$ it is easy to see that the properties of the Perron-Frobenius eigenvector ensure that $\alpha_1^{(0)}$ and $\alpha_2^{(0)}$ are both non-zero, distinct and linearly independent. Hence the $\mu = 0$ invariant subspace exists. Choose the Perron-Frobenius eigenvector to have all coefficients positive. We change notation and write

$$\alpha^{(i)} = \sum_{a \in \widehat{P}_i} \psi_a^{(0)} \alpha_a \,. \tag{5.54}$$

So that

$$\omega_i \, \alpha^{(j)} = \begin{cases} -\alpha^{(j)} & ; \text{ if } i = j. \\ \alpha^{(j)} + 2\,\alpha^{(i)} & ; \text{ if } i \neq j. \end{cases} \,. \tag{5.55}$$

We also define the weights

$$\rho^{(i)} = \sum_{a \in \widehat{P}_i} \psi_a^{(0)} \rho_a \,. \tag{5.56}$$

Their action upon the $\{\alpha^{(i)}\}$ is

$$\langle \rho^{(i)} , \alpha^{(j)\vee} \rangle = \tfrac{1}{2}\,\delta^{ij} \; ; \tag{5.57}$$

and upon roots in general, their action is to project onto the spaces $\mathrm{span}\{\alpha^{(1)}\}$ and $\mathrm{span}\{\alpha^{(2)}\}$ respectively. Equation (5.57) indicates that $2\,\rho^{(i)}$ is the dual of $\alpha^{(i)}$; therefore the projection operator $\mathcal{J}$ onto the space $V \equiv \mathrm{span}\{\alpha^{(1)}, \alpha^{(2)}\}$ is given by

$$\mathcal{J}\lambda \equiv 2\,\langle \rho^{(1)} , \lambda^{\vee} \rangle\, \alpha^{(1)} + 2\,\langle \rho^{(2)} , \lambda^{\vee} \rangle\, \alpha^{(2)} \; ; \tag{5.58}$$

where $\lambda \equiv \left(\overline{\lambda} , 0 , n \right)$ is any root. In particular $\mathcal{J}^2 = \mathcal{J}$. We let $\alpha \equiv \alpha^{(1)} + \alpha^{(2)} = \psi_0^{(0)}\delta$ and $\rho \equiv \rho^{(1)} + \rho^{(2)}$ so that $\langle \rho , \alpha \rangle = 1$.

We remark that ρ as defined, is a positive integer sum over the weights $\{\, \rho_a \mid a \in \mathcal{G} \,\}$. Thus recalling the property (4.27) that any root may be written as a positive or negative integer sum of the simple roots; we see that, by analogy with [21],

$$\begin{aligned} &\lambda \text{ is a positive root} \\ &\Leftrightarrow \langle \rho_a , \lambda^{\vee} \rangle > 0 \quad \text{for any } a \\ &\Leftrightarrow \langle \rho , \lambda^{\vee} \rangle > 0 \, . \end{aligned} \tag{5.59}$$

Thus we have:

Lemma 5.5 Any root of $\widehat{\Phi}$ is a positive root, iff the scalar product of its coroot with ρ is positive; i.e.

$$\lambda \equiv \left(\overline{\lambda} , 0 , n \right) \in \widehat{\Phi}^{+} \quad \text{iff} \quad \langle \rho , \lambda^{\vee} \rangle > 0 \, . \tag{5.60}$$

□

The following result is perhaps obvious; however we state it for clarity:

Proposition 5.6 The projection $\mathcal{J}$ commutes with the Weyl group operators ω_1 and ω_2; and hence with the Coxeter element. That is

$$[\mathcal{J}\,,\,\omega_i]\Big|_{\widehat{\Phi}} = 0\,, \quad \text{for } i = 1,2 \tag{5.61}$$

insofar as they act upon the roots $\widehat{\Phi}$. □

Proof The simple roots $\widehat{\Pi}$ provide a basis for $\widehat{\Phi}$. Therefore one need only examine to see if $\mathcal{J}\omega_i\alpha_a = \omega_i\mathcal{J}\alpha_a$ for each a and i. This follows easily using the properties (5.55) and the definition (5.58). ■

For convenience, for any operator Y, let:

$$[\![\mathsf{Y}]\!]_b \stackrel{\text{def}}{=} \begin{cases} \mathbb{I} & ;\text{ if } b \in \widehat{P}_1. \\ \mathsf{Y} & ;\text{ if } b \in \widehat{P}_2. \end{cases} \tag{5.62}$$

Theorem 5.7 For all a, $b \in \mathcal{G}$ and $p \in \mathbb{Z}^+$:

$$\left\langle \rho_a\,,\,\omega^{-p}\phi_b^\vee \right\rangle \geq 0\,. \tag{5.63}$$

□

Proof By lemma 5.5, we need only establish that $\langle \rho\,,\,\omega^{-p}\phi_b\rangle > 0$.

By proposition 5.6:

$$\begin{aligned} \mathcal{J}\omega^{-p}\phi_b &= \omega^{-p}\,[\![\omega_1]\!]_b\,\mathcal{J}\,\alpha_b \\ &= 2\left\langle \rho^{(1)}\,,\,\alpha_b^\vee\right\rangle \omega^{-p}\,[\![\omega_1]\!]_b\,\alpha^{(1)} + 2\left\langle \rho^{(2)}\,,\,\alpha_b^\vee\right\rangle \omega^{-p}\,[\![\omega_1]\!]_b\,\alpha^{(2)} \\ &= 2\left\langle \rho^{(P(b))}\,,\,\alpha_b^\vee\right\rangle \omega^{-p}\,[\![\omega_1]\!]_b\,\alpha^{(P(b))}\,; \end{aligned} \tag{5.64}$$

where we make use of the fact that $\langle \rho^{(i)}\,,\,\alpha_b^\vee\rangle = 0$ unless $b \in \widehat{P}_i$. Thus we need only examine the Coxeter orbits of $\alpha^{(1)}$ and $\omega_1\,\alpha^{(2)} \equiv 2\,\alpha^{(1)} + \alpha^{(2)}$.

We see from (5.55) that the application of ω^{-1} to $(n)\,\alpha^{(1)}+(n-1)\,\alpha^{(2)}$ yields $(n+2)\,\alpha^{(1)}+(n+1)\,\alpha^{(2)}$; i.e. n is replaced by $n+2$. The roots of both orbits follow this form. Hence, as $\mathcal{J}$ projects onto the invariant space V,

$$\begin{aligned}\left\langle \rho\,,\,\omega^{-p}\phi_b^\vee\right\rangle &= \left\langle \rho\,,\,\mathcal{J}\omega^{-p}\phi_b^\vee\right\rangle \\ &= \begin{cases} 2\left\langle \rho^{(1)}\,,\,\alpha_b^\vee\right\rangle(2p+1) & ;\text{ when } b\in\widehat{P}_1. \\ 2\left\langle \rho^{(2)}\,,\,\alpha_b^\vee\right\rangle(2p+3) & ;\text{ when } b\in\widehat{P}_2. \end{cases}\end{aligned} \tag{5.65}$$

This may be rewritten as

$$\left\langle \rho\,,\,\omega^{-p}\phi_b^\vee\right\rangle = 2\left\langle \rho\,,\,\alpha_b^\vee\right\rangle\left(2p+1+2\,\delta_{2,P(b)}\right)\,. \tag{5.66}$$

The scalar product appearing on the RHS clearly exceeds zero as α_b is a simple root and hence a positive root. The remaining factor is positive for all $p\geq 0$.

This completes the proof. ■

We already knew from generating polynomial arguments (section 2.5), that the coefficients of the Virasoro characters appearing in (5.49) were non-negative integers (which physically by (1.136) they have to be). We have now demonstrated this independently, and more importantly, *geometrically*. That they are integers follows trivially from the duality of the weights and coroots (4.37) together with the fact that the set $\widehat{\Phi}$ is closed under the action of $\widehat{W}$.

We mention as an aside that it might be interesting to investigate the relationship, if any, between the projection $\mathcal{J}$ and the defect map investigated by Berman *et al.* [6].

As is evident, much of the structure of an affine algebra $\widehat{\mathrm{g}}$ is related to the underlying structure of the horizontal subalgebra $\overline{\mathrm{g}}$. We may use the Euclidean Coxeter element of section 4.2.3 to examine separately the action of ω on the horizontal and lightlike parts of

the orbit representatives. Consider

$$\begin{aligned}\omega^{-1}\phi_b &= \omega^{-1}\left(\overline{\phi}_b\,,\,0\,,\,\delta_{0b}\right)\\ &= \breve{\omega}^{-1}\mathrm{t}\left(\overline{\phi}_b\,,\,0\,,\,\delta_{0b}\right)\\ &= \breve{\omega}^{-1}\left(\overline{\phi}_b\,,\,0\,,\,\delta_{0b}+\left(\overline{\phi}_b\,,\,\overline{\theta}^{\vee}\right)\right)\\ &= \left(\breve{\omega}^{-1}\overline{\phi}_b\,,\,0\,,\,\delta_{0b}+\left(\overline{\phi}_b\,,\,\overline{\theta}^{\vee}\right)\right)\,.\end{aligned} \tag{5.67}$$

Iterating, so that for $p \geq 0$,

$$\omega^{-p}\phi_b = \left(\breve{\omega}^{-p}\overline{\phi}_b\,,\,0\,,\,\delta_{0b}+\sum_{p'=0}^{p-1}\left(\breve{\omega}^{-p'}\overline{\phi}_b\,,\,\overline{\theta}^{\vee}\right)\right)\,. \tag{5.68}$$

As $\breve{\omega}$ has period h (section 4.2.3), we may write

$$\omega^{-(qh+r)}\phi_b = \left(\breve{\omega}^{-r}\overline{\phi}_b\,,\,0\,,\,\delta_{0b}+\sum_{r'=0}^{r-1}\left(\breve{\omega}^{-r'}\overline{\phi}_b\,,\,\overline{\theta}^{\vee}\right)+q\sum_{r'=0}^{h-1}\left(\breve{\omega}^{-r'}\overline{\phi}_b\,,\,\overline{\theta}^{\vee}\right)\right)\,; \tag{5.69}$$

where $p = qh + r$ and $r < h$ by the usual division algorithm. Thus to calculate the coefficient $\langle \rho_a\,,\,\omega^{-p}\phi_b\rangle$ we need only examine the behaviour of the "*Euclidean projection*" of the Coxeter orbits onto $\overline{\Phi}$, the root system of $\overline{\mathfrak{g}}$. In particular, due to the periodicity of $\breve{\omega}$, we find that one can calculate any coefficient from the knowledge of the $h(r+1)$ vectors

$$\left\{\,\breve{\omega}^{-r}\overline{\phi}_b\;\middle|\;r\in\mathbb{Z},\,0\leq r\leq h-1;\,b\in\mathcal{G}\,\right\}\,, \tag{5.70}$$

together with their inner products with the (dual of the) highest root $\overline{\theta}^{\vee}$; in particular, the sums

$$\left\{\sum_{r'=0}^{r-1}\left(\breve{\omega}^{-r'}\overline{\phi}_b\,,\,\overline{\theta}^{\vee}\right)\;\middle|\;r\in\mathbb{Z},\,0\leq r\leq h-1\right\}\,. \tag{5.71}$$

Note that it is the orbits $\langle\breve{\omega}\rangle\overline{\phi}_b$ of the Euclidean Coxeter element which appear in these quantities and *not* the orbits of the Coxeter element $\overline{\omega}$ of the algebra $\overline{\mathfrak{g}}$. However it is interesting to see that the *entire* structure of the affine Coxeter orbits can be determined by examining the orbits of $\breve{\omega}$ alone. These being of finite cardinality, allow one to determine the entire partition function (5.49) from a finite number of calculations. Indeed this

method of calculation was checked using Mathematica. The correct partition functions are obtained.

Chapter 6

Concluding Remarks

In this chapter, we summarise the main results of this thesis and attempt to place them within the context of current research.

We use the defining axioms of the affine Pasquier models on the cylinder to calculate their partition functions. This is motivated by a desire to extend the results of Saleur and Bauer [50] to the affine models. It is carried out by directly extending the result (1.149) of Saleur for the model A_∞ to the $\widehat{A}_n$ models (1.152) and using the derived intertwiner result (2.15) to relate the partition functions of the models based upon the graphs $\widehat{D}_n$ and $\widehat{E}_{6,7,8}$ to these partition functions.

The intertwiners relating the $\widehat{A}_{[h]}$, $\widehat{D}_{[h]}$ and $\widehat{E}_{[6,12,30]}$ models to the $\widehat{A}_{[2h]}$ models are found to be of a peculiar form:

$$\boxed{N_\lambda^{ab} \equiv \sum_{\mu \in \mathrm{v}^*(\mathcal{G})} \frac{\phi_\lambda^{(2\mu)}}{\phi_0^{(2\mu)}} \psi_a^{(\mu)*} \psi_b^{(\mu)}} \,. \tag{2.17}$$

This should be compared with the classical intertwiners (1.67). Unlike the classical intertwiners, typically these coefficients are of either sign and are integer or half-integer valued (see for example the results (2.20–2.23)). They also relate a model with affine Coxeter number h to a model with affine Coxeter number $2h$. In fact they even relate $\widehat{A}_n$ models with other $\widehat{A}_n$ models. However, as with classical intertwiners, the affine intertwiners (2.17) respect the parity of the boundary conditions, in that a model with even (odd) boundary

conditions is related to a $\widehat{A}_n$ models also with even (odd) boundary conditions.

The intertwining relationship is solved explicitly in all cases so that the partition functions can be expressly written as a positive integer sum over degenerate Virasoro characters (2.25). Generating functions for the coefficients are calculated (section 2.5) and phrased in terms of generating polynomials; the polynomials stated as tables 2.2–2.5, together with the parameters listed in table 2.1. These polynomial generators also manifest the positive integrality of the series derived and are observed on a case by case basis to respect the graph symmetries of the defining graph $\mathcal{G}$.

It is also observed (again individually for each model), that the Virasoro representation (i.e. character) of lowest weight appearing in the partition functions of the models is, in each case, of weight $h_{(a,b)} = \mathbb{K}^2/4$; where $\mathbb{K}$ is the length of the shortest path between the two nodes a and b on the defining diagram $\mathcal{G}$. This weight, $h_{(a,b)}$, is the weight of the 'ground state' field of each theory.

The result derived for the 4-state Potts model with free boundary conditions is found to be in precise agreement with that found by Saleur and Bauer [50] (section 2.4). In chapter 3, a numerical investigation of the partition functions is carried out. Within the limits of the analysis, the numerical calculations are found to be in agreement with the derived forms for a number of affine models. In addition, this numerical analysis allowed us to refute an alternative result, that of Baake *et al.* [2], for the 4-state Potts model. These checks combined, serve as a verification of the results found up to this point.

An analysis of the polynomial generators and the resulting Poincaré series, finds them to be related to the decomposition of tensor products of irreducible representations of the finite subgroup of SU(2) associated to the graph $\mathcal{G}$ under the McKay correspondence. Specifically, the generating polynomial $\mathsf{Q}^{(\mathcal{G};a,b)}(x)$ is the sum of the polynomials $\{K_j(x)\}$ associated with the representations $\{\gamma_j\}$ appearing in the tensor product decomposition of the representations associated with the nodes a and b (refer to equations (5.8) and (5.17)).

In summary therefore, we demonstrate two general forms for the affine partition functions,

namely

$$\boxed{\mathcal{Z}^{(\mathcal{G};a,b)}(q) = \sum_{n=0}^{\infty} \chi_{\frac{n^2}{4}}(q)\, \mathcal{U}_{ab}^{(n)}(\mathcal{G})} \,, \tag{5.18}$$

the "*Chebychev form*", and

$$\boxed{\mathcal{Z}^{(\mathcal{G};a,b)} = \sum_{p=p'}^{\infty} \chi_{\frac{(2p+v_{ab})^2}{4}}(q)\, \left\langle \rho_a \,,\, \omega^{-p} \phi_b^{\vee} \right\rangle} \tag{5.49}$$

with

$$p' = \begin{cases} 0 & ; \text{if } v_{ab} = 0 \text{ or } 1. \\ 1 & ; \text{if } v_{ab} = -1. \end{cases} \,,$$

the "*geometric form*", which relates the partition function of the affine model to the (Steinberg-ordered) Coxeter element of the associated affine Kac-Moody algebra.

Each form has its advantages: (5.18) manifests most clearly the graph symmetry of the partition functions. As is expected on purely physical grounds, $\mathcal{Z}^{(\mathcal{G};a,b)}(q)$ ought only to depend upon a and b insofar as their relative positions on the graph $\mathcal{G}$ are concerned. This is indeed the case (section 5.3). Equation (5.18) also manifests the connection these models have with the tensor decompositions of irreducible representations of SU(2).

The form (5.49) demonstrates that the affine extension of the Steinberg-ordered Coxeter element plays a role in the physics of the affine models. Mathematically, by theorem 5.7, it allows one to observe that the coefficients of the Virasoro characters in the expansion of the partition functions are positive integers. The expression also provides one with an exceptionally quick method of evaluating the partition function of any affine model. What initially appears to be an infinite sequence, may in fact be reduced to a finite number of evaluations by equation (5.69). It is possible that this can be used as a mechanism to collect the degenerate $c = 1$ Virasoro characters in the partition functions in such a way as to observe the action of higher symmetries, such as supersymmetry or those associated

with W-algebras, in the physics of these models.

Most importantly, this geometric result (5.49) and its consequences lends support to the idea that geometric structures have more general roles within conformal field theories. Another step in this direction has recently been made by Zuber [58], who has examined the possibility of constructing the "SU(3) analogue" (in the nomenclature of Di Francesco and Zuber [23]) of the Steinberg-ordered Coxeter element. Such an element and its generalisations may play a role in the more general SU(N) models of [23]. Indeed, we have demonstrated in this thesis, the relationship between the Chebychev polynomials and the Coxeter element for the SU(2) case. Could it be that a generalisation of this connection* to the SU(3) case, and beyond, can provide a useful tool in establishing the role of such a generalised Coxeter element?

*As an aside, we have constructed an "SU(3) analogue" of the Chebychev polynomials. This discussion is presented in appendix C.

Appendix A

Affine Eigenvectors

$\widehat{A}_{2h-1} \equiv \widehat{A}_{[2h]}$

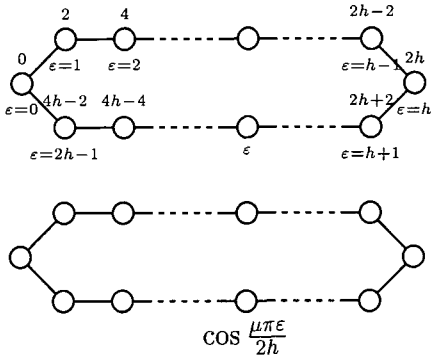

$\beta^{(\mu)} = 2\cos\frac{\mu\pi}{h}$.

Normalisation:

$$\left|\underset{\sim}{\phi}^{(\mu)}_{[2h]}\right|^2 = \begin{cases} 2h & ;\ \text{if } \mu = 0, 2h. \\ h & ;\ \text{if } \mu \neq 0, 2h. \end{cases} .$$

Table A.1: Labelling conventions for the nodes ($\varepsilon = \cdots$) and exponents μ (the numbers above the nodes on the first graph) for the graph $\widehat{A}_{2h-1}$. The components $\phi^{(\mu)}_{\varepsilon}$ of the eigenvectors $\underset{\sim}{\phi}^{(\mu)}$ together with the corresponding eigenvalue $\beta^{(\mu)}$ are given on the second graph. Note that the above choice is *not* an orthogonal set. The affine Coxeter number $h = n + 1$ for the graph $\widehat{A}_n$.

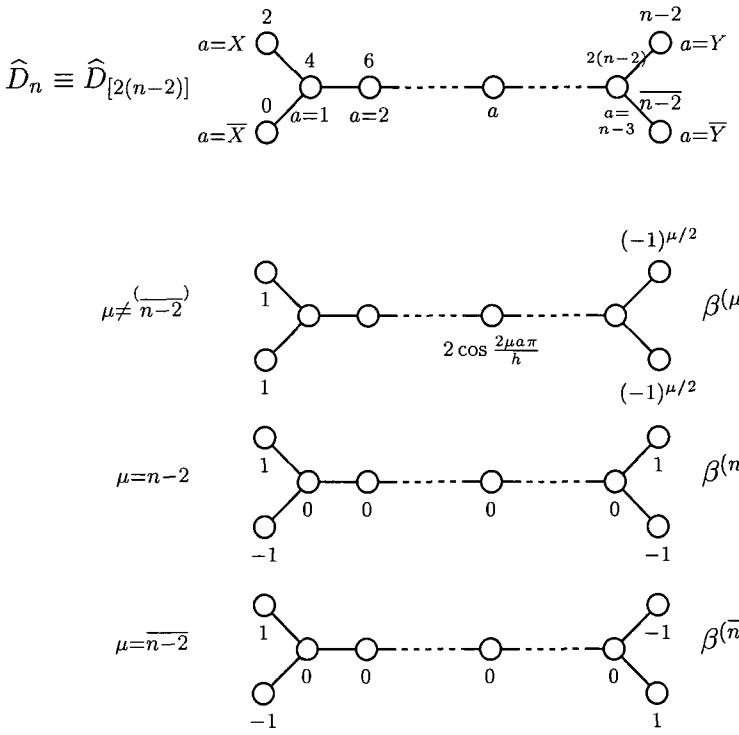

Normalisation:

$$\left|\underset{\sim}{\psi}^{(\mu)}\right|^2 = \begin{cases} 2(n-2) & ; \text{for } \mu \neq 0, \overline{n-2}, h \equiv 2(n-2). \\ 4(n-2) & ; \text{if } \mu = 0, h. \\ 4 & ; \text{if } \mu = \overline{n-2}. \end{cases} .$$

Table A.2: Labelling conventions for the nodes ($a = \cdots$) and exponents μ (numbers above the nodes on the first graph) for the graph $\widehat{D}_n$. The components $\psi_a^{(\mu)}$ of the orthogonalised eigenvectors $\underset{\sim}{\psi}^{(\mu)}$ together with the corresponding eigenvalue $\beta^{(\mu)}$ appear on subsequent graphs. The affine Coxeter number $h = 2(n-2)$ for the graph $\widehat{D}_n$.

$\widehat{E}_6$

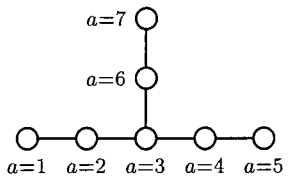

Exponents μ: $0, 2, 2, 3, 4, 4, 6$.

$\widehat{E}_7$

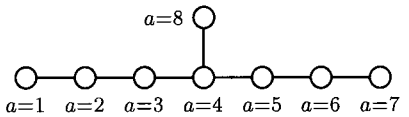

Exponents μ: $0, 3, 4, 6, 6, 8, 9, 12$.

$\widehat{E}_8$

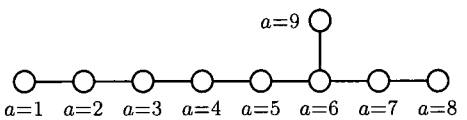

Exponents μ: $0, 6, 10, 12, 15, 18, 20, 24, 30$.

Table A.3: Labelling conventions for the nodes ($a = \cdots$) and exponents μ for the exceptional affine graphs $\widehat{E}_{6,7,8}$. The affine Coxeter numbers for the models are 6, 12 and 30 respectively.

Appendix B

The Kronecker Comb

We define the *generalised semi-infinite Kronecker comb* as

$$\Omega_{n,\varepsilon}^{(a_1,\ldots,a_k)} \equiv \sum_{m_1,\ldots,m_k=0}^{\infty} \delta_{n,\varepsilon+\sum_{i=1}^{k} m_i\, a_i} \; ; \tag{B.1}$$

where δ is the canonical Kronecker-δ. From this definition, it is easy to establish the following useful results:

$$\Omega_{n,\varepsilon}^{(\infty)} = \delta_{n,\varepsilon} \; , \tag{B.2}$$

$$\Omega_{n,\varepsilon}^{(\ldots,a,\ldots)} = \sum_{k'=0}^{\infty} \Omega_{n,\varepsilon+k'a}^{(\ldots\ldots)} \; , \tag{B.3}$$

$$\Omega_{n,\varepsilon}^{(\ldots,a,\ldots)} - \Omega_{n,\varepsilon+a}^{(\ldots,a,\ldots)} = \Omega_{n,\varepsilon}^{(\ldots\ldots)} \; , \tag{B.4}$$

$$\sum_{k'=0}^{k-1} \Omega_{n,\varepsilon+k'a}^{(\ldots,ka,\ldots)} = \Omega_{n,\varepsilon}^{(\ldots,a,\ldots)} \; , \tag{B.5}$$

$$\Omega_{n,\varepsilon+ka}^{(\ldots,a,a,\ldots)} = \left(\frac{n-\varepsilon}{a} + 1 - k \right) \Omega_{n,\varepsilon}^{(\ldots,a,\ldots)} \; . \tag{B.6}$$

Note that identity (B.3) is a special case of property (B.5) with $k \equiv \infty$ as

$$\Omega_{n,\varepsilon}^{(\ldots,\infty,\ldots)} = \Omega_{n,\varepsilon}^{(\ldots\ldots)} \; . \tag{B.7}$$

The sequence $\Omega_{n,\varepsilon}^{(a_1,\cdots,a_m)}$ is encoded by the generating function

$$\begin{aligned}\Omega_{\varepsilon}^{(a_1,\cdots,a_m)}(x) &\equiv \sum_{n=0}^{\infty} \Omega_{n,\varepsilon}^{(a_1,\cdots,a_m)}\, x^n \\ &= x^{\varepsilon} \prod_{m'=0}^{m} \frac{1}{1-x^{a_{m'}}} \,.\end{aligned} \tag{B.8}$$

So that

$$\Omega_{n,\varepsilon}^{(a_1,\cdots,a_m)} = \frac{1}{n!}\,\frac{\mathrm{d}^n}{\mathrm{d}x^n}\bigg|_{x=0} \Omega_{\varepsilon}^{(a_1,\cdots,a_m)}(x) \,. \tag{B.9}$$

Properties (B.2–B.6) follow for this generating function.

The function $\Omega_{\varepsilon}^{(a_1,\cdots,a_m)}(x)$ may also be interpreted as the generating function for the number of partitions of the integer $n-\varepsilon$ into sets of integers comprised only from the (possibly degenerate) set $\{a_1,\ldots,a_m\}$; this may be seen both from the result (B.8) and directly from the definition of the Kronecker comb (B.1).

Appendix C

SU(3) and Chebychev-like Polynomials

We begin by noting that there is an isomorphism θ_2 between the Chebychev polynomials (of the second kind) under multiplication and addition and the representations of SU(2) under the tensor product and direct sum (see also [23]):

$$\begin{aligned} \theta_2 : (\mathrm{SU}(2)^*, \otimes, \oplus) &\to (\mathfrak{H}^2, \cdot, +) \, , \\ \pi_0 &\mapsto 1 \, , \\ \pi_1 &\mapsto x \, , \\ \pi_n &\mapsto \mathcal{U}^{(n)}(x) \quad \forall \, n \in \mathbb{Z}^+. \end{aligned} \tag{C.1}$$

In fact the recursion relation (4.83) is given by the Clebsch-Gordon decomposition of the tensor product of the representation π_n and the fundamental representation π_1:

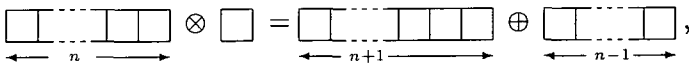

$$\mathcal{U}^{(n)}(x) \cdot x = \mathcal{U}^{(n+1)}(x) + \mathcal{U}^{(n-1)}(x) \, . \tag{C.2}$$

We recall that this recursion relation may be thought of as originating in the classical intertwiner relation (1.68) (see section 4.4).

Similarly we may establish an isomorphism:

$$\begin{aligned} \theta_3 : (\mathsf{SU}(3)^*, \otimes, \oplus) &\to (\mathfrak{H}^3, \cdot, +) \ , \\ \pi_{0,0} &\mapsto 1 \ , \\ \pi_{1,0} &\mapsto x \ , \\ \pi_{0,1} &\mapsto y \ , \\ \pi_{m,n} &\mapsto \mathcal{U}^{(m,n)}(x,y) \quad \forall \ m,n \in \mathbb{Z}^+ \ ; \end{aligned} \tag{C.3}$$

where $\mathfrak{H}^3$ is a set of polynomials.

We find the defining recursion relations of $\mathfrak{H}^3$ via the Clebsch-Gordon decompositions

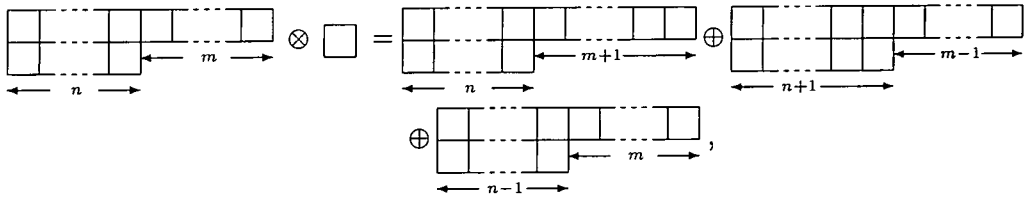

$$\begin{aligned} \mathcal{U}^{(m,n)}(x,y) \cdot x \ &= \mathcal{U}^{(m+1,n)}(x,y) + \mathcal{U}^{(m-1,n+1)}(x,y) \\ &\quad + \mathcal{U}^{(m,n-1)}(x,y) \end{aligned} \tag{C.4}$$

and

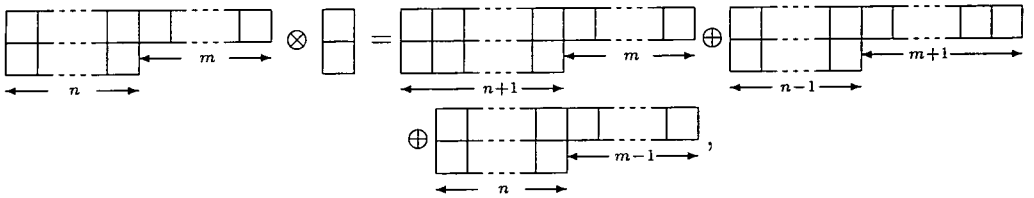

$$\begin{aligned} \mathcal{U}^{(m,n)}(x,y) \cdot y \ &= \mathcal{U}^{(m,n+1)}(x,y) + \mathcal{U}^{(m+1,n-1)}(x,y) \\ &\quad + \mathcal{U}^{(m-1,n)}(x,y) \ . \end{aligned} \tag{C.5}$$

As in the case of $\mathfrak{H}^2$ we require boundary conditions. Examining the Chebychev case, we

observe that $\mathcal{U}^{(-1)}(x) = 0$. Analogously, we choose

$$\begin{aligned}\mathcal{U}^{(-1,0)}(x,y) &= \mathcal{U}^{(-2,0)}(x,y) = \mathcal{U}^{(0,-1)}(x,y) \\ &= \mathcal{U}^{(-1,-1)}(x,y) = \mathcal{U}^{(-2,-1)}(x,y) = \mathcal{U}^{(0,-2)}(x,y) \\ &= \mathcal{U}^{(-1,-2)}(x,y) = \mathcal{U}^{(-2,-2)}(x,y) = 0\,,\end{aligned} \tag{C.6}$$

together with

$$\mathcal{U}^{(0,0)}(x,y) = 1\,, \tag{C.7}$$

for the trivial representation. In particular, this yields

$$\mathcal{U}^{(1,0)}(x,y) = x \quad \text{and} \quad \mathcal{U}^{(0,1)}(x,y) = y \tag{C.8}$$

for the fundamental representations $\pi_{1,0}$ and $\pi_{0,1}$ respectively.

With this choice of initial conditions, it is not difficult to calculate the generating function for the family of polynomials $\mathfrak{H}^3$. It is

$$\begin{aligned}\mathfrak{C}_3(p,q|x,y) &\equiv \sum_{m,n=0}^{m,n=\infty} \mathcal{U}^{(m,n)}(x,y)\, p^m\, q^n \\ &= \frac{1}{(1 - x\,p + y\,p^2 - p^3)(1 - y\,q + x\,q^2 - q^3)}\,,\end{aligned} \tag{C.9}$$

which is similar in form to (4.85).

Just as the algebraic properties Chebychev polynomials $\mathfrak{H}^2$ contain the tensor product decompositions of irreducible representations of SU(2), the properties of $\mathfrak{H}^3$ contain the tensor product decompositions of SU(3). Once a McKay-like correspondence relating the generators of a reflection group and the irreducible representations of the subgroups of SU(3) can be established, then hopefully, the link between $\mathfrak{H}^3$ and a generalised Coxeter element will follow. We remark that polynomials similar to the family $\mathfrak{H}^3$ are discussed by Di Francesco and Zuber [23], where they arise in connection with operators intertwining various SU(3) models.

References

[1] G. Andrews, R. Baxter and P. Forrester , "Eight-vertex SOS model and generalized Rogers-Ramanujan-type identities", *J. Stat. Phys.* ***35*** *(1984), 193–266.*

[2] M. Baake, G. von Gehlen, V. Rittenberg, "Operator content of the Ashkin-Teller quantum chain – superconformal and Zamolodchikov-Fateev invariance: I Free boundary conditions", *J. Phys.* ***A****: Math. Gen.* ***20*** *(1987), L479–L485.*

V. Rittenberg, "Operator content of some $c = 1$ models in statistical mechanics", *lectures presented at the international summer school "Conformal invariance and string theory", Poiana Brasov, Romania, 1–12 September 1987; University of Bonn (Germany) preprint BONN-HE-88-06.*

[3] M. Barber, "Finite-size scaling", *in "Phase transitions and critical phenomena, vol. 8", ed. by C. Domb and J. Lebowitz. Academic Press, London (1989).*

[4] R. Baxter, "Exactly solved models in statistical mechanics", *Academic Press, London (1982).*

[5] A. Belavin, A. Polyakov, A. Zamolodchikov, "Infinite conformal symmetry in two-dimensional quantum field theory", *Nucl. Phys.* ***B241*** *(1984), 333–380.*

[6] S. Berman, Y. S. Lee, R. V. Moody, "The spectrum of a Coxeter transformation, affine Coxeter transformations and the defect map", *J. Algebra* ***121*** *(1989), 339–357.*

[7] H. Blöte, J. Cardy, M. Nightingale, "Conformal invariance, the central charge, and universal finite-size amplitudes at criticality", *Phys. Rev. Lett.* ***56*** *(1986), 742–745.*

[8] D. O'Brien, P. Pearce, "Lattice realizations of unitary minimal modular invariant partition functions", *J. Phys.* ***A****: Math. Gen.* ***28*** *(1995), 4891–4906.*

[9] A. Cappelli, C. Itzykson, J.-B. Zuber, "Modular invariant partition functions in two-dimensions", *Nucl. Phys.* ***B280*** *(1987), 445–465.*

A. Cappelli, C. Itzykson, J.-B. Zuber, "The *A-D-E* classification of minimal and $A_1^{(1)}$ conformal field theories", *Commun. Math. Phys.* ***113*** *(1987), 1–26.*

[10] J. Cardy, "Conformal invariance and surface critical behaviour", *Nucl. Phys.* ***B240*** *(1984), 514–532.*

[11] J. Cardy, "Conformal invariance and universality in finite-size scaling", *J. Phys.* ***A****: Math. Gen.* ***17*** *(1984), L385–L387.*

[12] J. Cardy, "Operator content of two-dimensional conformally invariant theories", *Nucl. Phys.* ***B270*** *(1986), 186–204.*

[13] J. Cardy, "Effect of boundary conditions on the operator content of two-dimensional conformally invariant theories", *Nucl. Phys.* ***B275*** *(1986), 200-218.*

[14] J. Cardy, "Logarithmic corrections to finite-size scaling in strips", *J. Phys.* ***A****: Math. Gen.* ***19*** *(1986), L1093–L1098.*

[15] J. Cardy, "Conformal invariance and statistical mechanics", *in Les Houches, session XLIX, 1988, "Champs, cordes et phénomènes critiques", ed. by E. Brèzin and J. Zinn-Justin. Elsevier Science Publishers B.V., North-Holland, Amsterdam, The Netherlands (1989).*

[16] J. Cardy, "Boundary conditions, fusion rules and the Verlinde formula", *Nucl. Phys.* ***B324*** *(1989), 581–596.*

[17] A. Coleman, "Killing and the Coxeter transformation of Kac-Moody algebras", *Invent. Math.* ***95*** *(1989), 447–477.*

[18] J. Cornwell, "Group theory in physics", volumes I and II. *Academic Press, London (1984).*

[19] P. Dorey, "Root systems and purely elastic S-matrices, Part I", *Nucl. Phys.* ***B358*** *(1991), 654–676.*

P. Dorey, "Root systems and purely elastic S-matrices, Part II", *Nucl. Phys.* ***B374*** *(1992), 741–761.*

[20] P. Dorey, "Hidden geometrical structures in integrable models", *a talk given at the conference "Integrable quantum field theories" held in Como, Italy, 13–19 September 1992; hep-th/9212143.*

[21] P. Dorey, "Partition functions, intertwiners and the Coxeter element", *Int. J. Mod. Phys.* ***A8*** *(1993), 193–208.*

[22] P. Di Francesco, H. Saleur, J.-B. Zuber, "Modular invariance in non-minimal two-dimensional conformal theories", *Nucl. Phys.* ***B285*** *(1987), 454–480.*

[23] P. Di Francesco and J.-B. Zuber, "SU(N) lattice integrable models associated with graphs", *Nucl. Phys.* ***B338*** *(1990), 602–646.*

[24] P. Di Francesco and J.-B. Zuber, unpublished, *reported in section 3.6 of reference* [25] *and section 4 of* [21].

[25] P. Di Francesco, "Integrable lattice models, graphs and modular invariant conformal field theories", *Int. J. Mod. Phys.* ***A7*** *(1992), 407–500.*

[26] D. Friedan, Z. Qiu, S. Shenker, "Conformal invariance, unitarity, and critical exponents in two dimensions", *Phys. Rev. Lett.* ***52*** *(1984), 1575–1578.*

[27] J. Fuchs, "Affine Lie algebras and quantum groups", *Cambridge University Press, Cambridge, England (1995).*

[28] J. Fuchs, "Lectures on conformal field theory and Kac-Moody algebras", *in Lecture notes in physics vol. 498. Lectures held at the Eötvös graduate course, Budapest, Hungary, 13–18 August 1996, "Conformal field theories and integrable models", ed. by Z. Horváth and L. Palla. Springer-Verlag, Heidelberg, Germany (1997).*

[29] P. Ginsparg, "Curiosities at $c = 1$", *Nucl. Phys.* ***B295*** *(1988), 153–170.*

[30] P. Ginsparg, "Applied conformal field theory", *in Les Houches, session XLIX, 1988, "Champs, cordes et phénomènes critiques", ed. by E. Brèzin and J. Zinn-Justin. Elsevier Science Publishers B.V., North-Holland, Amsterdam, The Netherlands (1989).*

[31] P. Ginsparg, "Some statistical mechanical models and conformal field theories", *lectures given at Trieste spring school, 3–11 April 1989; Harvard University (Cambridge, Massachusetts) preprint HUTP-89-A027.*

[32] G. Golub, C. van Loan, "Matrix computations", *North Oxford Academic, Oxford, England (1983).*

[33] A. Hintermann, H. Kunz, F. Y. Wu, "Exact results for the Potts model in two dimensions", *J. Stat. Phys.* ***19*** *(1978), 623–632.*

[34] J. Humphreys, "Introduction to Lie algebra and representation theory", *Springer-Verlag, N.Y.C, New York (1972).*

[35] J. Humphreys, "Reflection groups and Coxeter groups", *Cambridge University Press, Cambridge, England (1990).*

[36] A. Iskandar, "On breathers in affine Toda theories", *University of Durham (England) Ph.D. thesis (1995).*

[37] V. Kac, "Contravariant form for infinite-dimensional Lie algebras and superalgebras", in *"Lecture notes in physics 94", 441–445, Springer, N.Y.C., New York (1979).*

[38] V. Kac, "Infinite dimensional Lie algebras", *Cambridge University Press, Cambridge, England (1990).*

[39] B. Kostant, "The principal three-dimensional subgroup and the Betti numbers of a complex simple Lie group", *Am. J. Math.* ***81*** *(1959), 973–1032.*

[40] B. Kostant, "On finite subgroups of SU(2), simple Lie algebras, and the McKay correspondence", *Proc. Natl. Acad. Sci. USA* ***81*** *(1984), 5275–5277.*

[41] B. Kostant, "The McKay correspondence, the Coxeter element and representation theory", *Société Mathématique de France Astérisque, hors série, (1985), 209–255.*

[42] B. Nienhuis, "Critical behaviour of two-dimensional spin models and charge asymmetry in the Coulomb gas", *J. Stat. Phys.* ***34*** *(1984), 636–761.*

[43] V. Pasquier, "Two-dimensional critical systems labelled by Dynkin diagrams", *Nucl. Phys.* ***B285*** *(1987), 162–172.*

[44] V. Pasquier, "Operator content of the *A-D-E* lattice models", *J. Phys.* ***A****: Math. Gen.* ***20*** *(1987), 5707–5717.*

[45] V. Pasquier, "Lattice derivation of modular invariant partition functions on the torus", *J. Phys.* ***A****: Math. Gen.* ***20*** *(1987), L1229–L1237.*

[46] R. B. Potts, "Some generalized order-disorder transformations", *Proc. Cambridge Philos. Soc.* ***48*** *(1952), 106–109.*

[47] Ph. Roche, "On the construction of integrable dilute *ADE* models", *Phys. Lett.* ***B285*** *(1992), 49–53.*

[48] H. Saleur, "Partition functions of the two-dimensional Ashkin-Teller model on the critical line", *J. Phys.* ***A****: Math. Gen.* ***20*** *(1987), L1127–L1133.*

[49] H. Saleur, "Off-critical integrable vertex models and conformal field theories in finite geometries", *J. Phys.* ***A****: Math. Gen.* ***22*** *(1988), L41–48.*

[50] H. Saleur and M. Bauer, "On some relations between local height probabilities and conformal invariance", *Nucl. Phys.* ***B320*** *(1989), 591–624.*

[51] N. Sochen, "Integrable models through representations of the Hecke algebra", *Nucl. Phys.* ***B360*** *(1991), 613–640.*

[52] R. Steinberg, "Finite reflection groups", *Trans. Amer. Math. Soc.* ***91*** *(1959), 493–504.*

[53] R. Steinberg, "Finite subgroups of SU(2), Dynkin diagrams and affine Coxeter elements", *Pac. J. Math.* ***118*** *(1985), 587–598.*

[54] H. Temperley, E. Lieb, "Relations between the 'percolation' and 'colouring' problem and other graph-theoretical problems associated with regular planar lattices: some exact results for the 'percolation' problem", *Proc. Roy. Soc. (London)* ***A322*** *(1971), 251–280.*

[55] S. Warnaar, B. Nienhuis, K. Seaton, "New construction of solvable lattice models including an Ising model in a field", *Phys. Rev. Lett.* ***69*** *(1992), 710–712.*

[56] F. Y. Wu and Y. K. Wang, "Duality transformation in a many-component spin model", *J. Math. Phys.* ***17*** *(1976), 439–440.*

[57] J.-B. Zuber, "Conformal field theories, Coulomb gas picture and integrable models", *in Les Houches, session XLIX, 1988, "Champs, cordes et phénomènes critiques", ed. by E. Brèzin and J. Zinn-Justin. Elsevier Science Publishers B.V., North-Holland, Amsterdam, The Netherlands (1989).*

[58] J.-B. Zuber, "Graphs and reflection groups", *Commun. Math. Phys.* ***179*** *(1996), 265–294.*